Chemical characterisation and source identification of PM$_{10}$ and PM$_{2.5}$ in Switzerland

- Project report -

View of the urban air quality monitoring station Zürich-Kaserne from above.

Dübendorf, 08.04.2021

Impressum

Contracting authority: Federal Office for the Environment (FOEN), Air Pollution Control and Chemicals Division, CH-3003 Bern.

Contractor: Empa, Swiss Federal Laboratories for Materials Science and Technology, Air Pollution/Environmental Technology Laboratory, CH-8600 Dübendorf.

Contact number: 16.0096.PJ/R152-0739

Authors: Christoph Hüglin and Stuart K. Grange

Contributions from: Andres Alastuey (IDAEA-CSIC), Andrea Fischer (Empa), Jean-Luc Jaffrezo (Université Grenoble Alpes), Juanita Rausch (Particle Vision), Gaëlle Uzu (Université Grenoble Alpes), David Jaramillo Vogel (Particle Vision), Claudia Zellweger-Fäsi (Empa)

Project monitoring FOEN, Air Quality Management Section: Brigitte Gälli Purghart, Rudolf Weber, Richard Ballaman

Disclaimer: This report was commissioned by the Federal Office for the Environment (FOEN). The contractor alone is responsible for the content.

Contact: christoph.hueglin@empa.ch

Contents

The main results in brief

Atmospheric particulate matter (PM) is a key air pollutant, which is composed of a large number of different chemical constituents and which is released by various emission sources or formed in the atmosphere by complex chemical processes. PM is usually defined and regulated by size, most commonly as the mass concentrations of particulate matter with diameters smaller than 10 and 2.5 micrometers and denoted as PM_{10} and $PM_{2.5}$, respectively.

Knowledge of the chemical composition and the contributions of the major sources of PM is needed for planning efficient measures to reduce particulate matter pollution and for assessing the effect of implemented measures. In this report, the detailed chemical composition of PM_{10} and $PM_{2.5}$ during a one year period (from June 2018 to May 2019) at five sites of the Swiss National Air Quality Monitoring Network (NABEL) representing rural, suburban, urban and urban roadside environments is presented. The chemical characterisation data is used for identification and quantification of main sources of particulate matter. The results are compared to similar measurement campaigns undertaken in 1998–1999 and 2008–2009.

The main constituents of PM in Switzerland are sulfate, nitrate and ammonium. They are all formed in the atmosphere by chemical transformation of gaseous compounds (SO_2, NO_x and NH_3) and contribute to a fraction of PM that is called secondary inorganic aerosol. Other large contributions to the mass concentration of atmospheric particulate matter come from organic matter (much of which is secondary organic aerosol and also formed in the atmosphere by conversion of organic gases), elemental carbon, mineral dust, and trace elements.

In addition to the various emission sources leading to the formation of secondary inorganic and organic aerosol, road traffic and residential wood burning have been identified to be important sources of atmospheric particulate matter. A gradual increase in the concentration of PM is observed when moving from rural to suburban, urban, and urban roadside locations. The higher concentration of PM in urban environments can largely be explained by contributions from road traffic, in particular the exhaust emissions from vehicles but also non-exhaust emissions released into the air from road and vehicle wear as well as from road dust.

In the past decades, policies to abate emissions of PM and its precursors have been implemented in Switzerland and in most parts of Europe. This led to decreasing concentrations of PM_{10} and $PM_{2.5}$ in Switzerland by about 40 % between 1998 and 2019. The trend of decreasing concentrations can be seen in all main constituents of particulate matter, except mineral dust. Most striking and of particular importance for the positive development of air quality in Switzerland is the large downward trend of elemental carbon (EC), which is mainly due to the implementation of diesel particulate filters.

Compared to the large decrease in PM_{10} and $PM_{2.5}$ mass concentration during the past two decades, the changes in the *relative* importance of the main constituents are rather modest. As an example, the figure below shows the change in relative composition of PM_{10} at the urban background site Zürich-Kaserne for three yearly measurement periods between 1998 and 2019.

Clear patterns in the changes of relative contributions to PM can, nevertheless, be identified for some constituents. Relative contributions of elemental carbon and sulfate in both PM_{10} and $PM_{2.5}$ size fractions have decreased at all five sampling locations included in this study. Inversely, the relative contribution of organic matter to PM_{10} and $PM_{2.5}$ mass increased over the monitoring periods. Similarly, mineral dust relative contributions have also consistently increased. Although crustal matter is mostly of natural origin, there is an anthropogenic component which is driven by resuspension processes, especially from traffic at roadside locations.
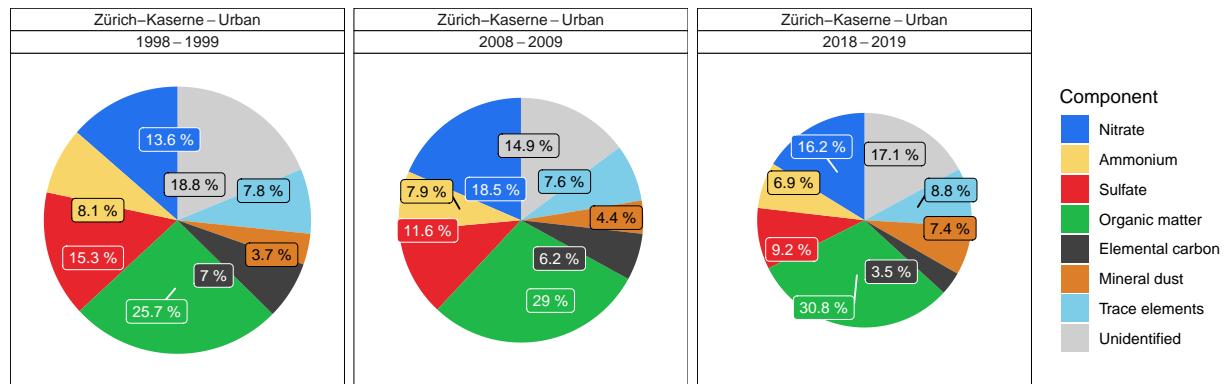
Chemical composition of PM_{10} at the urban background site Zürich-Kaserne for three one-year measurement periods between 1998 and 2019. The area of the shown circles is proportional to the PM_{10} concentration (1998–1999: 24.1 $\mu g\,m^{-3}$, 2008–2009: 20.2 $\mu g\,m^{-3}$, 2018–2019: 15.6 $\mu g\,m^{-3}$).

The temporal evolution of PM_{10} and $PM_{2.5}$ represents a success of the Swiss and European control of particulate matter and its precursors, especially in the area of combustion process control. However, there is still significant potential to improve air quality, e.g. by reducing road traffic emissions, emissions of ammonia from agriculture and emissions of organic matter from various sources. Road traffic emissions are most effectively reduced by focusing on non-exhaust emissions. This is also justified by the fact that non-exhaust emissions from road traffic are an important source of some transition metals that contribute negligibly to PM mass but are suspected to be important for the health effects of particulate matter. Finally, in more rural settlements, there are still opportunities to further abate emissions from wood burning activities.

Das Wichtigste in Kürze

Atmosphärischer Feinstaub (PM) ist ein wichtiger Luftschadstoff, der sich aus einer Vielzahl verschiedener chemischer Bestandteile zusammensetzt und von verschiedenen Emissionsquellen freigesetzt oder in der Atmosphäre durch komplexe chemische Prozesse gebildet wird. Die Definition von PM sowie die Regulierung im Rahmen von Immissionsgrenzwerten erfolgt vorwiegend anhand der Partikelgrösse, meistens als Massenkonzentration von Partikeln mit Durchmessern kleiner als 10 und 2.5 Mikrometer. Diese wird entsprechend als PM_{10} bzw. $PM_{2.5}$ bezeichnet.

Die Kenntnis der chemischen Zusammensetzung und der Beiträge der wichtigsten Feinstaub-quellen ist für die Planung effizienter Massnahmen zur Verringerung der Feinstaubbelastung und für die Bewertung der Wirkung umgesetzter Massnahmen notwendig. In diesem Bericht wird die detaillierte chemische Zusammensetzung von PM_{10} und $PM_{2.5}$ während eines Jahres (von Juni 2018 bis Mai 2019) an fünf Stationen des NABEL-Messnetzes beschrieben, welche ländliche, vorstädtische, städtische und verkehrsbelastete städtische Standorte repräsentieren. Die Konzentrationen der gemessenen chemischen Inhaltstoffe werden zur Identifizierung und Quantifizierung der Hauptquellen von Feinstaub verwendet. Die Ergebnisse werden mit Daten von ähnlichen Messkampagnen aus den Jahren 1998–1999 und 2008–2009 verglichen.

Hauptbestandteile des Feinstaubs in der Schweiz sind Nitrat, Ammonium und Sulfat, alle-samt Verbindungen, die in der Atmosphäre durch chemische Umwandlung von gasförmigem SO_2, NO_x und NH_3 gebildet werden und als sekundäres anorganisches Aerosol bezeichnet werden. Weitere grosse Beiträge zur Massenkonzentration des atmosphärischen Feinstaubs stammen von organischem Feinstaub, elementarem Kohlenstoff (EC), Mineralstaub und Spuren-elementen. Ein Grossteil des organischen Feinstaubs ist sekundäres organisches Aerosol und wird ebenfalls in der Atmosphäre durch Umwandlung organischer Gase gebildet.

Neben der Vielzahl von Emissionsquellen die zur Bildung von sekundärem anorganischem und organischem Aerosol beitragen, wurden der Strassenverkehr und die Holzverbrennung in Privathaushalten als Hauptquellen für atmosphärischen Feinstaub identifiziert. Ein gradueller Anstieg der PM-Konzentration von ländlichen zu vorstädtischen, städtischen und verkehrsbe-lasteten städtischen Standorten kann beobachtet werden. Die höheren PM-Konzentrationen in städtischen Umgebungen lassen sich grösstenteils durch Beiträge des Strassenverkehrs erklären, insbesondere durch Abgasemissionen von Fahrzeugen, aber auch durch Nicht-Abgasemissionen, die durch Strassen- und Fahrzeugabnutzung (z.B. Bremsabrieb) sowie durch Strassenstaub in die Luft gelangen.

In den vergangenen Jahrzehnten wurden in der Schweiz und in den meisten Teilen Europas

Massnahmen zur Verringerung der Emissionen von Feinstaub und seiner Vorläufersubstanzen ergriffen. Dies führte dazu, dass die Konzentrationen von PM_{10} und $PM_{2.5}$ in der Schweiz zwischen 1998 und 2019 um etwa 40 % abnahmen. Der Trend abnehmender Konzentrationen ist bei allen Hauptbestandteilen von Feinstaub zu beobachten, mit Ausnahme von Mineralstaub. Am auffälligsten und von besonderer Bedeutung für die positive Entwicklung der Luftqualität in der Schweiz ist der starke Rückgang der Konzentration von elementarem Kohlenstoff, der hauptsächlich auf die Einführung von Dieselpartikelfiltern zurückzuführen ist.

Angesichts des starken Rückgangs der Massenkonzentration von PM_{10} und $PM_{2.5}$ während der letzten zwei Jahrzehnte sind die Veränderungen in der relativen Bedeutung der Hauptbestandteile eher gering. Als Beispiel zeigt die folgende Abbildung die Änderung der relativen Zusammensetzung von PM_{10} am städtischen Standort Zürich-Kaserne für drei jährliche Messperioden zwischen 1998 und 2019.

Es lassen sich jedoch auch klare Muster in den Veränderungen der relativen Beiträge zum Feinstaub in der Schweiz erkennen. Die relativen Beiträge von elementarem Kohlenstoff und Sulfat in den beiden Grössenfraktionen PM_{10} und $PM_{2.5}$ haben an allen fünf in dieser Studie berücksichtigten Messorten abgenommen. Umgekehrt hat der relative Beitrag des organischen Feinstaubs zur Masse von PM_{10} und $PM_{2.5}$ während der vergangenen zwanzig Jahren zugenommen. In ähnlicher Weise haben auch die relativen Beiträge von mineralischem Staub durchweg zugenommen. Obwohl Mineralstaub zu einem grossen Teil natürlichen Ursprungs ist, gibt es eine anthropogene Komponente, die an strassennahen Standorten durch Aufwirbelung durch den Verkehr verursacht wird.
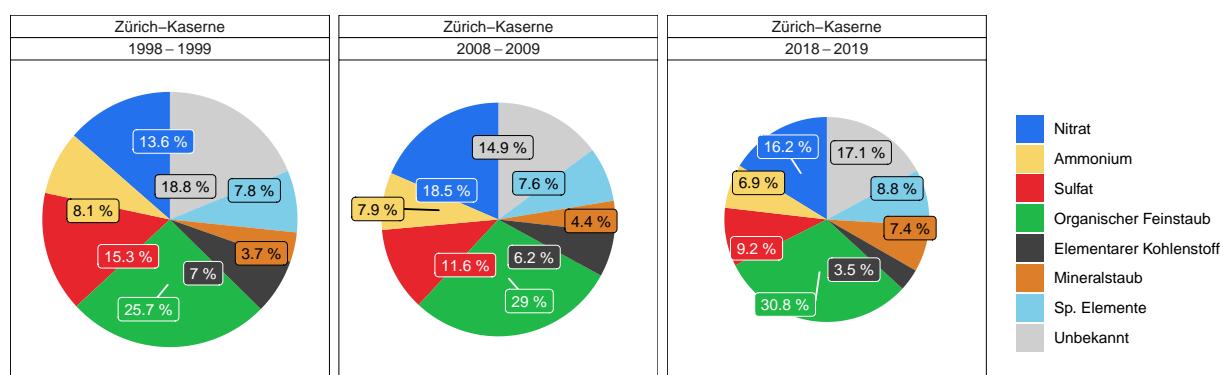
Chemische Zusammensetzung von PM_{10} am städtischen Standort Zürich-Kaserne während dreier jährlicher Messkampagnen zwischen 1998 und 2019. Die Fläche der dargestellten Kreise ist proportional zur PM_{10}-Konzentration (1998–1999: 24.1 $\mu g\,m^{-3}$, 2008–2009: 20.2 $\mu g\,m^{-3}$, 2018–2019: 15.6 $\mu g\,m^{-3}$).

Die zeitliche Entwicklung von PM_{10} und $PM_{2.5}$ stellt einen grossen Erfolg der schweizerischen und europäischen Massnahmen zur Minderung von Feinstaub und seinen Vorläufersub-

stanzen dar. Wichtige Verbesserungen bei den Emissionen aus Verbrennungsprozessen konnten erreicht werden. Es bestehen jedoch immer noch Möglichkeiten um die Luftqualität weiter zu verbessern, insbesondere durch weitere Reduktionen der Emissionen des Strassenverkehrs, von Ammoniak aus der Landwirtschaft und der Emissionen von organischen Stoffen aus verschiedenen Quellen. Weitere Emissionsreduktionen beim Strassenverkehr erfordern eine Konzentration auf die Nicht-Abgasemissionen. Anstrengungen zur Reduktion von Nicht-Abgasemissionen des Strassenverkehrs sind auch daher sinnvoll und notwendig, weil die nicht-abgasbedingten Emissionen des Strassenverkehrs eine wichtige Quelle für einige Metalle sind, welche zwar nur unwesentlich zur Feinstaubmasse beitragen, aber im Verdacht stehen, für die gesundheitlichen Auswirkungen von Feinstaub von spezieller Bedeutung zu sein. Schliesslich gibt es insbesondere in ländlichen Gebieten noch Möglichkeiten, die Emissionen aus Holzfeuerungen weiter zu verringern.

L'essentiel en bref

Les poussières fines (PM) constituent une importante source de pollution atmosphérique. Elles contiennent un grand nombre de composés chimiques et sont émises par différentes sources ou se forment dans l'atmosphère à travers des processus chimiques complexes. La définition des PM et la réglementation qui en précise les valeurs limites d'immission se basent en premier lieu sur leur taille. Sont généralement prises en compte les concentrations massiques de poussières d'un diamètre inférieur à 10 et à 2.5 micromètres, dénommées respectivement PM_{10} et $PM_{2.5}$.

Pour prendre des mesures efficaces de réduction de la charge en poussières fines puis en évaluer l'effet, il faut connaître la composition chimique des poussières ainsi que leurs principales sources et leurs immissions. Le présent rapport précise la composition chimique des PM_{10} et $PM_{2.5}$ relevées dans cinq stations suisses du réseau NABEL entre juin 2018 et mai 2019, en campagne, en périphérie urbaine, en ville et en milieu urbain fortement exposé au trafic. La concentration en composés chimiques permet d'identifier et de quantifier les principales sources de poussières fines. Les résultats sont comparés avec ceux de campagnes de mesure semblables conduites en 1998–1999 et en 2008–2009.

Les principaux composants des poussières fines en suspension dans l'air suisse sont des nitrates, l'ammonium et des sulfates, formés dans l'atmosphère par transformation chimique de SO_2, NO_x et NH_3 gazeux regroupés sous la dénomination d'aérosols inorganiques secondaires. Par ailleurs, une part importante de la masse des poussières fines atmosphériques se compose de poussières fines organiques, de carbone élémentaire (EC), de poussières minérales et d'éléments trace. Une bonne part de la poussière fine organique consiste en aérosols organiques secondaires et provient également de la transformation de composés organiques, présents sous forme gazeuse, dans l'atmosphère.

Si la formation d'aérosols inorganiques secondaires et d'aérosols organiques est attribuable à de nombreuses sources, on sait que le trafic routier et le chauffage individuel au bois, ainsi que l'agriculture sont les principales sources de poussières fines atmosphériques. La croissance graduelle des concentrations en PM des sites ruraux en banlieues, puis en villes, en zones urbaines très exposées au trafic est un fait établi. La concentration supérieure de PM en environnement urbain s'explique principalement par le trafic routier, en particulier par les gaz d'échappement, mais aussi l'usure des routes et des véhicules (entre autres de leurs freins et de leurs pneus) et par la poussière des rues.

Ces dernières décennies, la Suisse et un grand nombre de pays européens ont pris des mesures de réduction des émissions de poussières fines et de leurs précurseurs. Il s'en est suivi une réduction des concentrations en PM_{10} et $PM_{2.5}$ d'environ 40 % entre 1998 et 2019. Cette

réduction vaut pour tous les principaux composants des poussières fines à l'exception des poussières minérales. La réduction la plus frappante et la plus significative pour l'amélioration de la qualité de l'air est celle du carbone élémentaire, attribuable essentiellement à l'introduction des filtres à particules sur les moteurs diesel.

Si les concentrations en PM_{10} et $PM_{2.5}$ ont fortement baissé ces deux dernières décennies, la quote-part de leurs principaux composants n'a pas beaucoup changé. La figure ci-dessous illustre la modification relative de la composition des PM_{10} sur le site NABEL de Zürich-Kaserne lors des trois campagnes de mesure effectuées entre 1998 et 2019.

On peut toutefois observer dans notre pays quelques cas clairs de modification des teneurs relatives des poussières fines en divers composants. La quote-part du carbone élémentaire et des sulfates dans les deux classes PM_{10} et $PM_{2.5}$ a baissé sur les cinq sites. Inversement, la part relative des poussières fines organiques dans les PM_{10} et $PM_{2.5}$ a augmenté ces vingt dernières années. Il en va de même avec les poussières minérales. Bien que généralement d'origine naturelle, leur présence dans l'air en bordure de routes est liée aux tourbillons de poussière soulevées par le trafic et donc en relation avec les activités humaines.
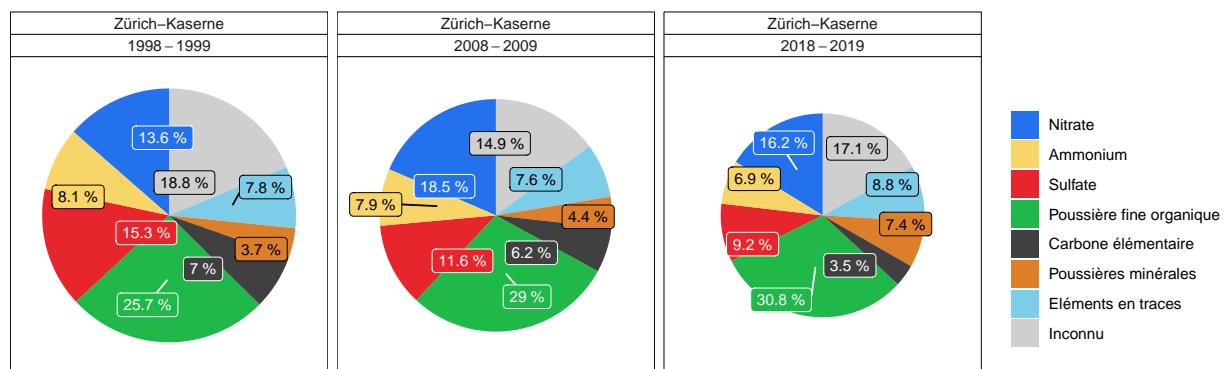
Composition chimique des PM_{10} sur le site urbain de Zürich-Kaserne lors des trois campagnes annuelles conduites entre 1998 et 2019. La surface des cercles est proportionnelle à la concentration en PM10 (1998–1999 : 24.1 $\mu g\,m^{-3}$, 2008–2009 : 20.2 $\mu g\,m^{-3}$, 2018–2019 : 15.6 $\mu g\,m^{-3}$).

L'évolution des concentrations en PM_{10} et $PM_{2.5}$ témoigne du succès des mesures prises en Suisse et en Europe pour lutter contre les poussières fines et leurs précurseurs. Il a été possible de nettement améliorer les émissions liées aux processus de combustion. L'effort doit cependant être poursuivi si l'on veut atteindre l'objectif fixé, soit un air pur et sain. Il existe d'autres possibilités de réduire les émissions du trafic routier, de l'ammoniac en provenance de l'agriculture et celles de substances organiques émises par diverses sources. La réduction des émissions du trafic routier passe par la prise en compte d'autres émissions que les seuls gaz d'échappement. C'est indispensable car c'est de là que proviennent certains métaux qui ne contribuent que marginalement à la masse totale des PM mais qu'on soupçonne de porter

gravement atteinte à la santé. Enfin, il reste une marge importante de réduction des poussières liées au chauffage au bois, en particulier dans les régions rurales.

Summary

Particulate matter (PM) is a key atmospheric pollutant which causes deleterious human health effects, perturbs the Earth's radiation balance, and reduces atmospheric visibility. PM is usually defined by size with the PM_{10} and $PM_{2.5}$ fractions being the most common in the domain of regulation, and these are defined as the mass concentration of PM with a diameter less than 10 and 2.5 micrometres (μm), respectively. PM_{10} and $PM_{2.5}$ are composed of a myriad of chemical constituents, either directly emitted into the atmosphere or formed in the atmosphere by chemical transformation of gaseous precursors. Routine measurement activities in air quality monitoring networks can capture total PM_{10} and $PM_{2.5}$ and the mass concentration of some main chemical constituents but not the very diverse nature of PM. Detailed knowledge of the chemical composition of PM can, however, be used for gaining a better understanding of the sources and processes contributing to atmospheric particulate matter.

Project goals. The primary objective of this study is to report a detailed chemical characterisation of PM_{10} and $PM_{2.5}$ in Switzerland. The results gained from an intensive sampling campaign involving five monitoring sites between June, 2018 and May, 2019 is the main focus. These data are then compared and put into context with two previous and similar sampling periods conducted in 1998–1999 and 2008–2009. The comparisons include changes in chemical composition over time and spatial patterns in different environments in Switzerland. In addition, source apportionment by using a widely used data analytical approach called positive matrix factorization (PMF) was used to identify the principal PM_{10} sources. This work, therefore, acts as an extension and an update to previous work (Hüglin et al. [1]).

Chemical composition of PM_{10} and $PM_{2.5}$ 2018–2019. Figure 1 and Figure 2 show the mean relative contribution of the main constituents of PM_{10} and $PM_{2.5}$ for the five sites of the 2018–2019 measurement period. The five selected sites represent typical air pollution situations. They include two urban settings: urban background (Zürich-Kaserne) and urban traffic (Bern-Bollwerk), at the kerbside of a major intra-urban road. The site Basel-Binningen is representative for a suburban environment, and two locations represent different rural surroundings: Magadino-Cadenazzo south of the Alps, and Payerne north of the Alps, on the Swiss plateau.

Particulate organic matter (OM) is the largest fraction of PM_{10} and $PM_{2.5}$ with a contribution of at least 30 %. A significant part of OM, although difficult to quantify, is so-called secondary OM (or secondary organic aerosol, SOA) that is formed in the atmosphere by chemical reaction of volatile organic compounds. In an earlier targeted study by the Paul Scherrer Institute on sources of OM in Switzerland, PM_{10} samples from all five sites considered in this study have

been analyzed using mass spectrometry (Daellenbach et al. [2]). It was found that between 43 % (Bern-Bollwerk) and 65 % (Payerne) of particulate organic matter was secondary OM. Further large contributors to total PM_{10} and $PM_{2.5}$ are sulfate, nitrate and ammonium. They are all formed in the atmosphere by chemical transformation of gaseous compounds (SO_2, NO_x and NH_3) and contribute to a fraction of PM that is called secondary inorganic aerosol. Consequently, a large and often dominating part of atmospheric PM is secondary particulate matter. The involved transformation processes occur on timescales of minutes to days resulting in secondary PM that is spatially homogeneous on the regional scale. Therefore, the concentrations of nitrate, sulfate and ammonium (as well as secondary OM) are very similar at the four sites north of the Alps.

Mineral dust, trace elements and elemental carbon are other important components of atmospheric PM. They are directly emitted into the air as particles (primary particulate matter) by various sources. With the applied analytical methods, a significant fraction of the PM mass could not be attributed. As detailed in the report, this unidentified mass results from underestimation of organic matter, mineral dust and trace elements as well as from particle bound water that has not been determined.
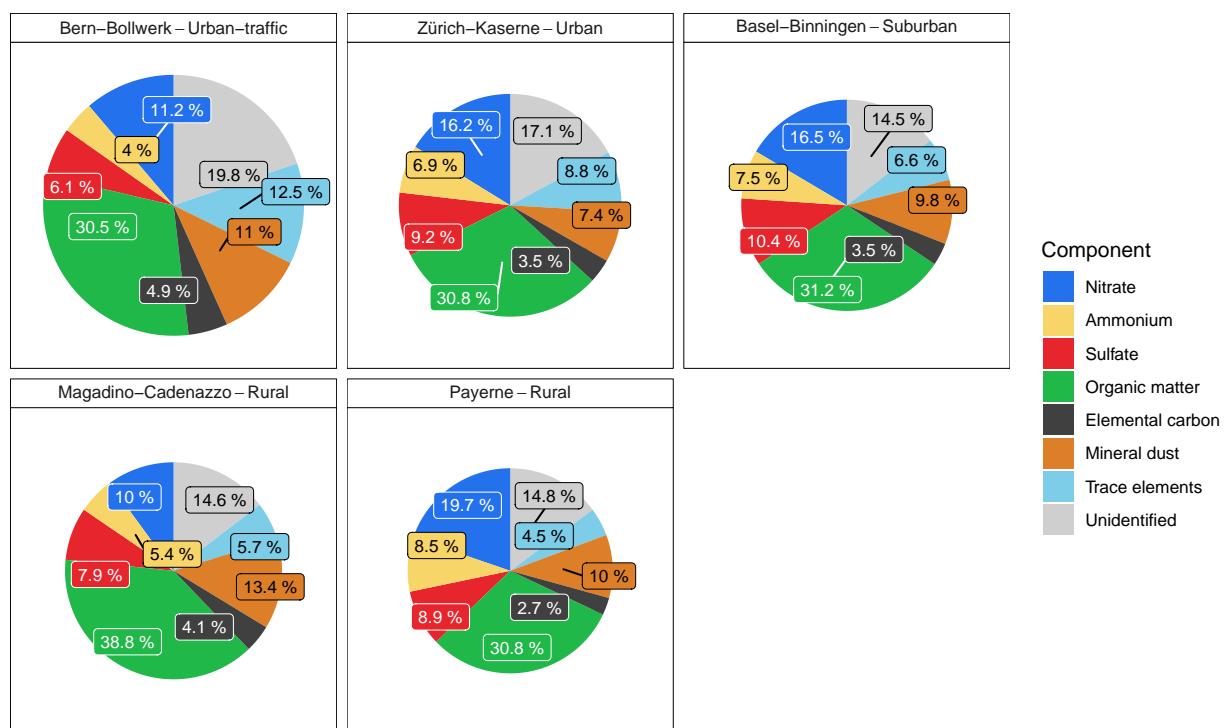
Figure 1 – Pie charts of the relative contribution of the main PM_{10} components for the five sites of the 2018–2019 measurement period. The area of the shown circles is proportional to the PM_{10} concentration at the different sites (Bern-Bollwerk: 21.3 μg m^{-3}, Zürich-Kaserne: 15.6 μg m^{-3}, Basel-Binningen: 14.0 μg m^{-3}, Magadino-Cadenazzo: 14.8 μg m^{-3}, Payerne: 13.2 μg m^{-3}).

Secondary particulate matter is predominantly associated with finer particle sizes, whereas mineral dust and many trace elements are mostly prevalent in larger particles. Accordingly, the contribution of secondary components in $PM_{2.5}$ is even larger than in PM_{10} as shown in Figure 2. In addition, there is a slightly increasing concentration gradient for PM_{10} and $PM_{2.5}$ from rural to urban and urban roadside environments. This gradient is driven by local emissions of primary PM_{10} and $PM_{2.5}$, in particular trace elements, mineral dust, elemental carbon and primary organic matter.
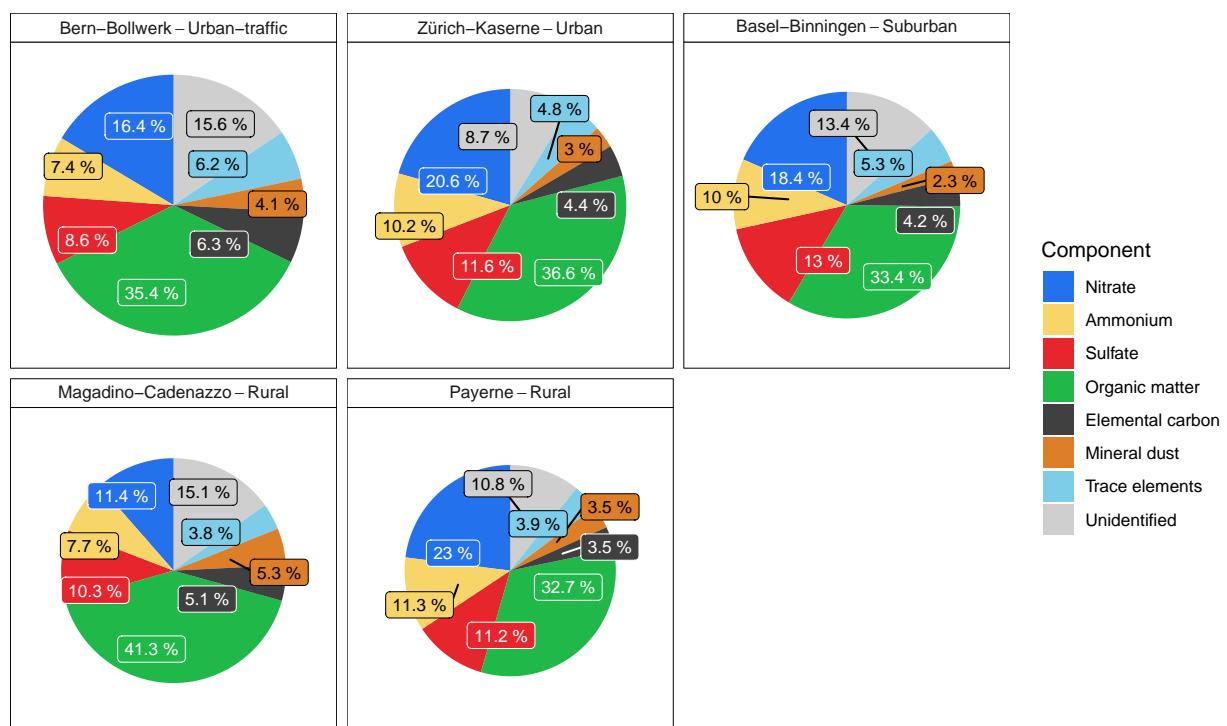

Figure 2 – Pie charts of the relative contribution of the main $PM_{2.5}$ components for the five sites of the 2018–2019 measurement period. The area of the shown circles is proportional to the $PM_{2.5}$ concentration at the different sites (Bern-Bollwerk: 14.0 $\mu g\,m^{-3}$, Zürich-Kaserne: 11.1 $\mu g\,m^{-3}$, Basel-Binningen: 10.6 $\mu g\,m^{-3}$, Magadino-Cadenazzo: 10.4 $\mu g\,m^{-3}$, Payerne: 9.2 $\mu g\,m^{-3}$).

Some chemical constituents, e.g. all metals except iron, do not contribute significantly to total mass of PM_{10} and $PM_{2.5}$. Despite their small contribution, some metals may, nevertheless, be highly important for health effects of particulate matter, as shown in recent studies.[3]. This work shows that the concentration of some metals (e.g. Ba, Cr, Cu, Fe, Sb, Sn, Mn, Co, Zn) show large concentration gradients from the urban roadside to urban and from urban to rural locations indicating that road traffic is an important source of these metals.

Changes in composition of PM_{10} and $PM_{2.5}$ since 1998. In Switzerland, PM_{10} and $PM_{2.5}$ mass concentrations are declining. The achieved reductions in PM_{10} and $PM_{2.5}$ are well documented in the annual reports of the Swiss national air pollution monitoring network NABEL
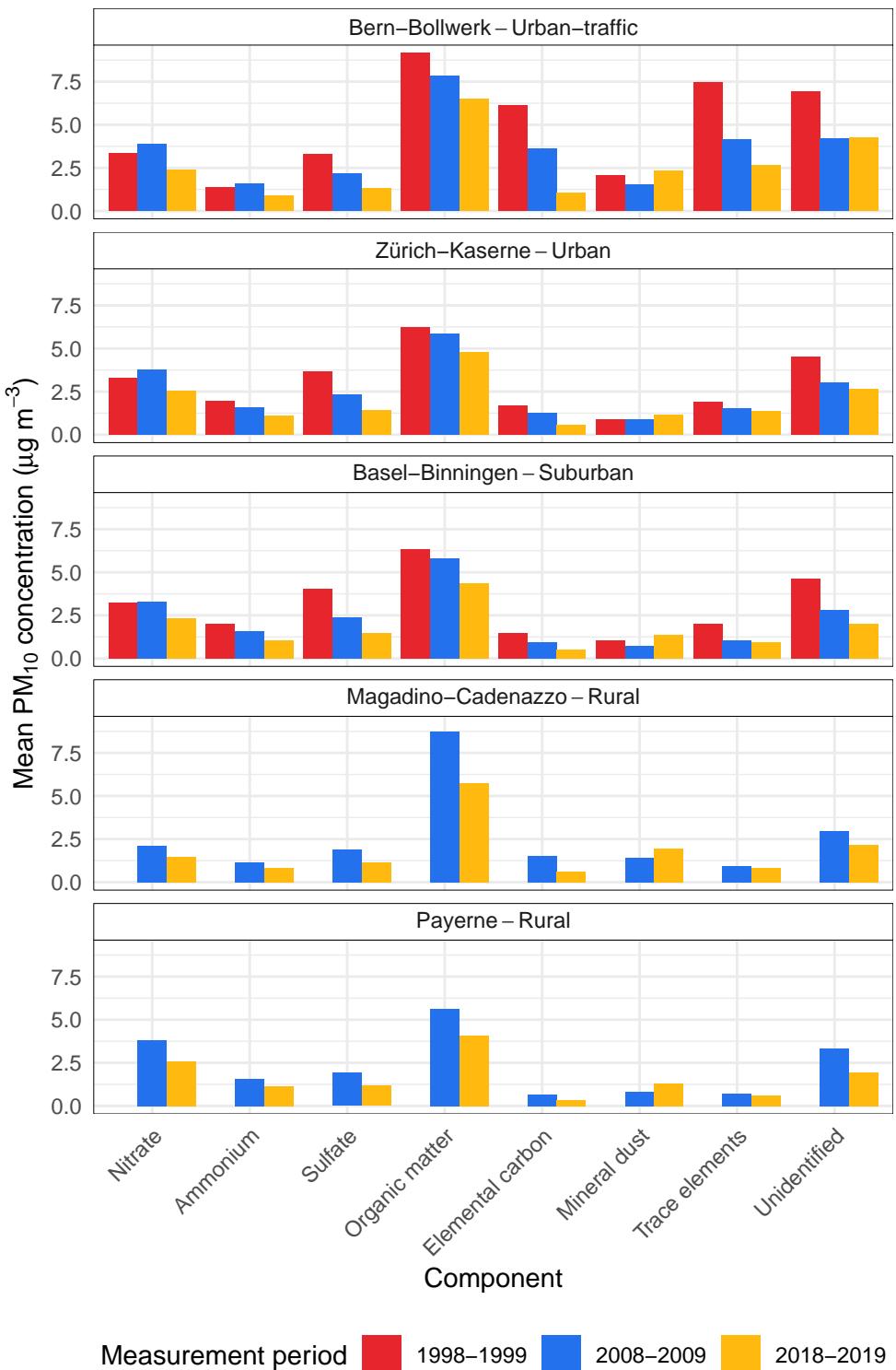
Figure 3 – Trend of mean concentrations of major components in PM_{10} for the three measurement periods between 1998 and 2019.

(Bundesamt für Umwelt [4]) and can be attributed to the implementation of air quality policies, within Switzerland itself and across large parts of Europe. Along with reductions in total mass, concentrations of all main components of PM_{10} except mineral dust have also decreased over time (Figure 3). Particularly remarkable is the change in elemental carbon (EC), a proxy for soot particles and predominantly emitted by diesel engines and residential wood burning. Since 1998, the concentration of EC decreased by 84 % at the urban traffic site Bern-Bollwerk, 71 % at the urban site Zürich-Kaserne, and 64 % at the suburban site Basel-Binningen. This marked decline in elemental carbon represents a significant improvement in air quality in Switzerland, which is mainly due to the introduction of particulate filters in diesel engines.
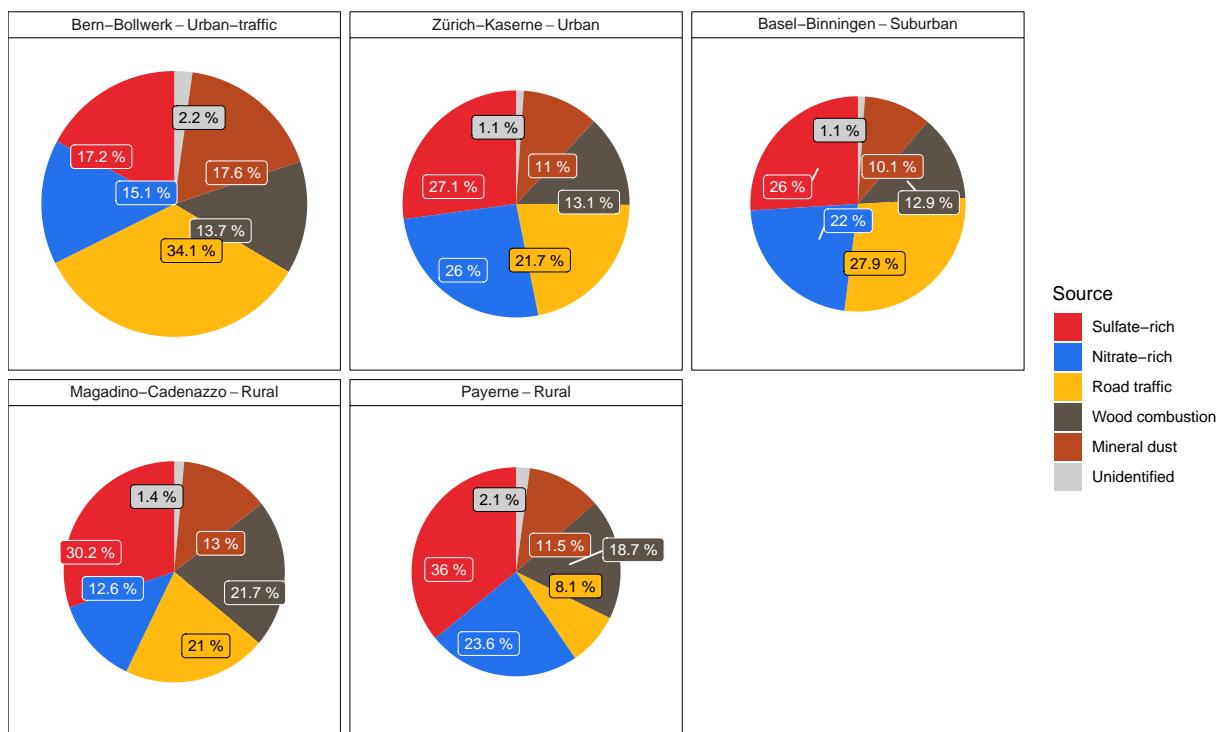
Figure 4 – Mean contribution of identified sources and components of PM_{10} for the measurement period 2018–2019. The area of the shown circles is proportional to the PM_{10} concentration at the different sites (Bern-Bollwerk: 21.3 µg m^{-3}, Zürich-Kaserne: 15.6 µg m^{-3}, Basel-Binningen: 14.0 µg m^{-3}, Magadino-Cadenazzo: 14.8 µg m^{-3}, Payerne: 13.2 µg m^{-3}).

Main sources of atmospheric particulate matter. A widely used receptor-oriented statistical model approach called Positive Matrix Factorization (PMF) was applied for relating emissions from main sources to the observed concentrations of PM_{10} (source apportionment). PMF identifies sources and determines their contributions to PM based on the temporal correlations of the concentrations of chemical constituents that are characteristic for specific source emissions. For chemical characterization of daily samples of PM_{10}, as performed in this study, PMF modeling can result in incomplete separation of identified source contributions because

temporal correlations might be due to confounding factors such as a similar annual cycle of source activities. This may have an impact on the calculated source contribution and increase the corresponding uncertainties. Nevertheless, PMF models applied to multiple sites provide a reliable estimate of the contribution of the main sources to the total mass concentration of PM. Another trait of receptor-oriented models like PMF is that source apportionment of secondary PM is difficult to achieve, because the information about the sources of the precursor gases gets largely lost upon secondary particle formation. The approach applied here allows the identification of different types of secondary PM_{10} and the most important sources of primary PM_{10}. The identified types of secondary PM_{10} are, for practical reasons, treated and labelled here as source emissions. For example, sulfate- and nitrate-rich secondary components were identified by PMF as important PM_{10} components across Switzerland. They were labelled as sulfate-rich and nitrate-rich sources (Figure 4). The sulfate-rich source was the greatest contributor to PM_{10} mass; this component contained beside sulfate a large amount of OM, likely secondary organic matter. The main sources of primary PM_{10} are road traffic, wood combustion and mineral dust. The yearly average contribution of mineral dust was between 1.4 $\mu g\,m^{-3}$ and 1.9 $\mu g\,m^{-3}$ except at the urban roadside site Bern-Bollwerk where the mean mineral dust contribution was 3.8 $\mu g\,m^{-3}$. The increment in mineral dust concentration in Bern-Bollwerk compared to the urban background site Zürich-Kaserne can be interpreted as resuspended road dust and add as non-exhaust emissions (Air Quality Expert Group [5]) to the total contribution from road traffic. Hence, the average total road traffic contribution in Bern-Bollwerk amounts to 9.4 $\mu g\,m^{-3}$ (34.1 %) and is, therefore, substantially higher than at the other sites where road traffic contributions ranged between 1.1 $\mu g\,m^{-3}$ (8.1 %) in Payerne and 3.9 $\mu g\,m^{-3}$ (27.9 %) in Basel-Binningen. The calculated concentration of the PMF-identified wood combustion source was between 1.8 $\mu g\,m^{-3}$ (12.9 %) in Basel-Binningen and 3.2 $\mu g\,m^{-3}$ (21.7 %) in Magadino-Cadenazzo. It is important to note that road traffic and wood combustion are additionally contributing to the formation of secondary PM_{10}.

We also evaluated PMF for the source apportionment of $PM_{2.5}$. However, the concentrations of some compounds that are characteristic for specific emission sources (e.g. metals) in $PM_{2.5}$ were often in the range or even below detection limits and it was not possible to obtain reliable results.

Contribution of tyre wear to PM_{10} and $PM_{2.5}$. An important result largely attributed to a parallel partner project relates to the contribution of tyre wear to PM_{10} and $PM_{2.5}$. Quantitative analysis of tyre wear particles by single particle analysis using SEM/EDX (see Rausch et al. [6] for details) resulted in an annual average contribution of tyre wear to total PM_{10} of 1.13 $\mu g\,m^{-3}$

(5.3%) at the urban traffic site Bern-Bollwerk and 0.16 $\mu g\, m^{-3}$ (1.0%) at the urban background site Zürich-Kaserne. Except at locations in the immediate vicinity of road traffic, tyre wear is only a small contributor to airborne fine particulate matter. Nevertheless, atmospheric deposition is assumed to be a relevant process for the input of tyre wear into soils and surface waters even in areas away from road traffic.

Zusammenfassung

Feinstaub (PM) ist ein wichtiger atmosphärischer Schadstoff mit negativen Auswirkungen auf die menschliche Gesundheit. Zudem schädigt Feinstaub Ökosysteme und beeinflusst den Strahlungshaushalt der Erde sowie die Sichtweite in der Atmosphäre. Die Definition von PM erfolgt vorwiegend anhand der Partikelgrösse, wobei die Fraktionen PM_{10} und $PM_{2.5}$ häufig durch Immissionsgrenzwerte reguliert werden. Diese sind definiert als die Massenkonzentration von luftgetragenen Partikeln mit Durchmesser von weniger als 10 bzw. 2.5 Mikrometern (μm). Chemisch sind PM_{10} und $PM_{2.5}$ aus einer Vielzahl von Inhaltsstoffen zusammengesetzt. Diese werden entweder direkt als Partikel in die Atmosphäre freigesetzt oder erst in der Atmosphäre durch chemische Umwandlung von gasförmigen Vorläufern gebildet. Bei den routinemässigen Messungen in Luftqualitätsmessnetzen können nur die gesamte Konzentration von PM_{10} und $PM_{2.5}$ sowie die Massenkonzentrationen einiger spezifischer Bestandteile erfasst werden, nicht jedoch die sehr vielfältige chemische Zusammensetzung von Feinstaub. Detaillierte Kenntnisse über die chemische Zusammensetzung von PM sind jedoch von grossem Nutzen, um ein besseres Verständnis der Emissionsquellen und der atmosphärischen Bildungsprozesse von Feinstaub zu erhalten.

Projektziele. Das Hauptziel dieser Studie ist eine detaillierte chemische Charakterisierung von PM_{10} und $PM_{2.5}$ in der Schweiz. Die Ergebnisse einer intensiven Messkampagne an fünf Messstationen des Nationalen Beobachtungsnetzes für Luftfremdstoffe (NABEL) zwischen Juni 2018 und Mai 2019 stehen im Vordergrund. Die fünf ausgewählten Messstationen repräsentieren unterschiedliche und typische Belastungssituationen: Ein städtischer Verkehrsstandort (Bern-Bollwerk), ein städtischer Hintergrundstandort (Zürich-Kaserne) sowie ein vorstädtischer Standort (Basel-Binningen). Ländliche Gegenden in der Schweiz sind durch zwei Standorte vertreten, einer im schweizerischen Mittelland nördlich der Alpen (Payerne), der zweite ausgewählte ländliche Standort befindet sich südlich der Alpen (Magadino-Cadenazzo). Die erhobenen Messwerte dieser Studie werden mit Daten aus zwei früheren und ähnlichen Messperioden aus den Jahren 1998–1999 und 2008–2009 verglichen. Die Vergleiche beinhalten die Beschreibung der zeitlichen Veränderungen sowie die standortabhängigen Unterschiede der chemischen Zusammensetzung. Darüber hinaus wurde eine etablierte datenanalytische Me-thode (positive matrix factorization PMF) verwendet, um die wichtigsten Emissionsquellen von PM_{10} zu identifizieren und deren Beiträge zur gesamten PM10-Belastung zu bestimmen. Diese Arbeit stellt somit eine Erweiterung und eine Aktualisierung früherer Arbeiten (Hüglin u. a. [1]) dar.

Chemische Zusammensetzung von PM_{10} und $PM_{2.5}$ 2018–2019. Die Abbildungen 1 und 2 zeigen die mittlere chemische Zusammensetzung von PM_{10} und $PM_{2.5}$ an den fünf Standorten der Messperiode 2018–2019. Organische Komponenten des Feinstaubs (organic matter OM) machen mit mindestens 30 % den größten Anteil von PM_{10} und $PM_{2.5}$ aus. Ein großer Teil von OM ist sekundärer organischer Feinstaub (oder sekundäres organisches Aerosol SOA), der in der Atmosphäre durch chemische Reaktion von flüchtigen organischen Verbindungen gebildet wird. Der Anteil von SOA am gesamten organischen Feinstaub ist schwer zu quantifizieren. In einer früheren Studie des Paul Scherrer Instituts wurden gezielt die Quellen und Bildungsprozesse von OM in der Schweiz untersucht. Dabei wurden PM_{10}-Proben von allen fünf in dieser Studie betrachteten Standorten mittels Massenspektrometrie analysiert (Daellenbach u. a. [2]) und festgestellt, dass sekundäre organische Aerosole zwischen 43 % (Bern-Bollwerk) und 65 % (Payerne) des gesamten organischen Feinstaubs im PM_{10} ausmachen. Neben den organischen Komponenten sind Sulfat, Nitrat und Ammonium wichtige Bestandteile von PM_{10} und $PM_{2.5}$. Diese sind ebenfalls sekundäre Komponenten, die in der Atmosphäre durch chemische Umwandlung von gasförmigem SO_2, NO_x und NH_3 entstehen und als sekundäres anorganisches Aerosol bezeichnet werden. Ein großer und häufig dominanter Teil von PM_{10} und $PM_{2.5}$ ist daher sekundärer Feinstaub. Die Bildung dieses sekundären Feinstaubs aus den gasförmigen Vorläufern erfolgt auf Zeitskalen von Minuten bis Tagen, was dazu führt, dass sekundärer Feinstaub regional räumlich homogen ist. Daher sind die Konzentrationen von Nitrat, Sulfat und Ammonium (sowie von sekundärem OM) an den vier Standorten nördlich der Alpen sehr ähnlich.

Mineralstaub, Spurenelemente und elementarer Kohlenstoff sind weitere wichtige Komponenten des Feinstaubs, welche von verschiedenen Quellen direkt als Partikel (primärer Feinstaub) in die Atmosphäre freigesetzt werden. Mit den eingesetzten Analysemethoden konnte ein Teil der Feinstaubmasse nicht zugeordnet werden. Diese nicht identifizierte (oder unbekannte) Feinstaubmasse lässt sich jedoch, wie im Bericht ausführlich dargestellt, auf systematisch leicht zu tief abgeschätzten Konzentrationen von organischem Feinstaub, Mineralstaub und Spurenelementen zurückführen, sowie auf partikelgebundenes Wasser, welches nicht bestimmt wurde.

Sekundäre Partikel sind überwiegend mit der feineren Partikelfraktion verbunden, während Mineralstaub und viele Spurenelemente meist in grösseren Partikeln vorherrschen. Entsprechend ist der relative Anteil von sekundärem Feinstaub in $PM_{2.5}$ grösser als in PM_{10}, wie aus einem Vergleich der beiden Abbildungen 1 und 2 entnommen werden kann. Für PM_{10} und $PM_{2.5}$ lassen sich eher kleine, ansteigende Konzentrationsgradienten von ländlichen zu städtischen
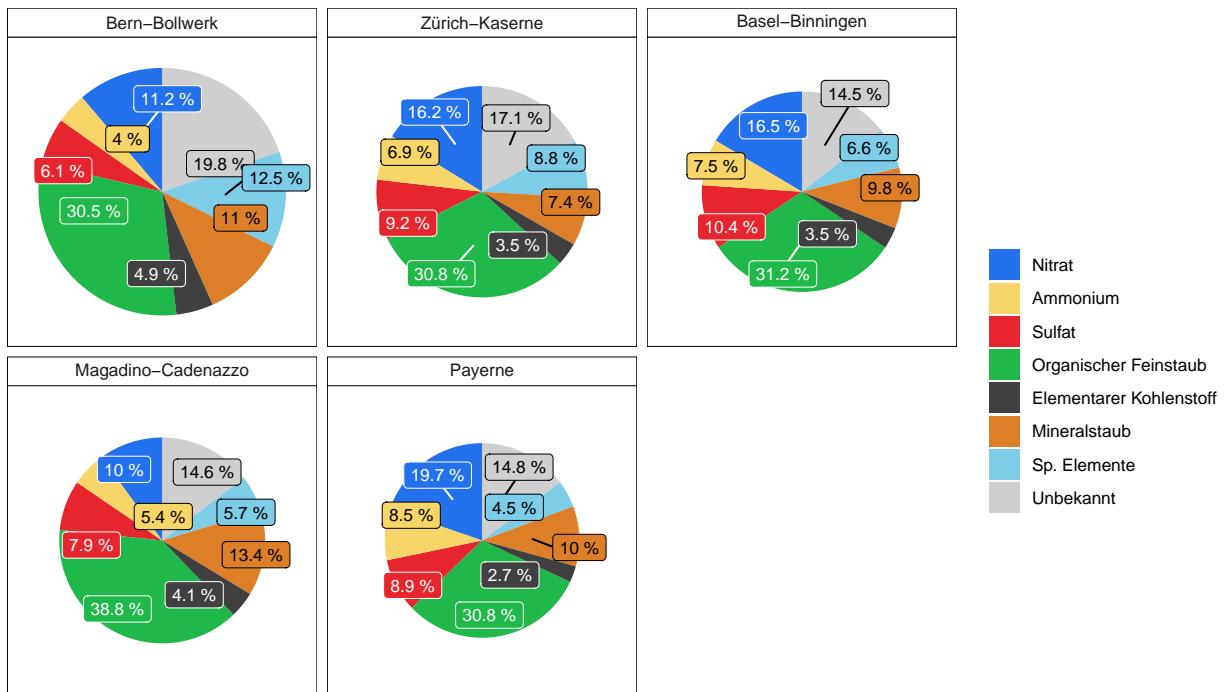
Abbildung 1: Mittlere chemische Zusammensetzung von PM_{10} an den fünf Messstationen der Messkampagne von 2018–2019. Die Fläche der Kreise ist proportional zur gesamten Konzentration von PM_{10} an den unterschiedlichen Standorten (Bern-Bollwerk: 21.3 $\mu g\,m^{-3}$, Zürich-Kaserne: 15.6 $\mu g\,m^{-3}$, Basel-Binningen: 14.0 $\mu g\,m^{-3}$, Magadino-Cadenazzo: 14.8 $\mu g\,m^{-3}$, Payerne: 13.2 $\mu g\,m^{-3}$).

und städtisch verkehrsbelasteten Standorten feststellen. Diese Gradienten werden durch lokale Emissionen von primärem PM_{10} und $PM_{2.5}$ verursacht, insbesondere von Spurenelementen, Mineralstaub, elementarem Kohlenstoff und primärem organischem Feinstaub.

Einige chemische Bestandteile, z.B. alle Metalle ausser Eisen, tragen nur unwesentlich zur Gesamtmasse von PM_{10} und $PM_{2.5}$ bei. Dennoch deuten neuere Studien darauf hin, dass einige Metalle für die gesundheitlichen Auswirkungen von Feinstaub sehr wichtig sein könnten.[3]. Die Konzentrationen einiger Metalle (z.B. Ba, Cr, Cu, Fe, Sb, Sn, Mn, Co, Zn) zeigen deutlich ansteigende Konzentrationen von ländlichen zu städtischen Standorten, mit den höchsten Konzentrationen am städtischen und verkehrsbelasteten Standort Bern-Bollwerk. Dies deutet darauf hin, dass der Strassenverkehr eine wichtige Quelle für diese Metalle ist.

Veränderungen in der Zusammensetzung von PM_{10} und $PM_{2.5}$ seit 1998. In der Schweiz sind die Massenkonzentrationen von PM_{10} und $PM_{2.5}$ rückläufig. Die erreichten Reduktionen sind in den Jahresberichten des Schweizerischen Nationalen Beobachtungsnetzes für Luftfremdstoffe NABEL (Bundesamt für Umwelt [4]) gut dokumentiert und können auf die ergriffenen Massnahmen zur Reduktion von PM_{10} und $PM_{2.5}$ sowie deren Vorläufergasen zurückgeführt werden, welche sowohl in der Schweiz als auch in weiten Teilen Europas umgesetzt wurden. Wie die gesamten Massenkonzentrationen haben auch die Konzentrationen aller Hauptbestandteile
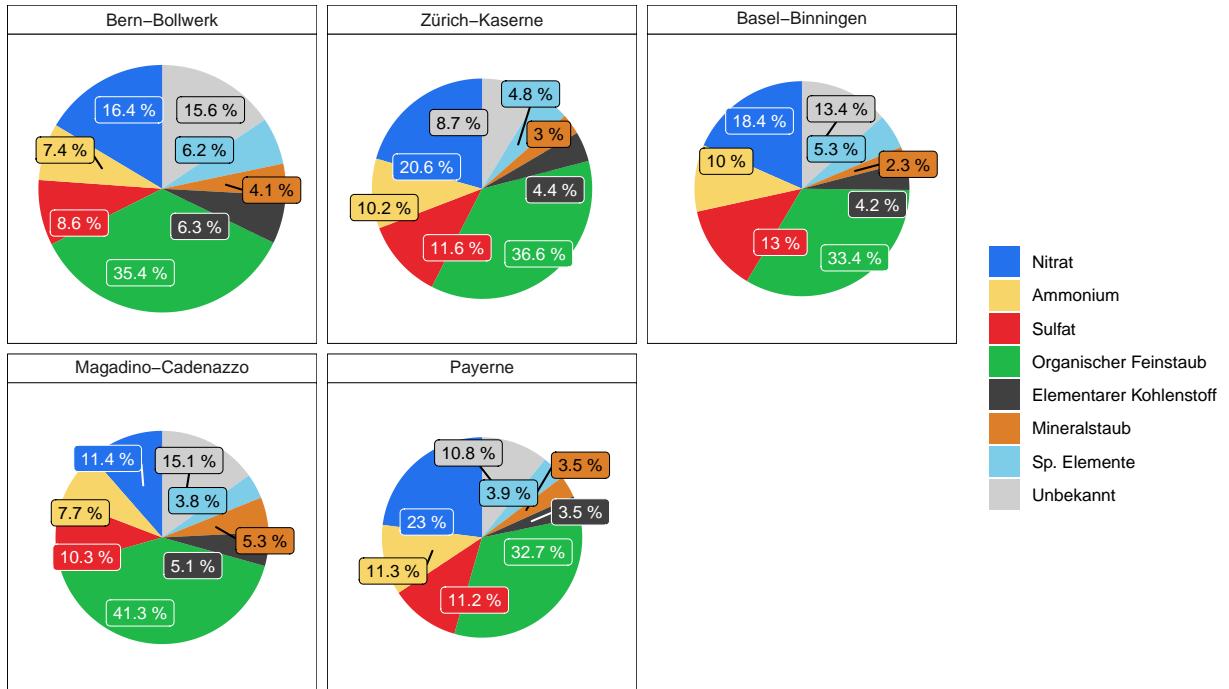
Abbildung 2: Mittlere chemische Zusammensetzung von PM$_{2.5}$ an den fünf Messstationen der Messkampagne von 2018–2019. Die Fläche der Kreise ist proportional zur gesamten Konzentration von PM$_{2.5}$ an den unterschiedlichen Standorten. (Bern-Bollwerk: 14.0 µg m^{-3}, Zürich-Kaserne: 11.1 µg m^{-3}, Basel-Binningen: 10.6 µg m^{-3}, Magadino-Cadenazzo: 10.4 µg m^{-3}, Payerne: 9.2 µg m^{-3}).

mit Ausnahme von Mineralstaub abgenommen (Abbildung 3). Besonders bemerkenswert ist die Veränderung von elementarem Kohlenstoff (EC), einer Messgrösse welche die Russpartikel repräsentiert und vorwiegend von Dieselmotoren und der Holzverbrennung in Haushalten emittiert wird. Seit 1998 nahm die Konzentration von EC am städtischen Verkehrsstandort Bern-Bollwerk um 84 %, am städtischen Standort Zürich-Kaserne um 71 % und am vorstädtischen Standort Basel-Binningen um 64 % ab. Dieser deutliche Rückgang der Konzentration von elementarem Kohlenstoff stellt eine grosse Verbesserung der Luftqualität in der Schweiz dar, welche vor allem durch die Einführung von Partikelfiltern bei Dieselmotoren zurückgeführt werden kann.

Hauptquellen von atmosphärischem Feinstaub. Die gemessenen Konzentrationen der chemischen Inhaltsstoffe in den Feinstaubproben können genutzt werden, um mittels statistischen Modellen (Rezeptormodelle wie Positive Matrix Factorization PMF) die Hauptquellen von Feinstaub zu identifizieren und deren Beiträge zu bestimmen (Quellenzuordnung). In dieser Studie wurde PMF für die Quellenzuordnung von PM$_{10}$ verwendet. Für das Verständnis dieser statistischen Modelle ist es hilfreich, den beobachteten Feinstaub als eine Überlagerung (Mischung) von Beiträgen durch verschiedene Emissionsquellen aufzufassen. Rezeptormodelle wie PMF versuchen eine Entmischung dieser Quellenbeiträge auf der Grundlage der zeitlichen Korrela-
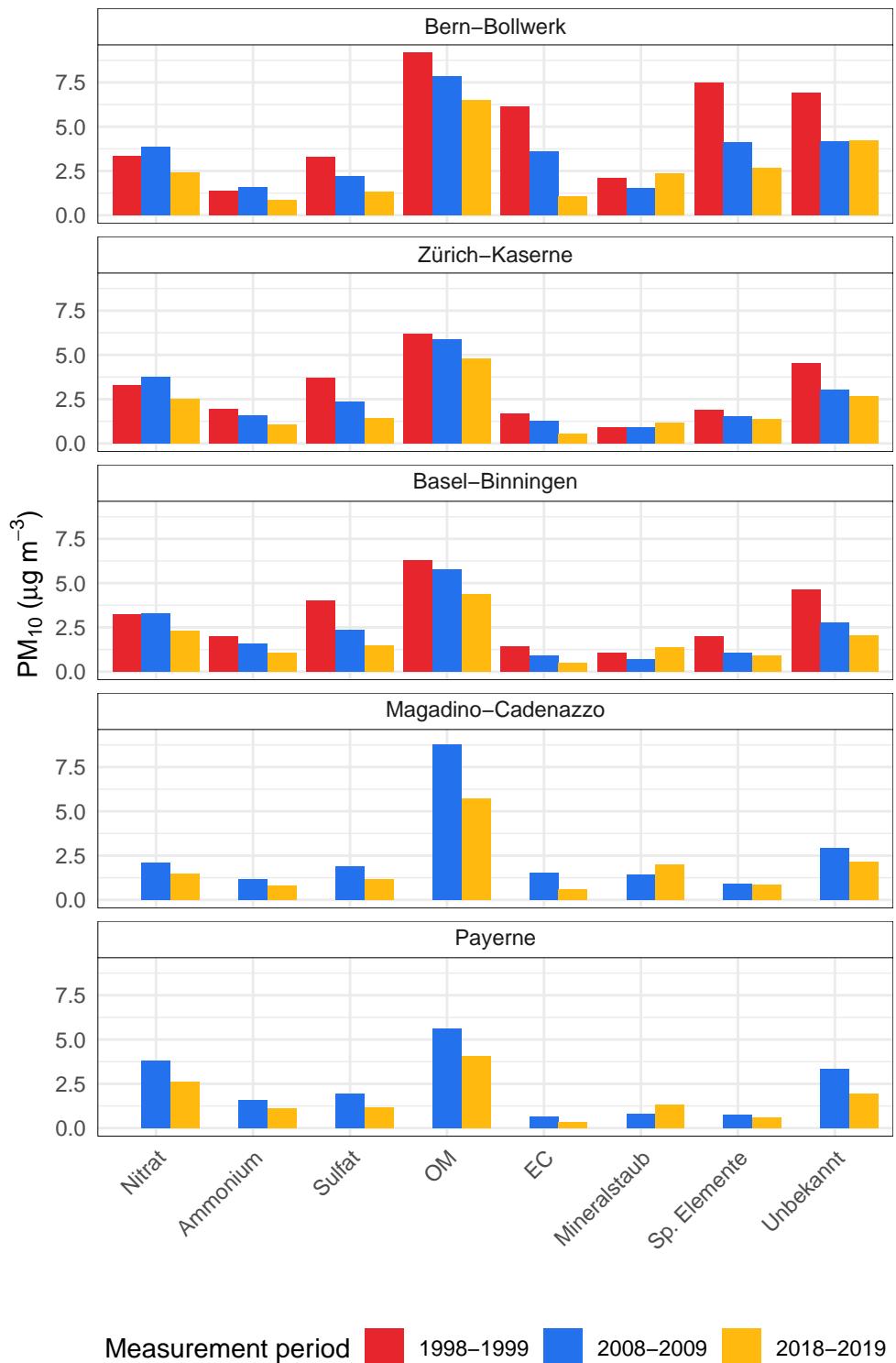
Abbildung 3: Mittlere Konzentration von Hauptbestandteilen in PM_{10} für die jährlichen Messperioden zwischen 1998 und 2019.

tionen der gemessenen Konzentrationen von chemischen Inhaltsstoffen, welche für Emissionen aus den verschiedenen Quellen charakteristisch sind. Werden Rezeptormodelle wie in dieser Studie auf die gemessenen Konzentrationen von Inhaltsstoffen in täglichen Proben von PM_{10} angewendet, dann kann die PMF-Modellierung jedoch zu einer unvollständigen Entmischung der Emissionsquellen führen, wenn zeitliche Korrelationen auch durch Faktoren wie einen ähnlichen Jahreszyklus der Aktivitäten von Emissionsquellen verursacht werden. Dies kann Auswirkungen auf die berechneten Quellenbeiträge haben, bzw. berechnete Quellenbeiträge können dann systematisch zu hoch oder zu tief sein. Dennoch bieten PMF-Modelle einen wertvollen Überblick über den Einfluss der Hauptquellen auf die Gesamtmassenkonzentration von Feinstaub, insbesondere, wenn Daten von mehreren Standorten unabhängig voneinander analysiert und die Resultate miteinander verglichen werden.
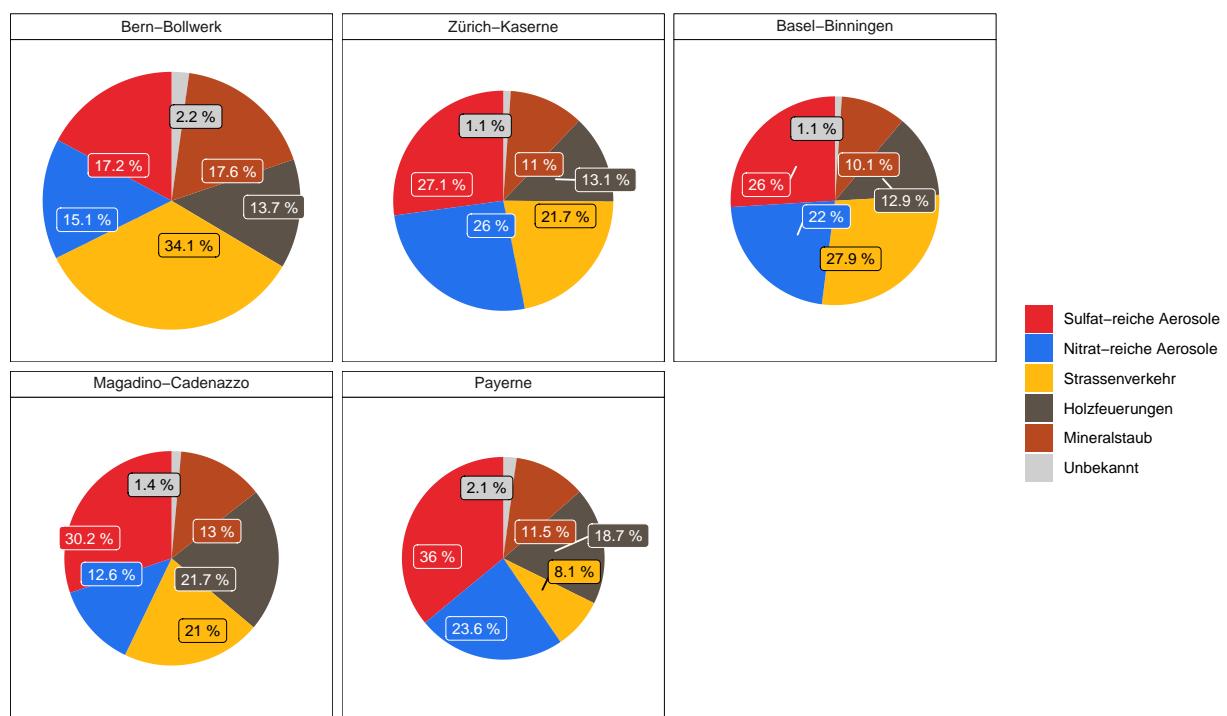
Abbildung 4: Mittlere Beiträge der mit einem statistischen Modell bestimmten Quellen von PM_{10} an den fünf Messstationen der Messkampagne von 2018–2019. Die Fläche der Kreise ist proportional zur gesamten Konzentration von PM_{10} an den unterschiedlichen Standorten (Bern-Bollwerk: 21.3 $\mu g\,m^{-3}$, Zürich-Kaserne: 15.6 $\mu g\,m^{-3}$, Basel-Binningen: 14.0 $\mu g\,m^{-3}$, Magadino-Cadenazzo: 14.8 $\mu g\,m^{-3}$, Payerne: 13.2 $\mu g\,m^{-3}$).

Ein weiteres wichtiges Merkmal von Rezeptormodellen wie PMF ist, dass eine Quellenzuordnung von sekundärem Feinstaub nur schwer möglich ist, da die Information über die Herkunft der emittierten Vorläufergase bei der Bildung von Sekundärpartikeln weitgehend verloren geht. Mit dem hier angewandten Ansatz werden verschiedene Arten von sekundärem PM_{10} neben den wichtigsten Emissionsquellen von primären PM_{10} identifiziert. Die identifizierten Arten

von sekundärem PM_{10} werden daher aus praktischen Gründen ebenfalls als Emissionsquellen behandelt und bezeichnet. Sulfat- und Nitrat-reiche sekundäre Aerosole wurden mit PMF als wichtige Komponenten von PM_{10} in der Schweiz erkannt und entsprechend gekennzeichnet (Abbildung 4). Die Sulfat-reichen Aerosole liefern den grössten Beitrag zur PM_{10} Massenkonzentration, diese Komponente enthielt neben Sulfat eine grosse Menge an organischem Feinstaub, wahrscheinlich sekundäre organische Aerosole. Die identifizierten Hauptquellen von primärem PM_{10} sind Strassenverkehr, Holzverbrennung und Mineralstaub. Der ermittelte jährliche Beitrag von Mineralstaub beträgt zwischen 1.4 $\mu g\,m^{-3}$ und 1.9 $\mu g\,m^{-3}$, ausser am städtischen verkehrsbelasteten Standort Bern-Bollwerk, an dem der Beitrag durch Mineralstaub mit 3.8 $\mu g\,m^{-3}$ deutlich höher ist. Die höhere Konzentration von Mineralstaub am verkehrsbelasteten Standort Bern-Bollwerk im Vergleich zum städtischen Standort Zürich-Kaserne kann als resuspendierter Strassenstaub interpretiert werden und kann als Teil der Nicht-Auspuffemissionen (Air Quality Expert Group [5]) zum Gesamtbeitrag des Strassenverkehrs hinzugezählt werden. Der Gesamtbeitrag des Strassenverkehrs am jährlichen PM_{10} beträgt in Bern-Bollwerk 9.4 $\mu g\,m^{-3}$ (34.1 %) und ist damit deutlich höher als an den anderen Standorten, wo die Strassenverkehrsbeiträge zwischen 1.1 $\mu g\,m^{-3}$ (8.1 %) in Payerne und 3.9 $\mu g\,m^{-3}$ (27.9 %) in Basel-Binningen betragen. Die berechneten Beiträge von Holzfeuerungen am PM_{10} liegen zwischen 1.8 $\mu g\,m^{-3}$ (12.9 %) in Basel-Binningen und 3.2 $\mu g\,m^{-3}$ (21.7 %) in Magadino-Cadenazzo. Es ist wichtig zu beachten, dass sowohl der Strassenverkehr als auch Holzfeuerungen zusätzlich zur Bildung von sekundärem PM_{10} beitragen.

Eine Quellenzuordnung für $PM_{2.5}$ wurde ebenfalls mittels PMF versucht. Da die Konzentrationen einiger quellenspezifischer Inhaltsstoffe (insbesondere Metalle) in $PM_{2.5}$ tief und häufig im Bereich oder unterhalb der analytischen Nachweisgrenze sind, lieferte die Quellenzuordnung mit PMF für $PM_{2.5}$ keine robusten und zuverlässigen Resultate.

Beitrag des Reifenabriebs zu PM_{10} und $PM_{2.5}$. Ein wichtiges Ergebnis, das vor allem einem parallelen Partnerprojekt zuzuschreiben ist, betrifft den Beitrag des Reifenabriebs zu PM_{10} und $PM_{2.5}$. Eine quantitative Einzelpartikelanalyse mittels SEM/EDX (siehe Rausch u. a. [6] für Details) ergab einen jährlichen durchschnittlichen Beitrag von Reifenabrieb zum gesamten PM_{10} von 1.13 $\mu g\,m^{-3}$ (5.3%) am städtischen verkehrsbelasteten Standort Bern-Bollwerk und 0.16 $\mu g\,m^{-3}$ (1.0%) am städtischen Standort Zürich-Kaserne. Ausser an Standorten in unmittelbarer Nähe des Strassenverkehrs trägt der Reifenabrieb nur gering zu PM_{10} und $PM_{2.5}$ bei. Anhand der gemessenen Konzentration von luftgetragenen Reifenabriebspartikel im Grössenbereich zwischen 10 und 80 Mikrometer am Standort Zürich-Kaserne kann jedoch erwartet werden, dass die atmosphärische Deposition ein relevanter Prozess für den Eintrag von Rei-

fenabrieb in Böden und Oberflächengewässer auch in Gebieten abseits des Strassenverkehrs ist.

Résumé

Les poussières fines (PM) constituent un polluant atmosphérique important aux effets nuisibles sur la santé humaine. Ces poussières nuisent également aux écosystèmes, modifient le bilan radiatif terrestre et réduisent la visibilité. Les PM sont principalement définies par leur taille. Celles qu'on évoque le plus fréquemment, les PM_{10} et $PM_{2.5}$, font l'objet de valeurs limites d'immission. Ces valeurs sont définies comme la concentration massique des poussières d'un diamètre aérodynamique inférieur à 10 respectivement 2.5 micromètres. Les PM_{10} et $PM_{2.5}$ contiennent un grand nombre de substances chimiques, libérées directement dans l'atmosphère, ou alors s'y sont formées par réactions entre précurseurs gazeux. Les réseaux d'observation des polluants atmosphériques peuvent en général mesurer la concentration totale en PM_{10} et $PM_{2.5}$ ainsi que leur teneur en certains composants spécifiques, mais sans pouvoir rendre compte de toute la variété de leurs composants. Il serait pourtant précieux de s'en faire une idée exacte pour en déterminer la source et les processus de formation dans l'atmosphère.

Objectifs du projet. Le principal objectif de cette étude est de préciser la nature chimique des PM_{10} et $PM_{2.5}$ en Suisse. Il s'agit en premier lieu d'exploiter les résultats de l'importante campagne de mesure conduite par cinq stations du réseau national d'observation des polluants atmosphériques (NABEL) entre juin 2018 et mai 2019. Les stations choisies sont représentatives de situations typiques bien distinctes : un site urbain exposé au trafic (Bern-Bollwerk), un site urbain éloigné de la chaussée (Zürich-Kaserne) et un site suburbain (Basel-Binningen) ; l'espace rural est représenté par deux sites, l'un au nord des Alpes (Payerne, sur le Plateau), le second au sud des Alpes (Magadino-Cadenazzo). Le résultat de ces mesures est comparé à celui de deux autres campagnes menées en 1998–1999 et 2008–2009, ce qui permet de préciser l'évolution locale et temporelle de la composition chimique des polluants atmosphériques. On recourt ensuite à une méthode éprouvée d'analyse des données, la factorisation matricielle positive (positive matrix factorization PMF), pour identifier les principales sources d'émission de PM10 et leur quote-part dans la pollution. Ce travail prolonge et actualise des travaux antérieurs.[1]

Composition chimique des PM_{10} et $PM_{2.5}$ en 2018–2019. Les figures 1 et 2 présentent la composition chimique moyenne des PM_{10} et $PM_{2.5}$ des cinq sites mentionnés durant l'année 2018–2019. Les poussières sont composées d'au moins 30 % d'éléments organiques (organic matter OM). Une grande part de l'OM est de la poussière organique secondaire (ou aérosol organique secondaire, AOS) formée dans l'atmosphère par réaction chimique entre liaisons organiques volatiles. La part totale des AOS dans les poussières fines est difficile à quantifier. Une étude antérieure a été consacrée aux sources et aux processus de formation d'OM en Suisse. On y a analysé des échantillons de PM_{10} des cinq sites par spectroscopie de masse[2] et constaté

que les aérosols organiques secondaires représentaient entre 43 % (Bern-Bollwerk) et 65 % (Payerne) de la matière organique des PM_{10}. Outre les composés organiques, les PM_{10} et $PM_{2.5}$ contiennent une proportion importante de sulfates, de nitrates et d'ammonium. Il s'agit là également de composés secondaires nés de la transformation dans l'atmosphère de SO_2, NO_x et NH_3 gazeux, dits aérosols anorganiques secondaires. Une part importante et souvent dominante de PM_{10} et $PM_{2.5}$ consiste ainsi en poussières fines secondaires. La formation de ces poussières fines secondaires à partir de leurs précurseurs gazeux s'opère à une échelle de temps allant de la minute à quelques jours, ce qui explique l'homogénéité des poussières fines secondaires au niveau régional. C'est pourquoi les concentrations en nitrates, sulfates et ammonium (ainsi que des OM secondaires) sont similaires sur les quatre sites du nord des Alpes.

Autres composants importants des poussières fines : les poussières minérales, les éléments trace et le carbone élémentaire que diverses sources libèrent directement dans l'atmosphère (poussières fines primaires). Les méthodes d'analyse utilisées n'ont pas permis de préciser la nature d'une part de la masse des PM. Le rapport explique toutefois comment cette masse non identifiée (ou inconnue) de poussières fines peut être mise en rapport avec la légère mais systématique sous-estimation des concentrations en poussières fines organiques, poussières minérales et éléments trace, ainsi qu'à l'eau liée aux poussières et dont la masse n'a pas été déterminée.
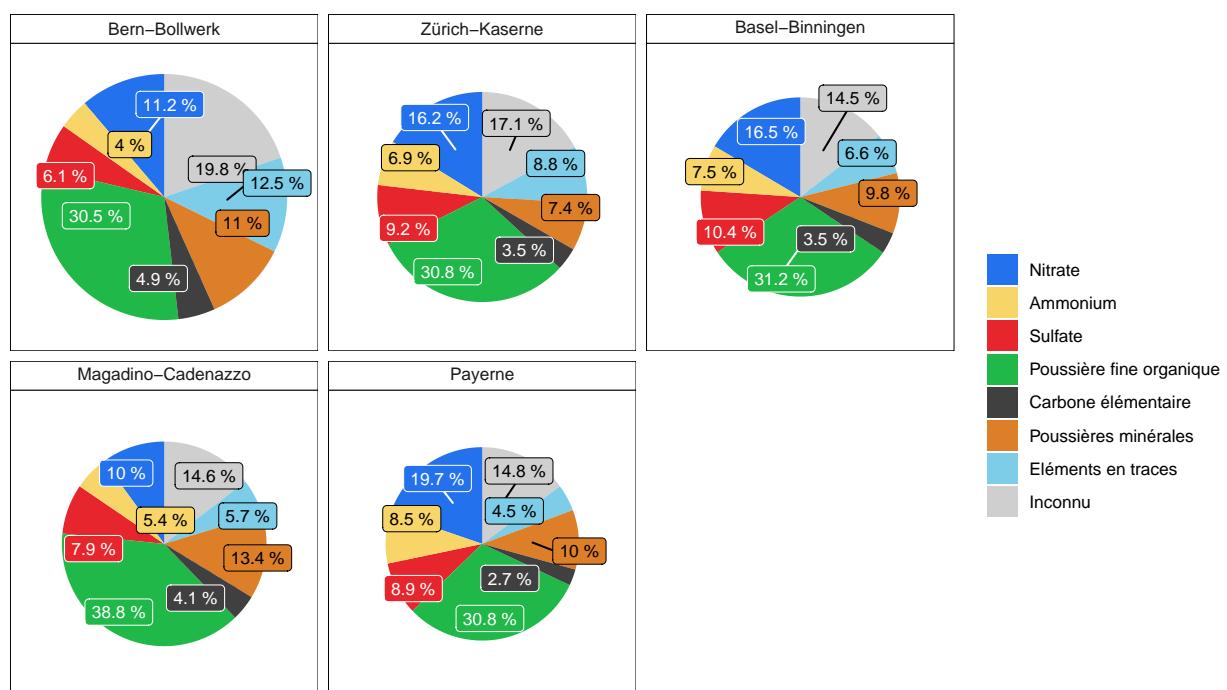

Figure 1 : Composition chimique moyenne des PM_{10} mesurée sur les cinq sites de la campagne 2018–2019. La surface des cercles est proportionnelle à la concentration totale en PM_{10} relevée sur chaque site (Bern-Bollwerk : 21.3 µg m^{-3}, Zürich-Kaserne : 15.6 µg m^{-3}, Basel-Binningen : 14.0 µg m^{-3}, Magadino-Cadenazzo : 14.8 µg m^{-3}, Payerne : 13.2 µg m^{-3}).

Les particules secondaires se lient majoritairement à la fraction des particules plus fines, alors que les poussières minérales et beaucoup d'éléments trace se lient généralement aux particules plus grossières. La part relative des poussières secondaires est donc plus élevée dans les $PM_{2.5}$ que dans les PM_{10}, comme l'illustrent les figures 1 et 2. On y constate aussi que la concentration tant en PM_{10} qu'en $PM_{2.5}$ présente un modeste gradient positif des sites ruraux aux villes, puis aux sites urbains très exposés au trafic. Ces gradients sont causés par les émissions locales de PM_{10} et $PM_{2.5}$ primaires, en particulier d'éléments trace, de poussières minérales, de carbone élémentaire et de poussières fines organiques primaires.

Certains constituants chimiques, par exemple tous les métaux à l'exception du fer, contribuent de façon négligeable à la masse totale des PM_{10} et $PM_{2.5}$. Néanmoins, des études récentes suggèrent que certains métaux peuvent jouer un rôle très important dans les effets des particules sur la santé.[3] Les concentrations de certains métaux (par exemple Ba, Cr, Cu, Fe, Sb, Sn, Mn, Co, Zn) montrent une nette augmentation des concentrations entre les sites ruraux et les sites urbains. Les concentrations les plus élevées étant enregistrées sur le site urbain et pollué par le trafic de Bern-Bollwerk. Cela indique que le trafic routier est une source importante de ces métaux.

Changements de composition des PM_{10} et $PM_{2.5}$ depuis 1998. En Suisse, les concentrations en PM_{10} et $PM_{2.5}$ diminuent. Ce fait est bien documenté par les rapports annuels du Réseau national d'observation des polluants atmosphériques NABEL publié par l'Office fédéral de l'environnement OFEV[4] et s'explique par les mesures de réduction des particules PM_{10} et $PM_{2.5}$ et de leurs gaz précurseurs prises tant en Suisse que dans une grande partie de l'Europe. Les concentrations totales ont diminué, tout comme celle de leurs principaux composants, à l'exception des poussières minérales (figure 3). On remarque en particulier un net recul du carbone élémentaire (EC) représenté par les particules de suie et provenant essentiellement des moteurs diesel et du chauffage au bois des ménages. Depuis 1998, la concentration en EC a reculé de 84 % sur le site urbain de Bern-Bollwerk, de 71 % sur le site urbain de Zürich-Kaserne et de 64 % sur le site de banlieue urbaine de Basel-Binningen. Cette importante amélioration de la qualité de l'air en Suisse est due avant tout à l'introduction de filtres à particules sur les moteurs diesel.

Principales sources de poussières fines atmosphériques. En introduisant les teneurs en composants chimiques des poussières fines dans des modèles statistiques (modèles récepteurs tels que la factorisation matricielle positive, dite PMF), on peut identifier les principales sources de poussières fines et en mesurer la contribution (attribution aux sources). Notre étude utilise une PMF pour l'attribution aux sources des PM_{10}. Pour comprendre ce modèle statistique,
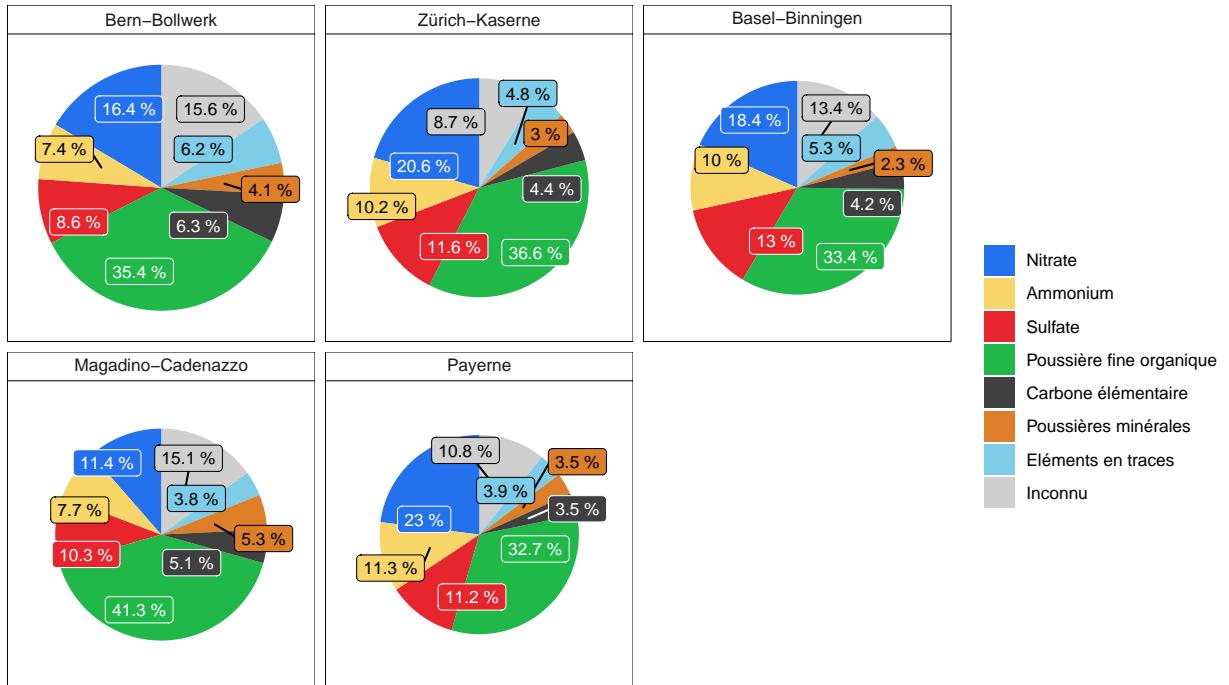
Figure 2 : Composition chimique moyenne des PM$_{2.5}$ des cinq stations de la campagne 2018–2019. La surface des cercles est proportionnelle à la concentration totale en PM$_{2.5}$ relevée sur chaque site. (Bern-Bollwerk : 14.0 µg m^{-3}, Zürich-Kaserne : 11.1 µg m^{-3}, Basel-Binningen : 10.6 µg m^{-3}, Magadino-Cadenazzo : 10.4 µg m^{-3}, Payerne : 9.2 µg m^{-3}).

il est utile de voir les poussières comme une superposition ou un mélange de poussières provenant de différentes sources. Les modèles récepteurs du type PMF cherchent à démêler la contribution de chaque source à partir de corrélations temporelles des teneurs mesurées en divers composants chimiques, sachant que chaque source a son propre profil de teneurs. Lorsqu'on utilise des modèles récepteurs tels que ceux de notre étude aux relevés quotidiens d'émissions de PM$_{10}$, on risque de ne pas entièrement démêler les sources si les corrélations temporelles sont également liées à certains autres facteurs tels que des cycles annuels d'activité. Cela peut se répercuter sur le calcul de la contribution des différentes sources, contributions qui peuvent être systématiquement surestimées ou sous-estimées. Les modèles PMF offrent cependant une précieuse vue d'ensemble du rôle des principales sources dans la concentration totale en PM, en particulier lorsque les données recueillies sur plusieurs sites sont analysées séparément et que les résultats de ces analyses sont comparés les uns aux autres.

Autre caractéristique importante des modèles récepteurs du type PMF : ils ne permettent pas de classer aisément les sources de poussières fines secondaires car une part des informations sur l'origine des émissions de gaz précurseurs se perd lors de la formation de particules secondaires. L'approche adoptée ici permet l'identification de différents types de PM$_{10}$ secondaires en plus de celle des sources d'émission des PM$_{10}$ primaires. C'est la raison pour laquelle les types identifiés de poussières secondaires PM$_{10}$ sont également désignés et traités comme des sources d'émission.

27
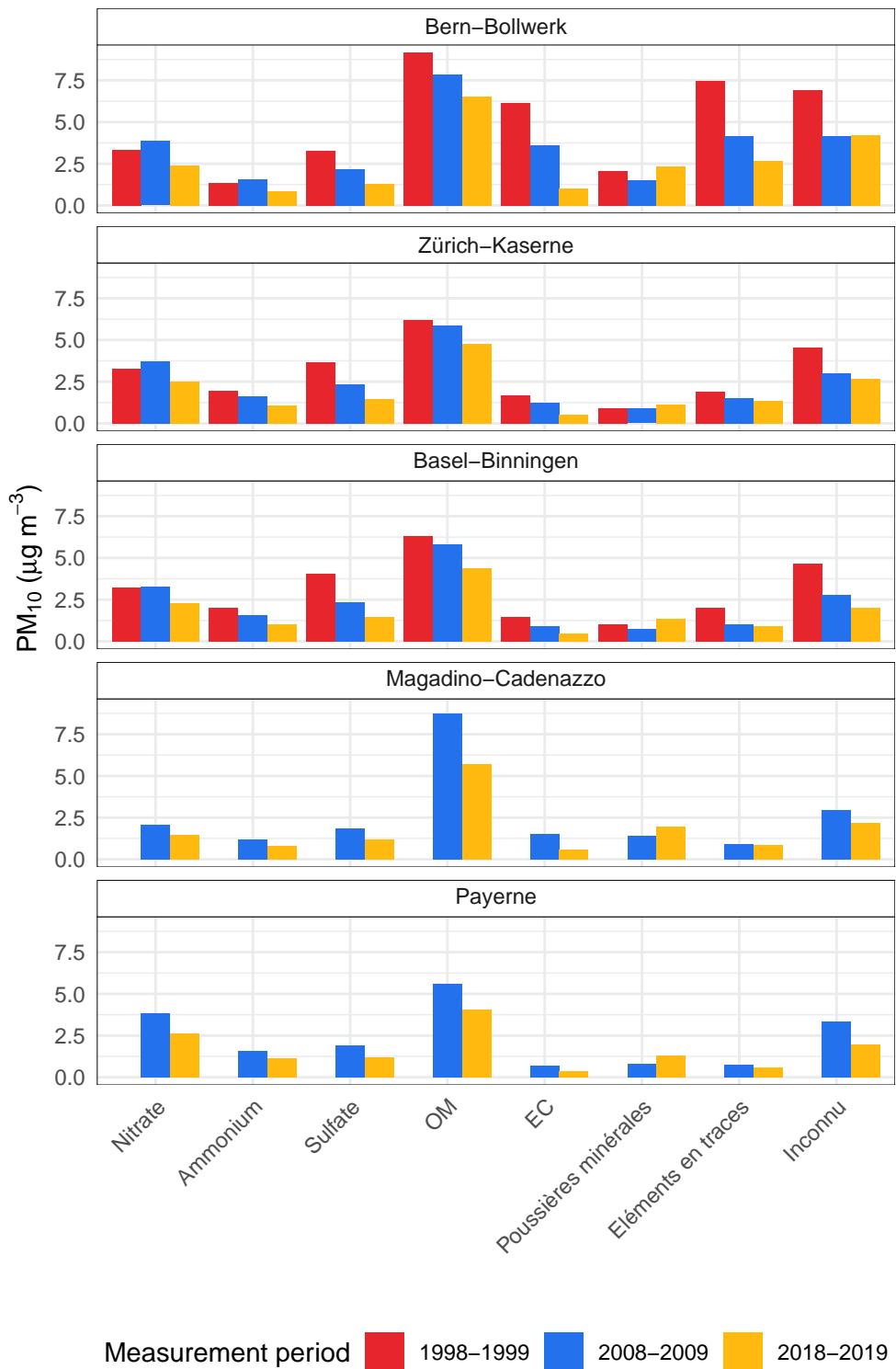
Figure 3 : Concentration moyenne des principaux composants de PM$_{10}$ lors des campagnes de mesure menées entre 1998 et 2019.
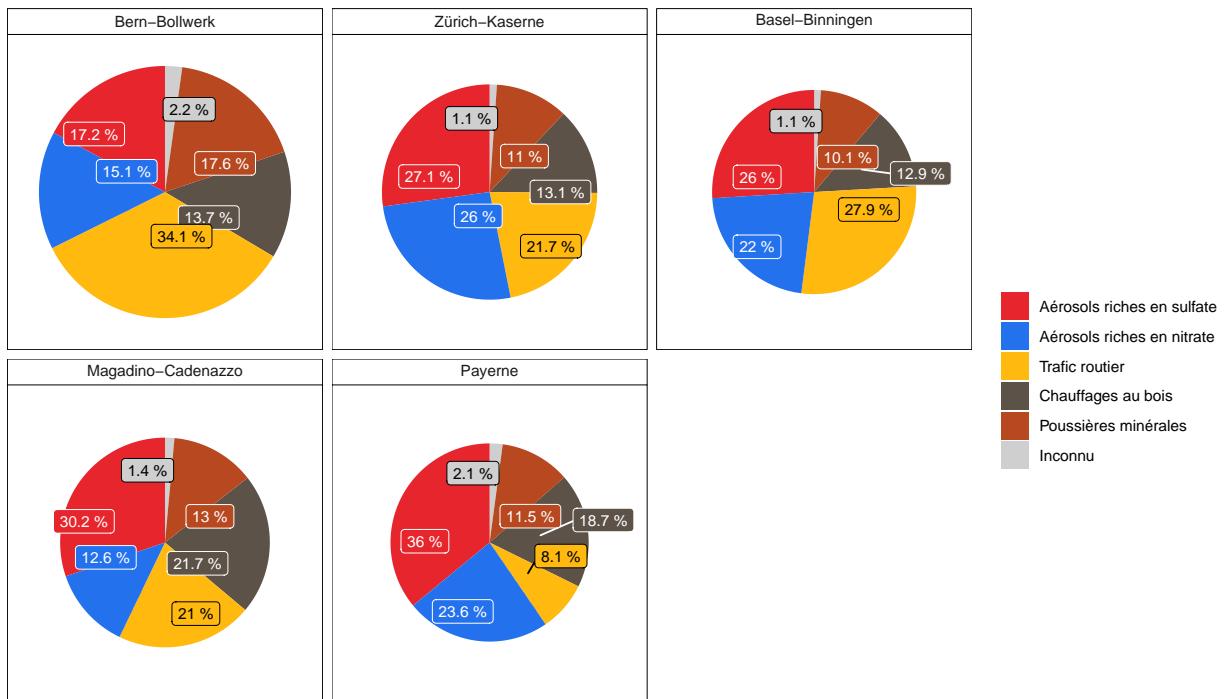
Figure 4 : Contributions moyennes d'une série de sources de PM_{10} évaluées au moyen d'un modèle statistique sur la base des mesures effectuées sur cinq stations au cours de la campagne de 2018–2019. La surface des cercles est proportionnelle à la concentration globale en PM_{10} relevée sur chaque site (Bern-Bollwerk : 21.3 $\mu g\,m^{-3}$, Zürich-Kaserne : 15.6 $\mu g\,m^{-3}$, Basel-Binningen : 14.0 $\mu g\,m^{-3}$, Magadino-Cadenazzo : 14.8 $\mu g\,m^{-3}$, Payerne : 13.2 $\mu g\,m^{-3}$).

La PMF a mis en évidence l'importance des aérosols secondaires riches en sulfates et en nitrates dans les PM_{10}, comme le montre la figure 4. Les aérosols riches en sulfates sont les principaux contributeurs en PM_{10} et contiennent, outre des sulfates, une grande quantité de poussières fines organiques, probablement des aérosols organiques secondaires. Les principales sources de PM_{10} primaires identifiées sont le trafic routier, le chauffage au bois et les poussières minérales. La contribution annuelle des poussières minérales varie entre 1.4 $\mu g\,m^{-3}$ et 1.9 $\mu g\,m^{-3}$, sauf sur le site urbain de Bern-Bollwerk – très exposé au trafic – où elle atteint la valeur notablement plus élevée de 3.8 $\mu g\,m^{-3}$. Cette concentration en poussières minérales, supérieure à celles du site urbain de Zürich-Kaserne, peut être attribuée à la poussière routière resuspendue qui, à titre d'émission autre que les gaz d'échappement (Air Quality Expert Group [5]), vient compléter les émissions dues au trafic routier. La contribution totale du trafic routier aux PM10 relevées à Bern-Bollwerk est avec 9.4 $\mu g\,m^{-3}$ (34,1 %) très supérieure à celle des autres sites qui atteint 1.1 $\mu g\,m^{-3}$ (8.1 %) à Payerne, 3.9 $\mu g\,m^{-3}$ (27.9 %) à Basel-Binningen et 3.2 $\mu g\,m^{-3}$ (21.7 %) à Magadino-Cadenazzo. Il est important de remarquer que tant le trafic routier que le chauffage au bois contribuent en outre à la formation de PM_{10} secondaires.

Nous avons également tenté de classer les sources de $PM_{2.5}$ par PMF. La teneur en certains composants spécifiques aux sources (en particulier en métaux) étant faible, souvent à la limite

ou sous la limite de détection, le classement des sources de $PM_{2.5}$ n'est ni robuste ni fiable.

Contribution de l'usure de pneus aux PM_{10} et $PM_{2.5}$. L'usure des pneus contribue aux PM_{10} et $PM_{2.5}$, comme l'a mis en évidence un projet partenaire conduit parallèlement au nôtre. Il ressort de l'analyse quantitative des poussières par microscopie électronique à balayage SEM/EDX (voir Rausch et al. [6]) que la moyenne annuelle de cette contribution au PM_{10} s'élève à 1.13 $\mu g\,m^{-3}$ (5,3 %) sur le site urbain exposé au trafic de Bern-Bollwerk et 0.16 $\mu g\,m^{-3}$ (1,0 %) sur le site urbain de Zürich-Kaserne. Dès qu'on s'écarte du trafic routier, la contribution s'amenuise et ne contribue plus que peu aux PM_{10} et $PM_{2.5}$. La concentration en poussières de pneus d'un diamètre de 10 à 80 micromètres aéroportées sur le site de Zürich-Kaserne suggère toutefois que le transport par voie atmosphérique contribue de manière non négligeable à la présence de particules fines de pneus dans les sols et les eaux superficielles éloignées du trafic automobile.

1 Introduction

1.1 Background

Particulate matter (PM) is an atmospheric pollutant which can be directly emitted or generated within the atmosphere either by natural or anthropogenic processes. PM causes deleterious human health effects, can be harmful for ecosystems, perturbs the Earth's radiation balance, and reduces atmospheric visibility and these features make PM a principal atmospheric and well studied pollutant.[7] A key feature of PM is that is it composed of a myriad of heterogeneous liquid and solid components, all of which combine to give PM its features. This allows for a number of data analysis techniques to be used to identify emission or generation sources which cannot be used for gaseous pollutants such as oxides of nitrogen (NO_x), or ozone (O_3).[8]

PM has a very diverse number of both natural and anthropogenic sources and the primary natural emission sources include: wind blown dust, volcanos, sea spray and forest fires.[9] Anthropogenic activities which result in PM emissions are generally combustion processes from the burning of fossil fuels or biomass. However, PM is also generated by secondary processes which occur in the atmosphere itself and secondary PM generation requires precursors, which are often of anthropogenic origin.[10] The oxidation of NO_x, sulfur dioxide, and ammonia emissions occur and produce nitrate, sulfate, and ammonium-borne PM which are especially relevant for many locations where secondary PM contributes the majority, or a large proportion of the PM load.

PM is usually defined by size with the PM_{10} and $PM_{2.5}$ fractions being the most common and these are defined as PM with a diameter less than 10 and 2.5 micrometres (μm) respectively. $PM_{2.5}$ is often denoted as fine particulate matter, PM with diameter between 2.5 and 10 μm is often called coarse PM ($PM_{2.5-10}$) and can be determined from the difference of PM_{10} and $PM_{2.5}$. Primarily due to the negative health effects of PM, Switzerland has like many other countries legal limits for ambient outdoor PM_{10} and $PM_{2.5}$. To ensure compliance to these ambient air quality standards, PM is monitored in ambient air routinely within air quality monitoring networks.

Although PM is commonly monitored, such routine activities do not capture the very diverse nature of PM because in ambient monitoring operations, generally, only PM mass or particle number is reported. Therefore, there is substantial value in determining the constituents which form the PM mix in any given location.[11,12] With such knowledge, PM can be characterised and this information can be used to inform policy makers to make decisions which more effectively control PM sources and reduce the negative effects of this pollutant – a goal of all compliance-driven monitoring activities.[13]

1.2 Objectives of this project

The primary objective of this work is to report a detailed characterisation project of PM_{10} and $PM_{2.5}$ for Switzerland. Results gained from an intensive sampling campaign involving five monitoring sites between June, 2018 and May, 2019 will be the main focus, however, these data will be compared and put into context with two previous and similar sampling periods conducted in 1998–1999 and 2008–2009.

This study was accompanied by a second project also supported by the Swiss Federal Office for the Environment (FOEN) and lead by Particle Vision GmbH. In this second project, complementary information on the chemical composition and sources of coarse PM was attained by using single particle analysis, *i.e.* Scanning Electron Microscopy combined with Energy-dispersive X-ray spectroscopy (SEM/EDX). Although the findings of this latter project are described in detail in a separate report[6], some aspects and results will be incorporated in this work for validation of obtained results and for leveraging our understanding of atmospheric PM. Therefore, this work acts as an extension and an update to previous work to report on atmospheric fine particulate matter ($PM_{2.5}$ and PM_{10}) in Switzerland.[1,14–16]

1.3 Switzerland's PM concentrations

Across all of Switzerland, both PM_{10} and $PM_{2.5}$ concentrations have significantly decreased during the past decades.[17–19] Such reductions have been achieved in urban areas and isolated mountainous sites and therefore, the reductions can be attributed to air quality management strategies, within Switzerland itself and across large parts of Europe (Figure 5).

A detailed knowledge about the chemical composition of PM is important as it allows an assessment of the effect of implemented air quality management strategies. In addition, detailed characterisation of PM will be very useful to identify pollutant sources and processes which need to be targeted to achieve further reductions in PM concentrations in Switzerland. To this end there have been two previous PM characterisation projects conducted: the first between April, 1998 and March, 1999 and a second between August, 2008 and July, 2009.[1,14–16] A third PM characterisation measurement period between June, 2018 and May, 2019 was undertaken and the findings are reported here and put in context with the previous measurement efforts.

2 Methods

2.1 Sampling sites and periods

PM_{10} and $PM_{2.5}$ sampling was conducted at five Swiss sites of the National Air Pollution Monitoring Network (NABEL), see Table 1 and Figure 6. Four of the five monitoring sites are
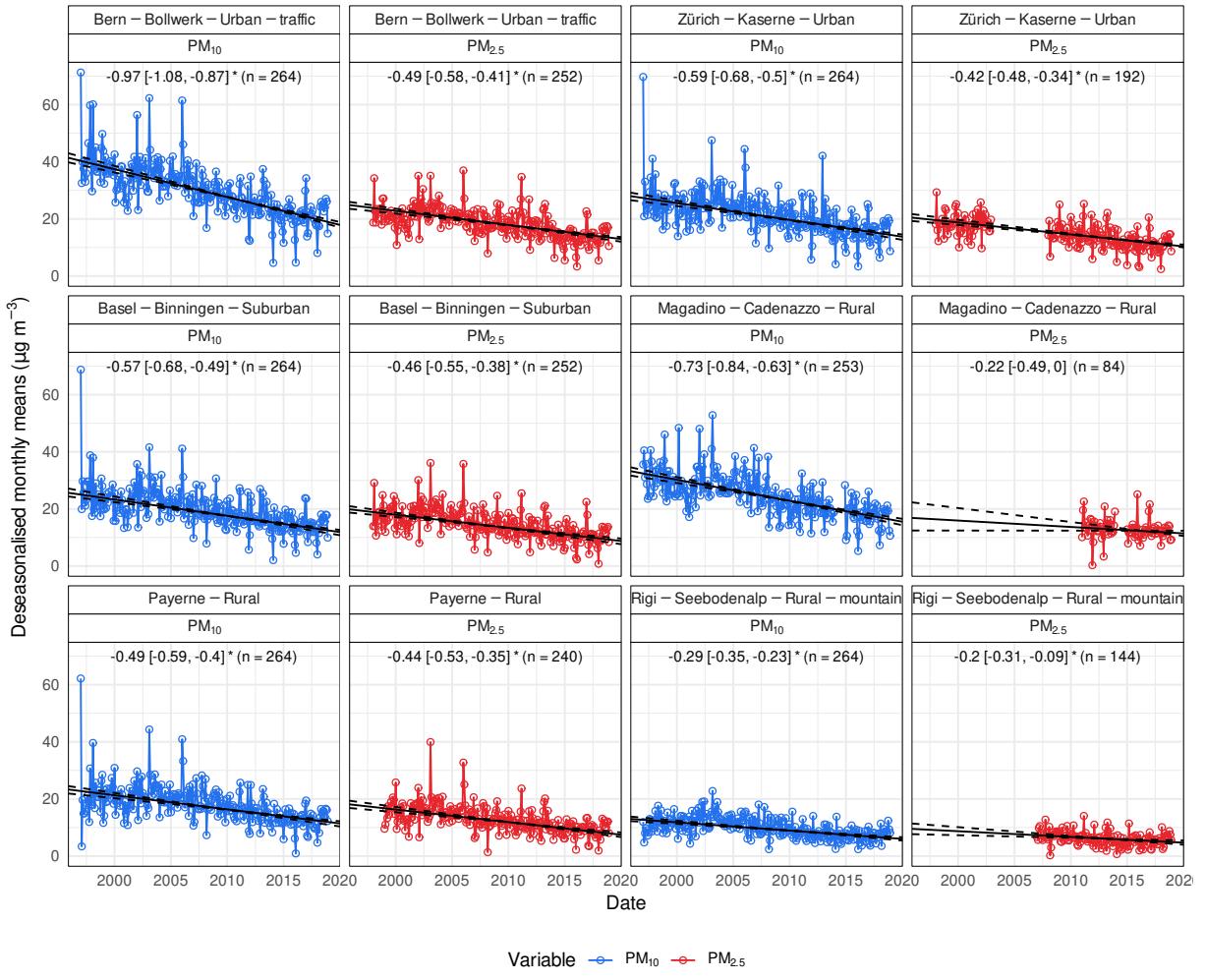
Figure 5 – PM$_{10}$ and PM$_{2.5}$ deseasonalised monthly means and trends for six monitoring locations in Switzerland between 1997 and 2020.

located on the Swiss plateau where the majority of the human population resides, however, Magadino-Cadenazzo is located in a rural area south of the Alps in the canton of Ticino. Bern-Bollwerk is classified as an urban traffic site and is located within a partial street canyon while the other locations are background locations in urban (Zürich-Kaserne), suburban (Basel-Binningen) and rural (Payerne) environments.

Table 1 – Basic information for the five monitoring sites in Switzerland which were used for intensive PM characterisation measurements.

Site name	Local ID	Canton	Lat.	Long.	Elev. (m)	Site type
Basel-Binningen	BAS	Basel-Landschaft	47.5	7.6	316	Suburban
Bern-Bollwerk	BER	Bern/Berne	47.0	7.4	536	Urban Traffic
Magadino-Cadenazzo	MAG	Ticino	46.2	8.9	203	Rural
Payerne	PAY	Vaud	46.8	6.9	489	Rural
Zürich-Kaserne	ZUE	Zürich	47.4	8.5	409	Urban

Three intensive measurement periods have been conducted: (*i*) April 1, 1998 to March

31, 1999, (*ii*) August 1, 2008 to July 31, 2009, and (*iii*) June 1, 2018 to May 31, 2019. These three periods all had durations of 12 months, but began and ended at different times of the year and therefore were not aligned with one-another. There was not a uniform sampling programme for PM_{10} and $PM_{2.5}$ across the five monitoring sites among the three measurement periods (Figure 7). Notably, chemical PM characterization was in the first measurement period (1998–1999) not conducted in Magadino-Cadenazzo and only partially conducted at Payerne (only EC and OC in PM_{10}). In addition, $PM_{2.5}$ was sampled but not chemically characterised at all the sites for the second measurement period (2008–2009).
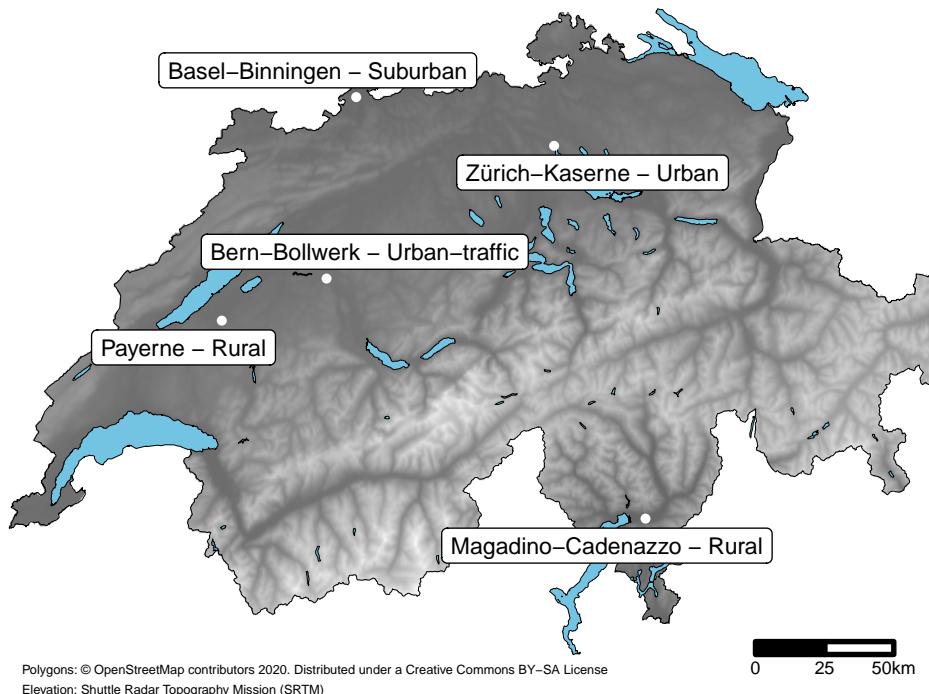
Figure 6 – The five monitoring sites in Switzerland which were used for intensive PM characterisation measurements. The shading indicates the elevation of the terrain and filled black areas show larger lakes and reservoirs.

2.2 Data

2.3 Filter samples and PM mass

Daily PM_{10} and $PM_{2.5}$ filter samples were collected using Digitel DA-80H high-volume samplers with flow rates of $30\,\mathrm{m^{-3}\,h^{-1}}$ with the appropriate PM_{10} or $PM_{2.5}$ inlets. The quartz filters used had diameters of $150\,\mathrm{mm}$ (Pallflex Tissuquartz 2500 QAT-UP) and the sampling duration was between midnight and midnight. The mass concentration of the deposited PM_{10} and $PM_{2.5}$ has been determined using the standard gravimetric measurement method according to European Committee for Standardization [20].

Although PM samples were collected every day, punches from only every fourth day were
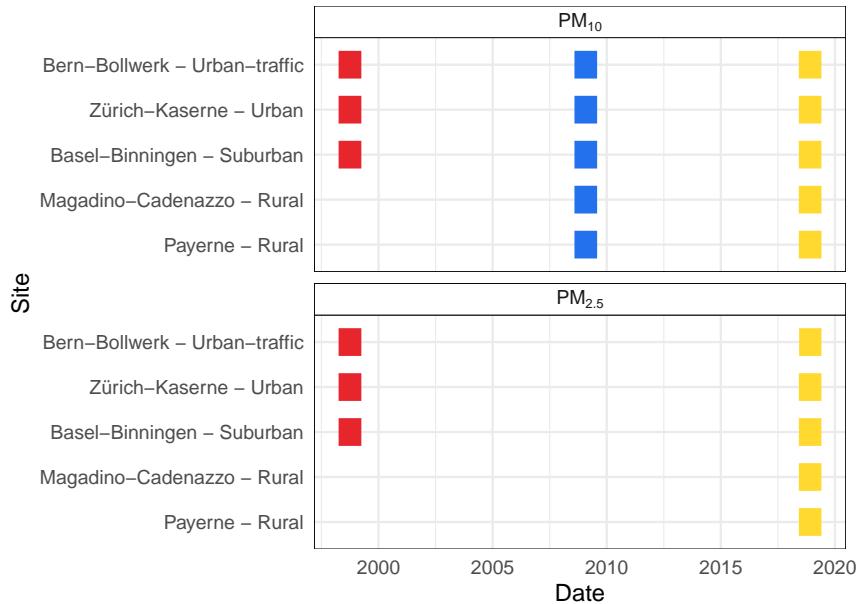
Figure 7 – Time line of PM_{10} and $PM_{2.5}$ sampling for the five monitoring sites in Switzerland for the three measurement periods.

taken and delivered to laboratories and analysed with a number of analytical techniques. A very small number of filter samples were not sent for analysis due to sampling issues and the numbers of filter samples analysed are shown in Table 2. For the third measurement period 2018–2019 a total of 899 filters were included in the analysis with 450 and 449 PM_{10} and $PM_{2.5}$ samples respectively.

Table 2 – Counts of PM filters with valid observations between June, 2018 and May, 2019.

Site name	PM_{10}	$PM_{2.5}$
Basel-Binningen	90	90
Bern-Bollwerk	88	88
Magadino-Cadenazzo	90	90
Payerne	91	90
Zürich-Kaserne	91	91

2.4 Analytical techniques

Elemental and organic carbon (EC and OC) concentrations were determined by the thermal optical transmission (TOT) method using the EUSAAR2 temperature protocol.[21] Water soluble inorganic ion concentrations (ammonium, calcium, chloride, magnesium, nitrate, potassium, sodium, sulfate) were detected by ion chromatography. The determination of EC, OC, and ions were conducted at Empa. For the transformation of OC to organic matter (OM), a 1.6 multiplier was used. This multiplier accounts for the mass of other elements than the detected carbon in organic particle bound matter, in particular the mass of hydrogen, oxygen and nitrogen and has been chosen to be in agreement with the scientific literature and the transformation done

in the past study.[15]. It should be noted that experimental values for average OM to OC ratios of PM in Switzerland are missing and the true conversion multiplier is unknown. However, it has been reported that the OM to OC ratio of primary PM emitted by road traffic is around 1.3, while OM to OC ratios in PM from wood burning are around 1.6–1.8.[2] Secondary organic PM is typically highly oxidized and OM to OC ratios are in the range of 1.9–2.2.[2] The chosen multiplier for transformation of measured OC to OM is therefore rather too low and might lead to an underestimation of the true OM mass concentration in PM_{10} and $PM_{2.5}$. Nevertheless, the chosen 1.6 multiplier can be justified by the lack of knowledge of the true value.

Acid digestion of $15.9\,cm^2$ filter punches was undertaken using $25\,mL$ of a $HF:HNO_3:HClO_4$ mixture for determination of elemental concentrations in PM by inductively coupled plasma atomic emission spectrometry (ICP-AES) and inductively coupled plasma mass spectrometry (ICP-MS). The analyses have been performed at the Institute of Environmental Assessment and Water Research (IDAEA), Consejo Superior de Investigaciones Científicas (CSIC), Barcelona, Spain, details of the applied analytical procedure are described in Pérez et al. [22]. The applied acid digestion method using HF allows a complete dissolution of the PM sample and therefore complete recovery of the elements. This was regularly tested by analysis of few milligrams of an reference material (NIST 1633b) that was added to laboratory blank filter samples.

Sugar alcohols including arabitol, mannitol, and mannosan as well as other organics, notably levoglucosan were determined by liquid chromatography-mass spectrometry (LC-MS) at Institut des Géosciences de l'Environnement, IGE Grenoble, France. Additionally, oxidative potential assays were conducted by IGE Grenoble (subsection 2.7).

The above descriptions are for the third measurement period between 2018 and 2019, but for the two previous measurement periods, there were some differences. For the first measurement period, the EC and OC concentrations were determined by the VDI2465/1 method.[23] Some of these old filters were reanalysed with the TOT/EUSAAR2 method and the carbon measurements as determined by VDI2465/1 were adjusted to their TOT/EUSAAR2 values. The details of this procedure is discussed in Gianini et al. [15], data adjustment has been applied to all PM_{10} and $PM_{2.5}$ samples from the 1998-1999 measurement period. For the two previous measurement periods 1998–1999 and 2008–2009, the elemental analysis was conducted at Empa using a milder acid digestion in a $HNO_3:H_2O_2$ mixture as described in Hueglin et al. [14] and Gianini et al. [16]. This milder acid digestion resulted in a incomplete digestion of some elements. However, the recovery rates of all elements measured was determined based on the analysis of certified reference material and the measured element concentrations were corrected for incomplete recovery.[14,16] The comparability of the two analytical methods for determination

of element concentrations used for the different measurement periods has been tested within an inter-laboratory comparison performed in 2009. Eight PM_{10} filter samples have then been analysed using both methods. The agreement of the concentrations obtained with the two methods is for most elements good. As shown in Figure A.1, the correlation of the measured concentrations is high ($R^2 > 0.7$) for all elements except for Ni, Se, Mo and Y. The analytical procedure performed by IDAEA-CSIC for the measurement period 2018–2019 results for Na, Mg, Al, Ca, V, Mn, Ba and Ce in systematically higher concentrations (Figure A.2). Since these differences in concentration values have been determined based on a small number of parallel measurements, it was decided not to apply a data correction. However, the systematically higher concentration obtained with the IDAEA-CSIC analytical method should be kept in mind when discussing the temporal change of the concentrations of the corresponding elements in PM_{10} and $PM_{2.5}$.

2.5 Estimation of mineral dust

The determination of mineral dust in PM is often done by summing common crustal elements together while assuming these elements are within oxide forms.[24] Calcium, iron, and potassium have significant anthropogenic sources however, and therefore, a pragmatic "aluminium ratios" approach was applied to these three elements to split their mass into crustal and anthropogenic components. Calcium, iron, and potassium ratios to aluminium were calculated with simple least-squares regression using the observations with the lowest 10 % of these aluminium ratio values. Extra models were used for calcium at Magadino-Cadenazzo because of the different geological makeup of the crust south of Alps when compared to the Swiss plateau.[15] The regression slopes used for calculation of the crustal component of the three elements are displayed in Table 3. The obtained regression slopes are somewhat smaller than the values used in Gianini et al. [15]. In order to ensure a consistent mineral dust estimation for the three measurement periods, mineral dust concentrations for the two earlier measurement periods have been re-calculated using the regression slopes given in Table 3. Consequently, the numbers reported here are slightly different from the values reported by Gianini et al. [15].

Table 3 – Simple least-squares regression slopes to calculate crustal component of three elements based on aluminium concentrations for PM_{10} and $PM_{2.5}$. Calcium south of the Alps have individual models because of different geology.

Model	Element	PM_{10}	$PM_{2.5}$
Representative of Switzerland	Calcium	1.00	0.43
Calcium south of the Alps	Calcium	0.59	0.25
Representative of Switzerland	Iron	0.65	0.37
Representative of Switzerland	Potassium	0.38	0.49

Once the crustal and anthropogenic splits were calculated using the aluminium ratios in Table 3, the mineral dust contributions were calculated in agreement with Gianini et al. [15] by using Equation 1:

$$\text{Mineral dust} = \text{aluminium} \times 1.89 + \text{magnesium} \times 1.66 + \text{calcium}_{\text{crustal}} \times 1.4 + \\ \text{potassium}_{\text{crustal}} \times 1.21 + \text{iron}_{\text{crustal}} \times 1.43 + \text{silicon} \times 2.14 \tag{1}$$

The multipliers are oxide multipliers and silicon was not analytically determined because of the use of quartz filters and was therefore calculated by aluminium $\times$ 3.62 where the multiplier represents the average ratio of silicon and aluminium in the Earth's crust.[25] The validity of this average global ratio for calculation of silicon is supported by the analysis of $PM_{2.5-10}$ in Zürich-Kaserne during the parallel project by using SEM/EDX where an average ratio of silicon and aluminum of 3.79[6] was found. For the urban traffic site Bern-Bollwerk, elemental analysis of $PM_{2.5-10}$ by SEM/EDX resulted in an average silicon to aluminum ratio of 4.73, indicating an impact of other sources than crustal mineral dust to the concentration of these two elements at the Bern-Bollwerk site. Other sources containing silicon and aluminum in unknown amounts are likely road dust that is re-suspended by traffic on the road nearby the measurement site and possibly dust from construction works. In addition, silicon is also contained in tyre wear,[26] but not aluminium. In an earlier study by Amato et al. [27], the PM_{10} fraction of road dust collected from sweeping the pavement of roads at several locations in the city centre of Zürich has been analysed and an average Si to Al ratio of 3.45 has been found. The similar Si to Al ratio in road dust and natural mineral dust implies that the mineral dust concentration as calculated using Equation 1 might be influenced by contributions from resuspended road dust.

2.6   Mass closure calculation

The applied analytical methods account for most of the mass of PM_{10} and $PM_{2.5}$. However, elements like oxygen, nitrogen, hydrogen and silicon are not quantitatively measured. Their mass has been accounted for through the assumptions and estimations described in subsection 2.4 and subsection 2.5. In addition, all elements other than the four elements used for mineral dust estimation have been assumed to be present in oxide forms. Consequently, a mass closure of PM_{10}, $PM_{2.5}$ has been tried by adding up the measured and assumed mass and by comparison of the calculated values with the mass concentrations obtained from the gravimetric measurement of the filter samples. The mass closure for the coarse PM fraction ($PM_{2.5-10}$) has been also done on daily basis from the difference of determined mass concentrations in PM_{10} and $PM_{2.5}$. Note that for the measurement period 1998–1999 only about 70 daily $PM_{2.5}$

38

samples per sampling location were chemically characterised.[14] Therefore, the calculated annual statistics for $PM_{2.5-10}$ from 1998-1999 are based on a smaller number of observations compared to the 2018–2019 measurement period.

2.7 Oxidative potential assays

Oxidative potential (OP) was analysed with three different assays: ascorbic assay (AA), dithio-threitol (DTT), and dichlorofluorescein (DCFH) and these analyses were conducted at the Institute of Environmental Geosciences, University of Grenoble, Grenoble, France. The AA assay measures antioxidant depletion, DTT measures the consumption of the reagent which is consumed by redox reactions (DTT to O_2 transfer), while DCFH is a fluorescence method which quantifies reactive organic species (ROS). All filter samples were analysed with five replicates of each assay to ensure reproducibility.

The three assays have the same objective of determining the amount of oxidative stress an analyte can elicit, but the three assays have differing sensitivities to various components which form the PM mix. The three assays have these general characteristics: AA is primarily sensitive to transition metals, DTT is the most reported OP assay and is sensitive to organics and to a lesser extent, metals[28,29], and DCFH also shows a greater sensitivity to organic compounds.

It should be noted that OP can be represented in two forms: OP per PM mass, or OP per volume of air. The air value is a superior unit when representing population exposure and therefore, this unit is used in this analysis. Because there are three OP assays reported, a subscript notation is used, *i.e.*, OP_{AA} m^{-3}, OP_{DTT} m^{-3}, and OP_{DCFH} m^{-3}.

2.8 Source apportionment

Source apportionment refers to a diverse family of techniques which link ambient concentrations to pollution emission sources which is particularity relevant for PM data analysis. Receptor models are a prominent method to enable source apportionment and such models use multivariate analysis to solve mass balance equations.[30] A widespread and internationally used model is called positive matrix factorisation (PMF) and generally, in modern usage, the algorithm used to solve the equation is the multilinear engine (ME-2).[31]

Discussions of the mechanics of PMF and ME-2 have been covered in depth in very many previous publications (see Hopke [30], Comero et al. [32], and Olivier et al. [33] for detailed overviews), but in a practical sense, a data user requires two inputs: a concentration table and an error or uncertainty table. The two tables (sometimes called matrices) are used to perform a weighted least squares fit where a goodness of fit parameter, usually called the *Q-value* is optimised. PMF is constrained to non-negativity and allows for every observation to have its

own error in the model which gives a user much flexibility and choices in how to handle missing observations, observations below detection limit of a particular analytical technique, or variables with a low signal-to-noise ratio. Data users explore the stability of the models and determine an optimal number of factors (which represent emission sources or atmospheric processes) which can also be aided with the use of molecular markers; other pollutants not included in the models but are considered tracers for certain processes.

The main advantage of PMF is that it is a dimensionality reduction technique which allows the transformation of (typically) dozens of measured variables or species to be reduced to a handful of factors. Critically, these factors can be mapped to distinct PM sources which makes the technique highly utilitarian and useful for research and air quality management and policy informing purposes.[34]

Receptor modelling by PMF for the three measurement periods and the five monitoring locations (a total of 13 models) was conducted on PM_{10} samples with the EPA PMF 5.0 software tool.[35,36] The PMF procedure followed was consistent for all models and the steps followed are outlined and discussed in Olivier et al. [33], Weber et al. [34], and Belis et al. [37]. Note that PMF-modelling was also tried for $PM_{2.5}$. However, the concentrations of some compounds that are characteristic for specific emission sources are in $PM_{2.5}$ often in the range or even below the detection limits and reliably unmixing of source contributions was not possible and no additional knowledge could be gained. The results of $PM_{2.5}$ source apportionment are therefore not included in this report.

Construction of observation's errors used for PMF has no standard procedure. However, errors are expressed in the same units of the observations and should encompass analytical uncertainty, variations in reproducibility, and other sources of noise. Here, the error for each observation was calculated by Equation 2.

$$s = \sqrt{DL^2 + (CV \times x)^2 + (\alpha \times x)^2} \tag{2}$$

Where, DL is the detection limit and calculated by two times the standard deviation of the blanks of each species, CV is the coefficient of variation (also known as the relative standard deviation; μ/σ), x is the concentration of the species, and finally, α is an additional error term set at 0.03 to include other, miscellaneous sources of uncertainty. For the mass measurements, Equation 2 was not used, the errors were simply set at four times the concentration value which resulted in the mass variable having very little weighting to the PMF solution.

The concentrations and errors were evaluated together and a species was only included in

the PMF model if the signal-to-noise ratio (Equation 3) of the variable was greater than one.

$$SN = \sum_{i=1}^{n} \frac{\left(\frac{x}{s}\right)}{n} \tag{3}$$

An additional filter was applied where if 50 % of the concentration values for a species were below the detection limit, the species was not included in the PMF model.

For values which were below the detection limit, they were replaced by half of the detection limit and the errors were replaced with 5/6 of the detection limit. PMF does not accept missing values and therefore, a final manipulation was conduced where missing values were replaced by the species median and the errors were set to four times the concentration's median. These preliminary data preparation steps were aided by the **pmfr** R package.[38]

2.8.1 Number of factors and valid solutions

The number of factors for any PMF model must be declared before models are run. To identify the optimal number of factors, many models were run with a varying number of factors. To determine valid and stable model solutions and the correct number of factors, the residuals of the input species, rotational ambiguity of the solutions, Fpeak values, G-space plots, stability of factors after model bootstrapping, and the Qtrue/Qrobust ratio (Q-ratio) were investigated.[35] For additional confirmations, molecular markers such as levoglucosan were used to validate the sources after they had been mapped.

The number of sources was conserved among the different measurement periods. Bern-Bollwerk, the single urban traffic site had the best solutions with six sources while all the four remaining sites' models were best with five sources. Summaries of the PMF runs are shown in Table 4. After the EPA PMF tool was used, the outputs were loaded and analysed with the **pmfr** package.[38]

Table 4 – Summary of the 13 PMF models used for the source apportionment analysis.

Site	Period	No. of observations	No. of species	No. of factors
Basel-Binningen	1998-1999	103	28	6
Bern-Bollwerk	1998-1999	104	33	7
Zürich-Kaserne	1998-1999	104	30	6
Basel-Binningen	2008-2009	91	32	6
Bern-Bollwerk	2008-2009	91	33	7
Magadino-Cadenazzo	2008-2009	91	31	6
Payerne	2008-2009	91	30	6
Zürich-Kaserne	2008-2009	91	31	6
Basel-Binningen	2018-2019	90	28	6
Bern-Bollwerk	2018-2019	88	31	6
Magadino-Cadenazzo	2018-2019	90	30	5
Payerne	2018-2019	91	28	5
Zürich-Kaserne	2018-2019	91	28	5

3   Chemical composition of PM for the 2018–2019 measurement period

The mean chemical composition of PM_{10} and $PM_{2.5}$ for the three measurement periods is shown in Table 5 and Table 6. Table 7 lists the mean composition of coarse PM calculated as the difference of the mean concentrations of the main constituents in PM_{10} and $PM_{2.5}$ and denoted as $PM_{2.5-10}$. A graphical representation of the mean concentration of the main constituents in PM_{10}, $PM_{2.5}$ and $PM_{2.5-10}$ is given in Figure 8, Figure 9 and Figure 10. The figures for the mean relative composition of PM_{10}, $PM_{2.5}$ and $PM_{2.5-10}$ are provided in the Appendix (section 8).

For the four sites north of the Alps a site-type continuum is present. There is a weak, but consistent increase in PM_{10} and $PM_{2.5}$ from rural (Payerne) to suburban (Basel-Binningen) and urban (Zürich-Kaserne) environments. The highest PM levels are present at urban roadside locations, here represented by the urban traffic site Bern-Bollwerk. Magadino-Cadenazzo, a rural site south of the Alps, does not follow this order of PM levels in Switzerland. The region south of the Alps show generally higher PM concentrations than the region north of the Alps due to the different climate, the alpine topography and the proximity to the industrialised areas in northern Italy.

3.1   Chemical Composition of PM_{10} and $PM_{2.5}$

Like in the earlier field campaigns, organic matter (OM) was the most abundant compound of both PM_{10} and $PM_{2.5}$ sampled in the 2018–2019 measurement period. The absolute and relative contribution of OM ranges from 4.1–6.5 $\mu g\,m^{-3}$ (30.5–38.8 %) in PM_{10} and 3.0–5.0 $\mu g\,m^{-3}$ (32.7–41.3 %) in $PM_{2.5}$ respectively. OM is known to be mainly formed from the transformation of gaseous organic species in the atmosphere (secondary organic aerosol, SOA), but also resulting from primary emissions of organic PM including biological particles. Consequently, the largest part of OM is in the $PM_{2.5}$ size fraction, however, there is a substantial part of OM also present in

Table 5 – Mean concentrations and contributions to PM_{10} mass for five PM monitoring sites in Switzerland for three measurement periods between 1998 and 2019. All values have been rounded to one decimal place. Note that values can slightly differ from those reported before[1,14,15] due to the slightly different logic for selection of valid filter samples and due to the different methodology for the calculation of mineral dust (subsection 2.5). For the 2008–2009 measurement period the Saharan dust event from 15.10.2008 has not been excluded.

Period	Variable	Bern-Bollwerk $\mu g\,m^{-3}$	%	Zürich-Kaserne $\mu g\,m^{-3}$	%	Basel-Binningen $\mu g\,m^{-3}$	%	Magadino-Cad. $\mu g\,m^{-3}$	%	Payerne $\mu g\,m^{-3}$	%
1998-1999	Mass	39.7	100.0	24.1	100.0	24.7	100.0	–	–	–	–
1998-1999	Organic matter	9.2	23.1	6.2	25.7	6.3	25.6	–	–	–	–
1998-1999	Nitrate	3.3	8.4	3.3	13.6	3.2	13.1	–	–	–	–
1998-1999	Sulfate	3.3	8.3	3.7	15.3	4.0	16.4	–	–	–	–
1998-1999	Mineral dust	2.1	5.2	0.9	3.7	1.0	4.2	–	–	–	–
1998-1999	Trace elements	7.5	18.8	1.9	7.8	2.0	8.1	–	–	–	–
1998-1999	Ammonium	1.4	3.5	1.9	8.1	2.0	8.0	–	–	–	–
1998-1999	Elemental carbon	6.1	15.4	1.7	7.0	1.4	5.9	–	–	–	–
1998-1999	Missing mass	6.9	17.4	4.5	18.8	4.6	18.8	–	–	–	–
2008-2009	Mass	28.9	100.0	20.2	100.0	18.5	100.0	20.7	100.0	18.5	100.0
2008-2009	Organic matter	7.8	27.1	5.9	29.0	5.8	31.3	8.7	42.3	5.6	30.5
2008-2009	Nitrate	3.9	13.4	3.7	18.5	3.3	17.8	2.1	10.1	3.8	20.6
2008-2009	Sulfate	2.2	7.5	2.3	11.6	2.4	12.8	1.9	9.1	1.9	10.4
2008-2009	Mineral dust	1.5	5.3	0.9	4.4	0.7	3.9	1.4	6.9	0.8	4.4
2008-2009	Trace elements	4.1	14.3	1.5	7.6	1.0	5.7	0.9	4.4	0.7	4.0
2008-2009	Ammonium	1.6	5.5	1.6	7.9	1.6	8.4	1.2	5.6	1.6	8.5
2008-2009	Elemental carbon	3.6	12.4	1.3	6.2	0.9	5.0	1.5	7.3	0.7	3.6
2008-2009	Missing mass	4.2	14.4	3.0	14.9	2.8	15.0	3.0	14.3	3.3	18.0
2018-2019	Mass	21.3	100.0	15.6	100.0	14.0	100.0	14.8	100.0	13.2	100.0
2018-2019	Organic matter	6.5	30.5	4.8	30.8	4.4	31.2	5.7	38.8	4.1	30.8
2018-2019	Nitrate	2.4	11.2	2.5	16.2	2.3	16.5	1.5	10.0	2.6	19.7
2018-2019	Sulfate	1.3	6.1	1.4	9.2	1.5	10.4	1.2	7.9	1.2	8.9
2018-2019	Mineral dust	2.3	11.0	1.1	7.4	1.4	9.8	2.0	13.4	1.3	10.0
2018-2019	Trace elements	2.7	12.5	1.4	8.8	0.9	6.6	0.8	5.7	0.6	4.5
2018-2019	Ammonium	0.9	4.0	1.1	6.9	1.0	7.5	0.8	5.4	1.1	8.5
2018-2019	Elemental carbon	1.0	4.9	0.5	3.5	0.5	3.5	0.6	4.1	0.4	2.7
2018-2019	Missing mass	4.2	19.8	2.7	17.1	2.0	14.5	2.2	14.6	2.0	14.8

Table 6 – Mean concentrations and contributions to $PM_{2.5}$ mass for five PM monitoring sites in Switzerland for two measurement periods between 1998 and 2019. All values have been rounded to one decimal place. Note that for main components that are almost entirely abundant in $PM_{2.5}$ (e.g. ammonium), it is possible that listed mean concentrations in $PM_{2.5}$ are slightly higher than the values listed for PM_{10} (Table 9), because the exact dates and/or the total number of samples analysed can be different.

Period	Variable	Bern-Bollwerk $\mu g\,m^{-3}$	%	Zürich-Kaserne $\mu g\,m^{-3}$	%	Basel-Binningen $\mu g\,m^{-3}$	%	Magadino-Cad. $\mu g\,m^{-3}$	%	Payerne $\mu g\,m^{-3}$	%
1998-1999	Mass	24.2	100.0	20.0	100.0	19.0	100.0	–	–	–	–
1998-1999	Organic matter	8.5	35.0	5.5	27.4	5.3	27.7	–	–	–	–
1998-1999	Nitrate	2.9	12.1	3.4	17.1	3.3	17.3	–	–	–	–
1998-1999	Sulfate	2.8	11.7	3.5	17.7	4.1	21.8	–	–	–	–
1998-1999	Mineral dust	0.2	0.8	0.5	2.4	0.3	1.5	–	–	–	–
1998-1999	Trace elements	1.3	5.2	0.9	4.3	1.1	5.7	–	–	–	–
1998-1999	Ammonium	1.6	6.7	2.1	10.4	2.1	11.2	–	–	–	–
1998-1999	Elemental carbon	4.2	17.4	1.8	8.9	1.6	8.7	–	–	–	–
1998-1999	Missing mass	2.7	11.1	2.3	11.7	1.1	6.1	–	–	–	–
2018-2019	Mass	14.0	100.0	11.1	100.0	10.6	100.0	10.4	100.0	9.2	100.0
2018-2019	Organic matter	5.0	35.4	4.1	36.6	3.5	33.4	4.3	41.3	3.0	32.7
2018-2019	Nitrate	2.3	16.4	2.3	20.6	1.9	18.4	1.2	11.4	2.1	23.0
2018-2019	Sulfate	1.2	8.6	1.3	11.6	1.4	13.0	1.1	10.3	1.0	11.2
2018-2019	Mineral dust	0.6	4.1	0.3	3.0	0.2	2.3	0.6	5.3	0.3	3.5
2018-2019	Trace elements	0.9	6.2	0.5	4.8	0.6	5.3	0.4	3.8	0.4	3.9
2018-2019	Ammonium	1.0	7.4	1.1	10.2	1.1	10.0	0.8	7.7	1.0	11.3
2018-2019	Elemental carbon	0.9	6.3	0.5	4.4	0.4	4.2	0.5	5.1	0.3	3.5
2018-2019	Missing mass	2.2	15.6	1.0	8.7	1.4	13.4	1.6	15.1	1.0	10.8

Table 7 – Mean concentrations and contributions to $PM_{2.5-10}$ mass for five PM monitoring sites in Switzerland for two measurement periods between 1998 and 2019. All values have been rounded to one decimal place.

Period	Variable	Bern-Bollwerk $\mu g\,m^{-3}$	%	Zürich-Kaserne $\mu g\,m^{-3}$	%	Basel-Binningen $\mu g\,m^{-3}$	%	Magadino-Cad. $\mu g\,m^{-3}$	%	Payerne $\mu g\,m^{-3}$	%
1998-1999	Mass	15.6	100.0	4.2	100.0	5.7	100.0	–	–	–	–
1998-1999	Organic matter	0.7	4.4	0.7	17.4	1.0	18.4	–	–	–	–
1998-1999	Nitrate	0.4	2.5	0.0	0.0	0.0	0.0	–	–	–	–
1998-1999	Sulfate	0.5	3.1	0.2	3.8	0.0	0.0	–	–	–	–
1998-1999	Mineral dust	1.9	12.2	0.4	10.3	0.8	13.2	–	–	–	–
1998-1999	Trace elements	6.2	39.9	1.0	24.7	0.9	15.8	–	–	–	–
1998-1999	Ammonium	0.0	0.0	0.0	0.0	0.0	0.0	–	–	–	–
1998-1999	Elemental carbon	1.9	12.4	0.0	0.0	0.0	0.0	–	–	–	–
1998-1999	Missing mass	4.0	25.5	1.8	43.9	3.0	52.5	–	–	–	–
2018-2019	Mass	7.3	100.0	4.5	100.0	3.4	100.0	4.4	100.0	4.0	100.0
2018-2019	Organic matter	1.6	21.1	0.7	16.4	0.8	24.7	1.4	33.0	1.1	26.5
2018-2019	Nitrate	0.1	1.3	0.2	5.3	0.4	10.6	0.3	6.7	0.5	12.3
2018-2019	Sulfate	0.1	1.5	0.1	3.3	0.1	2.4	0.1	2.3	0.1	3.6
2018-2019	Mineral dust	1.8	24.1	0.8	18.1	1.1	33.0	1.4	32.6	1.0	24.7
2018-2019	Trace elements	1.8	24.6	0.8	18.9	0.4	10.8	0.5	10.3	0.2	5.7
2018-2019	Ammonium	0.0	0.0	0.0	0.0	0.0	0.0	0.0	0.0	0.1	2.1
2018-2019	Elemental carbon	0.2	2.1	0.1	1.3	0.0	1.2	0.1	1.7	0.0	0.9
2018-2019	Missing mass	1.9	25.3	1.6	36.7	0.6	17.3	0.6	13.4	1.0	24.1

$PM_{2.5-10}$ (Figure 10). OM in the coarse PM fraction is mostly primary biological particles[39] and minor additional contributions from aerosol dynamic processes such as coagulation of particles and condensation of semi-volatile organic compounds. However, it is known that with the applied analytical method carbon in carbonates (e.g. $CaCO_3$) can add to the measured amount of OC and consequently to the calculated OM concentration.[40] Carbonates are prevalent in natural mineral dust in Switzerland. Like mineral dust, carbonates are predominantly abundant in the coarse fraction of PM_{10}, *i.e.* in $PM_{2.5-10}$. The quantification of the contribution from
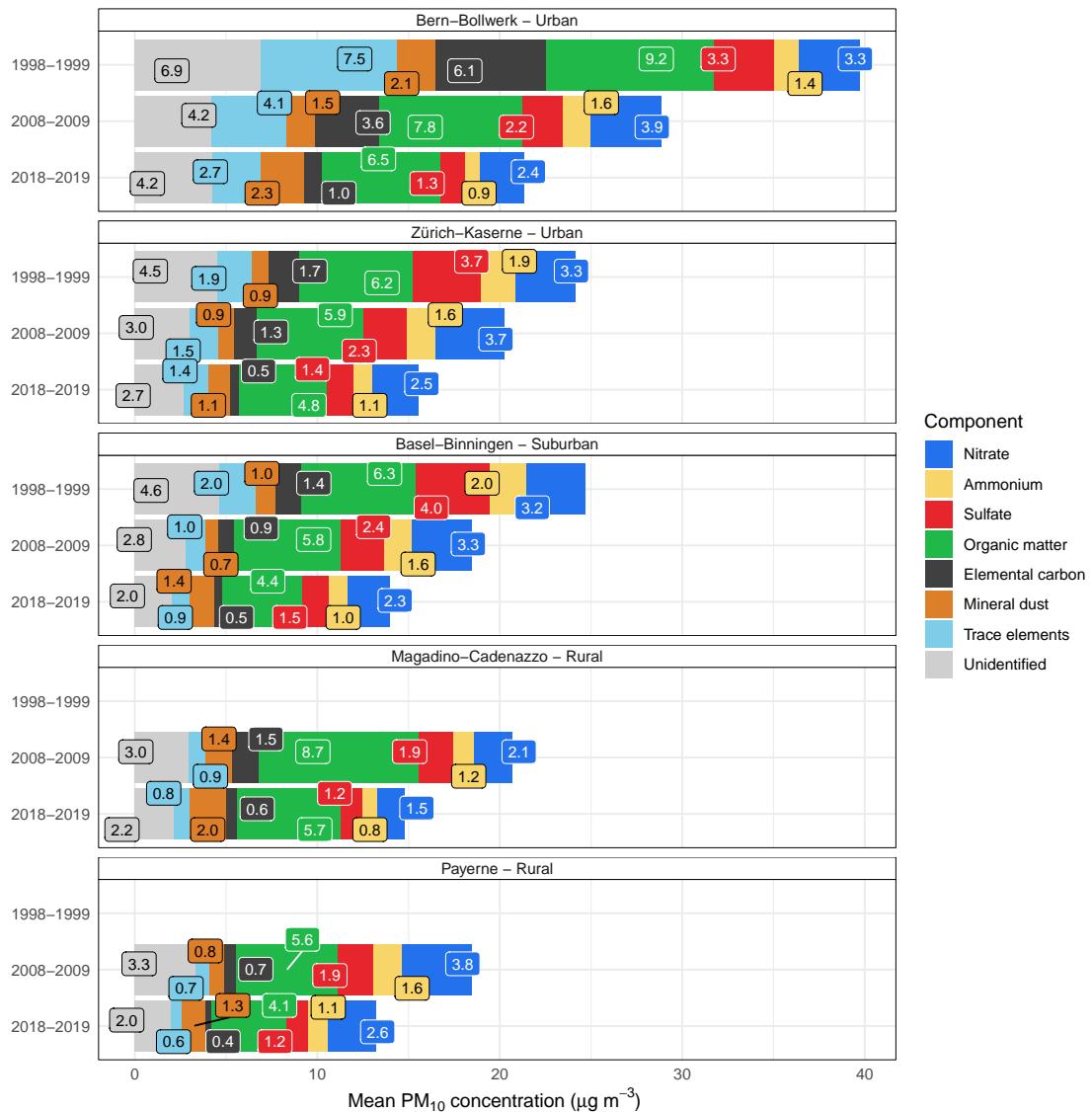
Figure 8 – Mean concentration of PM_{10} and the main chemical components of PM_{10} for five monitoring sites in Switzerland for the duration of the three field campaigns.

carbonates to OC is not possible with the analytical methods at hand. Nevertheless, it is clear that the interference from carbonates is largest at sites with high mineral dust concentrations, in particular the urban traffic site Bern-Bollwerk. The fact that the average OM concentration in $PM_{2.5-10}$ is clearly highest in Bern-Bollwerk might be an indication of a significant contribution from carbonates at this site.

Large fractions of PM_{10} and $PM_{2.5}$ are secondary inorganic aerosols, *i.e.* the sum of nitrate, sulfate and ammonium. The share of secondary inorganic aerosols in PM_{10} is between $3.5 \, \mu g \, m^{-3}$ (23.4 %) in Magadino-Cadenazzo and $5.0 \, \mu g \, m^{-3}$ (32.4 %) in Zürich-Kaserne. Secondary inorganic aerosols are predominantly abundant in the fine particle fraction, meaning that the percentage of secondary inorganic aerosols is for $PM_{2.5}$ even larger (29.4 % in Magadino-Cadenazzo and 42.5 % in Zürich-Kaserne). The lower relative as well as absolute share of
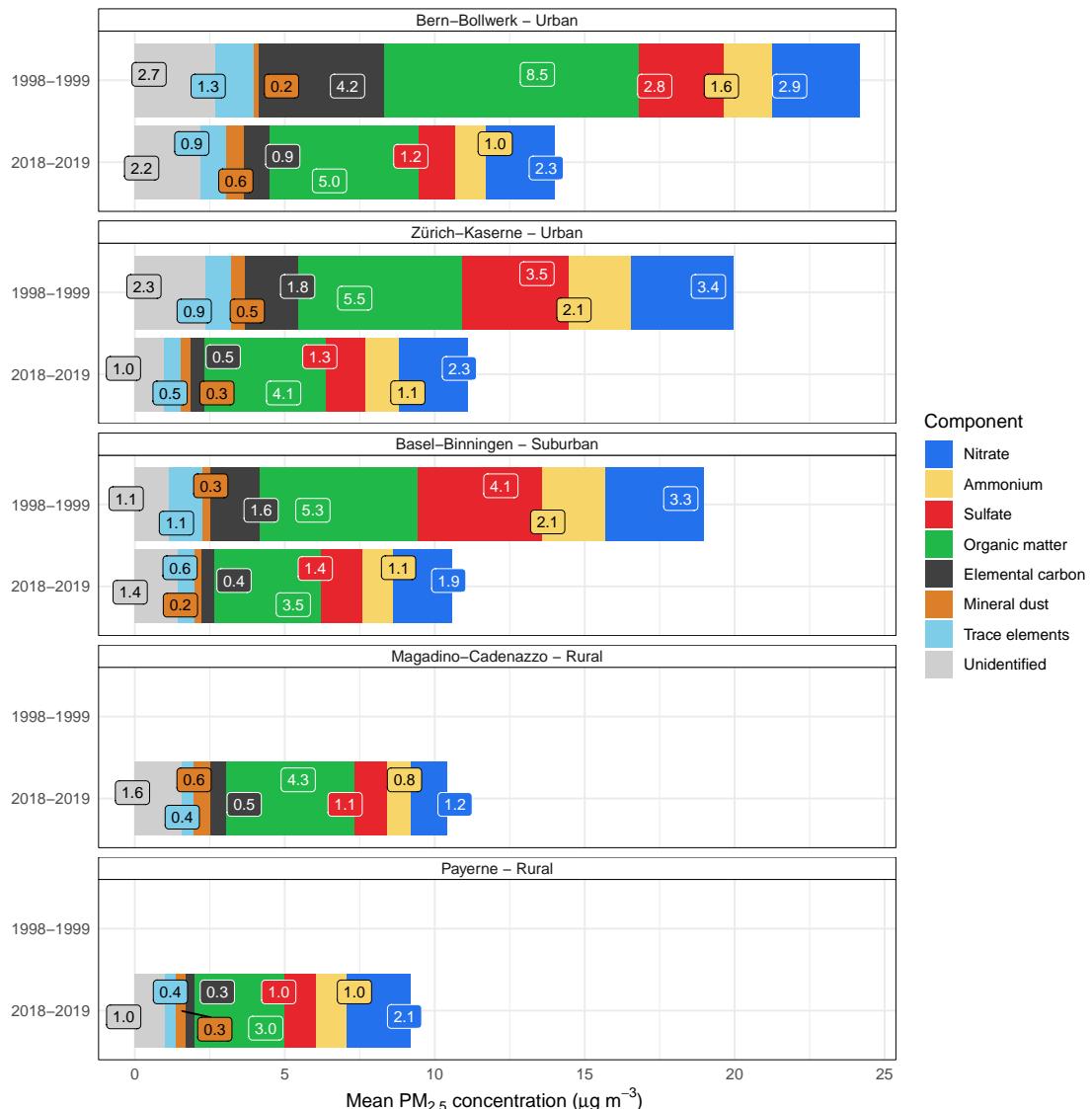
Figure 9 – Mean concentration of $PM_{2.5}$ and the main chemical components $PM_{2.5}$ for five monitoring sites in Switzerland for the duration of the field campaigns in 1998-1999 and 2018–2019. Note that $PM_{2.5}$ was not included in the field campaign in 2008–2009.

secondary inorganic aerosols in Magadino-Cadenazzo has already been described in Gianini et al. [15] and is explained by lower ammonium nitrate concentrations due to the warmer climate in Magadino-Cadenazzo. Warmer temperatures shift the thermodynamic equilibrium between particulate ammonium nitrate and gaseous ammonia and nitric acid towards the gas phase. The annual wet deposition of nitrate is, however, in Magadino-Cadenazzo higher than at Payerne and other sites north of the Alps.[4] In addition, it is interesting to note that a small fraction of nitrate in PM_{10} is found in the coarse fraction $PM_{2.5-10}$. Such coarse-mode nitrate is likely resulting from the reaction of nitric acid with calcium and magnesium carbonates.[41]

The large fraction of organic matter and secondary inorganic aerosols shows that the domi-nating part of PM_{10} and $PM_{2.5}$ in Switzerland is secondary PM, *i.e.* formed in the atmosphere by

chemical transformation of gaseous precursors. The involved transformation processes occur on hourly or daily timescales resulting in secondary PM that is spatially homogeneous on the regional scale. Consequently, the concentrations of nitrate, sulfate and ammonium are very similar at the three sites north of the Alps as shown in Figure 11 and Figure 12, where an alternative representation of the measured concentration of the main components of PM_{10} and $PM_{2.5}$ during the 2018–2019 period is given.

The increasing concentration gradient for PM_{10} and $PM_{2.5}$ from rural to urban and urban roadside environments is driven by local emissions of primary PM. Increasing primary particle emissions from anthropogenic sources lead to increasing concentrations of elemental carbon, organic matter and trace elements when moving from rural to urban environments. The effect of local emissions of primary PM_{10} and $PM_{2.5}$ is particularly visible at the urban traffic site Bern-Bollwerk, where resuspension of road dust as well as road and vehicle wear (e.g. break dust and tyre wear) lead to elevated concentrations of the calculated mineral dust component (see also subsection 2.5) as well as of trace elements (subsection 3.3).

Finally, 2.0–4.2 $\mu g \, m^{-3}$ of PM_{10} cannot be attributed with the applied analytical methods and remains missing (missing mass concentration in $PM_{2.5}$ ranges from 1.0–2.2 $\mu g \, m^{-3}$). Missing PM of this amount is known from the previous measurement periods and is typical for chemical PM characterisation studies.[13] The missing mass of PM_{10} and $PM_{2.5}$ can mainly be explained by three factors: First, main chemical constituents like ammonium, nitrate and sulfate are hygroscopic and take up water depending on the relative humidity of the air. Consequently, atmospheric PM contains an unaccounted amount of particle-bound water. Second, the mass concentration of OM has been calculated assuming an OM to OC ratio of 1.6 which is possibly too small and is likely resulting in too low OM concentrations (subsection 2.4). Third, the total concentration of mineral dust and trace elements is reported with assumptions about the oxidation state of the measured elements. The assumed mass of oxygen might be too small. Further discussions and insights in the nature of the unaccounted mass of PM in this study are given in subsection 3.2.

3.2 Chemical Composition of $PM_{2.5-10}$

The coarse PM fraction consists predominantly of trace elements, mineral dust, and organic matter (Figure 10; Table 7). The concentrations of secondary inorganic aerosols (*i.e.* ammonium, nitrate and sulfate) and elemental carbon are small. A significant part of the mass of $PM_{2.5-10}$ remains unaccounted for. The average relative share of the unaccounted mass in $PM_{2.5-10}$ is in all sampling locations except Magadino-Cadenazzo larger than in $PM_{2.5}$ and ranges from 13.4 % in Magadino-Cadenazzo to 36.7 % in Zürich-Kaserne. In absolute terms, the amount
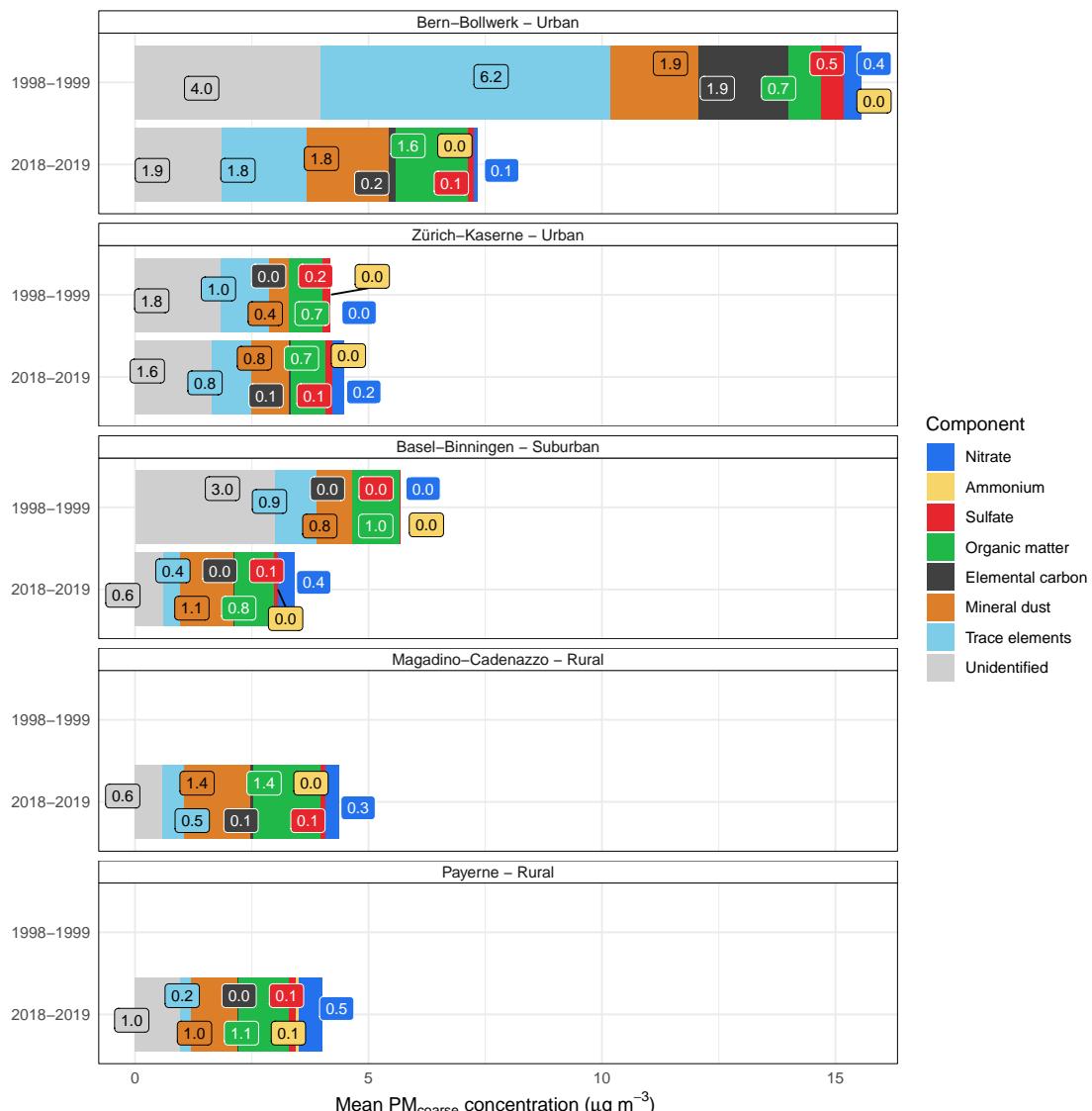
Figure 10 – Mean concentration of of coarse PM (PM$_{2.5-10}$) and the main chemical components of PM$_{2.5-10}$ for five monitoring sites in Switzerland for the duration of the field campaign 2018–2019. Note that PM$_{2.5}$ was not included in the field campaign in 2008–2009.

of unaccounted mass in PM$_{2.5-10}$ ranges from 0.6 µg m^{-3} in Basel-Binningen and Magadino-Cadenazzo up to 1.6 µg m^{-3} and 1.9 µg m^{-3} in Zürich-Kaserne and Bern-Bollwerk, respectively (Table 7).

The chemical composition of PM$_{2.5-10}$ as determined during the 2018–2019 measurement period by chemical analysis of PM$_{10}$ and PM$_{2.5}$ filter samples can be compared with the results from single particle analysis using SEM/EDX as obtained in the parallel project by Particle Vision GmbH[6]. In this accompanying project, SEM/EDX analysis was performed on PM samples that were independently collected with passive samplers. Two-weekly PM samples were collected at Bern-Bollwerk and Zürich-Kaserne using a so-called Sigma-2 sampler.[42] At Bern-Bollwerk an additional passive sampler that allows PM sampling for pre-defined time

48
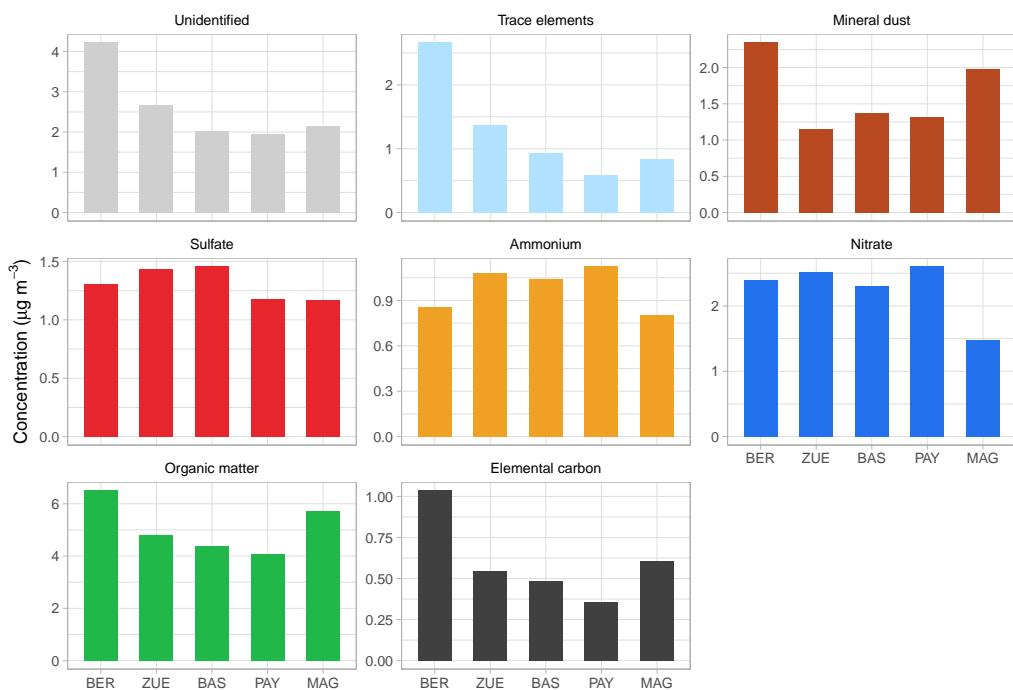
Figure 11 – Mean concentration of the main chemical components of PM_{10} during the field campaign 2018–2019 sorted for the type of site.
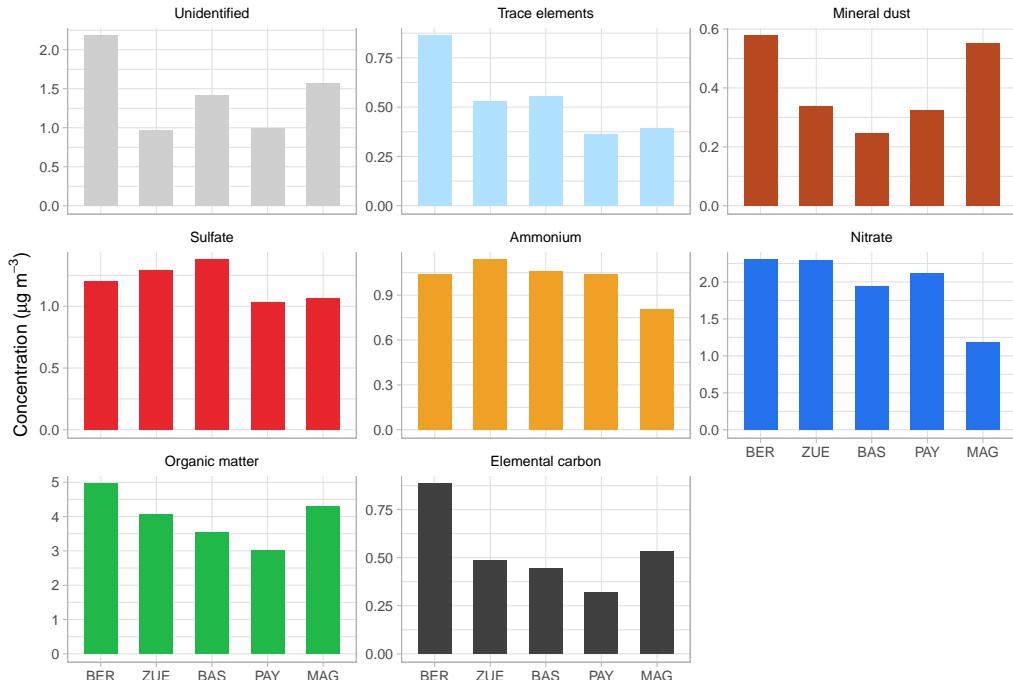

Figure 12 – Mean concentration of the main chemical components of $PM_{2.5}$ during the field campaign 2018–2019 sorted for the type of site.

intervals was operated (Sigma-Z sampler). The Sigma-Z sampler was deployed during periods of 32 days and PM sampling was synchronised with PM_{10} and $PM_{2.5}$ filter sampling for the 2018–2019 measurement period. Details of the sampling methods used are given in the separate project report.[6]

The agreement of the element concentrations in $PM_{2.5-10}$ from Bern-Bollwerk and Zürich-Kaserne obtained by SEM/EDX and ICP-MS/AES was for most elements remarkably good. An exception was Calcium, where SEM/EDX resulted in about 50 % higher concentrations compared to ICP-AES. Details of this comparison of sampling and analytical methods can again be found in the full report.[6] In contrast to ICP-MS/AES, SEM/EDX allowed quantitative measurements of all elements except hydrogen that contribute significantly to total PM mass, including oxygen, nitrogen and silicon. Consequently, adding up the mass concentrations of all elements gives an estimate of the total $PM_{2.5-10}$ mass concentration. Passive sampling combined with SEM/EDX resulted in mean $PM_{2.5-10}$ mass concentrations of 8.1 $\mu g\,m^{-3}$ in Bern-Bollwerk and 4.0 $\mu g\,m^{-3}$ in Zürich-Kaserne. Given the fundamentally different approaches, these values can be considered to be in good agreement with $PM_{2.5-10}$ determined by the gravimetric method (7.3 $\mu g\,m^{-3}$ in Bern-Bollwerk and 4.5 $\mu g\,m^{-3}$ in Zürich-Kaserne or percentage difference of -11.0 % and 11.1 %, respectively).

It can be summarised that on the one hand the mass closure calculation done for $PM_{2.5-10}$ within this study results in a large fraction of unaccounted mass. On the other hand, a good agreement of mass concentrations and element concentrations found in Bern-Bollwerk by the two above describe approaches has been observed. This indicates potential underestimation of PM mass that has not been measured but calculated based on sensible assumptions, in particular the estimation of silicon mass based on an assumed silicon to aluminum ratio (subsection 2.5) and the assumption of the mass contribution of non-carbon atoms in organic matter (e.g. oxygen, nitrogen and hydrogen, see subsection 2.4). As mentioned in subsection 2.5, the Si to Al ratio found by SEM/EDX were slightly higher (4.73 in Bern-Bollwerk and 3.79 Zürich-Kaserne) than the value of 3.62 that was used in this study. This difference in assumed and observed Si to Al ratio leads to an unaccounted silicon mass of 0.2 $\mu g\,m^{-3}$ in Bern-Bollwerk (or unaccounted mass of 0.43 $\mu g\,m^{-3}$ of SiO_2). In Zürich-Kaserne the difference is negligible.

Comparison of the oxygen mass concentration measured by SEM/EDX and the assumed oxygen mass concentration in $PM_{2.5-10}$ in this study is more difficult and care must be taken to avoid double counting. However, the average oxygen concentration measured by SEM/EDX was 2.9 $\mu g\,m^{-3}$ in Bern-Bollwerk and 1.5 $\mu g\,m^{-3}$ in Zürich-Kaserne.[6] For this project, the assumed oxygen mass concentration in the calculated contributions from mineral dust and trace elements

to $PM_{2.5-10}$ were 1.2 $\mu g\,m^{-3}$ in Bern-Bollwerk and 0.6 $\mu g\,m^{-3}$ in Zürich-Kaserne. Based on the used OM/OC multiplier of 1.6 and assuming that all non-carbon atoms in organic matter is oxygen, additional maximum oxygen mass concentration of 0.6 $\mu g\,m^{-3}$ in Bern-Bollwerk and 0.3 $\mu g\,m^{-3}$ in Zürich-Kaserne can be added, leading to a total assumed oxygen mass concentration of 1.8 $\mu g\,m^{-3}$ in Bern-Bollwerk and 0.9 $\mu g\,m^{-3}$ in Zürich-Kaserne. Although this is a rather simple and rough calculation, it indicates that in the mass closure performed within this study, the mass concentration of oxygen is underestimated by about 1.1 $\mu g\,m^{-3}$ in Bern-Bollwerk and 0.6 $\mu g\,m^{-3}$ in Zürich-Kaserne. This underestimation of oxygen explains a substantial fraction of the unaccounted mass in $PM_{2.5-10}$ (Table 7). It is interesting to note that the mass concentration of nitrogen and also phosphor in $PM_{2.5-10}$ as found by SEM/EDX was small (< 0.1 $\mu g\,m^{-3}$ in Bern-Bollwerk and Zürich-Kaserne).[6]

Finally, the amount of carbon determined by SEM/EDX was about double the concentration of total carbon measured by using the TOT/EUSAAR2 method. Lighter elements like carbon can only semi-quantitatively be detected by the SEM/EDX technique, its concentration is therefore likely overestimated. On the other hand, it is known from the literature, that carbonate carbon adds to the OC signal when using the TOT/EUSAAR2 method.[40] This can lead to a misclassification of carbonate carbon as organic carbon. For this reason, the TOT/EUSAAR2 method is only defined as a reference method for $PM_{2.5}$ where the amount of carbonate is minor.[21] Despite this potential misclassification of carbonate carbon, the total amount of carbon in $PM_{2.5-10}$ as determined with the TOT/EUSAAR2 method can expected to be accurate.

3.2.1 Identified particle types and main chemical components of $PM_{2.5-10}$

SEM/EDX analysis allowed the identification and quantification of four dominating types of particles in coarse PM: biogenic-organic particles dominated by carbon and oxygen (pollen, spores, etc.); mineral particles (road dust and road wear, crustal matter, dust from construction works); mixed tyre wear particles (tyre rubber including encrusted road wear particles); and, finally, metallic particles dominated by iron and oxygen (vehicle wear, railway related wear, industry). The mean concentration of $PM_{2.5-10}$ and the concentration of the identified particle types in $PM_{2.5-10}$ at Bern-Bollwerk and Zürich-Kaserne are listed in Table 8.

The concentrations of the different particle classes as identified by SEM/EDX cannot directly be compared with the chemical composition data of this study, because the identified particle classes do not exactly match the determined main chemical components of $PM_{2.5-10}$. Nevertheless, some of the results are worth to be discussed.

The mass concentration of the class of biogenic-organic particles in $PM_{2.5-10}$ agrees reason-

ably well with the concentration of organic matter. It should, however, be kept in mind that the mass concentration of carbon as measured by SEM/EDX as well as by TOT/EUSAAR2 have high measurement uncertainties as detailed in subsection 3.2. Nevertheless, the concentration of OM as calculated based on TOT/EUSAAR2 analyses is in Bern-Bollwerk slightly larger than the mass concentration of the biogenic-organic class (1.6 $\mu g\,m^{-3}$ compared to 1.4 $\mu g\,m^{-3}$), whereas in Zürich-Kaserne the concentration of OM is smaller than the concentration of carbonaceous particles (0.7 $\mu g\,m^{-3}$ compared to 1.0 $\mu g\,m^{-3}$). However, some fraction of the particles classified by SEM/EDX as an internal mixture of tyre wear and road wear certainly contain additional organic compounds. The average mass fraction of tyre wear (*i.e.* tyre rubber) in this class of particles was determined to be 49%, the remaining 51% of the mass was attributed to road wear.[6] Organic compounds in tyre wear particles can therefore assumed to be more than sufficient for closing the gap between the mass concentration of organic particulate matter in $PM_{2.5-10}$ as determined by SEM/EDX and by TOT/EUSAAR2 in Bern-Bollwerk. For Zürich-Kaserne, the amount of tyre wear in $PM_{2.5-10}$ is small and its contribution to the total mass concentration of organic compounds determined by SEM/EDX is therefore minor. The reason for the smaller mass concentration of OM (based on TOT/EUSAAR2) compared to the mass concentration of the biogenic-organic particle class (based on SEM/EDX) at the Zürich-Kaserne site remains unknown. However, it can be speculated that this concentration gap results from the combined limitations associated with the applied analytical techniques (see subsection 3.2). Nevertheless, the particle classification based on SEM/EDX analysis confirms the higher concentration of organic matter in $PM_{2.5-10}$ at the urban traffic site Bern-Bollwerk compared to the urban background site Zürich-Kaserne.

For comparison of the concentration of mineral particles in $PM_{2.5-10}$ as obtained by the two different methods, it is sensible to add the mass fraction of road wear in the mixed tyre wear and road wear particle class to the mass concentration of the mineral particles class. This simple calculation leads to a total mineral particles concentration of 4.3 $\mu g\,m^{-3}$ in Bern-Bollwerk and 2.3 $\mu g\,m^{-3}$ in Zürich-Kaserne. These values are clearly higher than the mineral dust concentration based on the element analysis using ICP-AES and ICP-MS (1.6 $\mu g\,m^{-3}$ in Bern-Bollwerk and 0.8 $\mu g\,m^{-3}$ in Zürich-Kaserne). In order to achieve a good agreement between the mineral dust concentration as determined from element analysis of PM filter samples and mineral particles determined by SEM/EDX, it is necessary to attribute all of the missing mass to be mineral dust. A detailed comparison of the quantification of those elements that could potentially have a large influence on the calculation of mineral dust concentrations (i.e. Si, O and C) has been discussed in subsection 3.2.

The concentration of the class of metallic particles identified by SEM/EDX and found to be dominated by iron and oxygen Rausch et al. [6], can be compared to the iron concentration in $PM_{2.5-10}$ measured by ICP/AES. Subtracting the mass of the mineral dust contribution to the measured iron concentrations in $PM_{2.5-10}$ (subsection 2.4) and assuming that the remaining iron of antropogenic origin is present as iron oxide (Fe_2O_3), leads to iron oxide concentrations in $PM_{2.5-10}$ of 1.1 $\mu g\,m^{-3}$ in Bern-Bollwerk and 0.5 $\mu g\,m^{-3}$ in Zürich-Kaserne. These values are lower but reasonably close to the concentration of metallic particles listed in Table 8.

In summary, a good agreement of the results deduced from the two complementary chemical characterization approaches can be noted. Moreover, it can be concluded from these analyses that $PM_{2.5-10}$ in Switzerland is almost exclusively composed of primary particles.

Table 8 – Mean concentration of the dominating types of particles in $PM_{2.5-10}$ as identified by single particle analysis (SEM/EDX) of samples collected using a passive sampling method. For Bern-Bollwerk, the results obtained from samples collected with the Sigma-Z sampler are listed. For details see the full project report by Rausch et al. [6]

Particle class	Bern-Bollwerk $\mu g\,m^{-3}$	Zürich-Kaserne $\mu g\,m^{-3}$
Biogenic/organic particles	1.4	1.0
Mineral particles	3.4	2.1
Mixed tyre wear and road wear particles	1.8	0.3
Metallic particles	1.4	0.6
Total mass	8.1	4.0

3.2.2 Tyre wear particles in $PM_{2.5-10}$ and PM_{10}

One of the important results of the single particle analysis using SEM/EDX is the identification and quantification of tyre wear particles (Table 8). Based on the above mentioned mass fractions of tyre wear and road wear particles in the corresponding mixed particles class, the mass concentration of tyre wear (tyre rubber) in $PM_{2.5-10}$ can easily be calculated. The mass concentration of tyre rubber in $PM_{2.5-10}$ at the urban traffic site Bern-Bollwerk is 1.08 $\mu g\,m^{-3}$ or 14.8% in relation to the $PM_{2.5-10}$ mass concentration determined with the gravimetric method. At the urban background site Zürich-Kaserne, tyre rubber contributes 0.15 $\mu g\,m^{-3}$ (3.5%) to $PM_{2.5-10}$.

Tyre wear particles were almost exclusively found in the coarse fraction of PM_{10}. The mean concentration of tyre wear in the size range between PM_1 and $PM_{2.5}$ was 0.03 $\mu g\,m^{-3}$ in Bern-Bollwerk and 0.01 $\mu g\,m^{-3}$ in Zürich-Kaserne.[6] Note that the applied passive PM sampling method is not capable of quantitative sampling of particles smaller than 1 μm and the amount of tyre wear in PM_1 could not be determined. However, it is known from the literature, that virtually all tyre wear particles are larger than 1 μm and the mass contribution of tyre wear

to PM_1 is negligible.[26] Consequently, the annual mean mass fraction of tyre wear in PM_{10} at the urban traffic site Bern-Bollwerk and the urban background site Zürich-Kaserne can be calculated to be 1.13 $\mu g\,m^{-3}$ (5.3%) and 0.16 $\mu g\,m^{-3}$ (1.0%), respectively. Again, the percentage contribution of tyre wear was calculated relative to the mass concentration of PM_{10} obtained with the gravimetric method (Table 5). Although beyond the scope of this study, it is worth mentioning that most of the airborne tyre wear was associated with particles larger than ten micrometer. At the urban traffic site Bern-Bollwerk and the urban background site Zürich-Kaserne, the mass concentration of tyre rubber in the particle size range from 10 μm to 80 μm was found to be 5.49 $\mu g\,m^{-3}$ and 0.59 $\mu g\,m^{-3}$, respectively.[6] Strongly decreasing concentrations with the distance to busy roads can be expected for the larger tyre wear particles with diameters from 10 μm to 80 μm. However, the found concentration in the urban background in Zürich-Kaserne appears to be surprisingly high. Typical deposition velocities of supermicron particles as available in textbooks (e.g. Seinfeld and Pandis [43]) and a simple calculation of the dry atmospheric deposition leads for Zürich-Kaserne to remarkably high dry deposition rates in the order of one gram per square metre and year at the Zürich-Kaserne site. Note that this estimate is only very rough, however, the observed mean concentration of tyre wear particles at Zürich-Kaserne could be an argument for targeted and more detailed investigations at locations not directly exposed to road traffic.

3.3   Trace elements in PM_{10} and $PM_{2.5}$

The concentration of the measured trace elements in PM_{10} and $PM_{2.5}$ are listed in Table 9 and Table 10. Only a few trace elements contribute noticeably to the total PM mass concentrations. These are Aluminum, Calcium, Iron, Potassium, Sodium and Chlorine, the latter is represented by Chloride. Furthermore, average Sulfur concentrations in PM_{10} and $PM_{2.5}$ are about 0.4–0.5 $\mu g\,m^{-3}$, the comparison with measured sulfate concentration indicates that sulfur is entirely present as sulfate. Since Aluminum is exclusively attributed to mineral dust, the mass concentration of the main chemical component in PM_{10} and $PM_{2.5}$ denoted as trace elements is dominated by the concentrations of Sodium, Chloride and the anthropogenic fractions of Calcium, Iron and Potassium. The concentration of all other measured elements in PM_{10} and $PM_{2.5}$ is small and well below 0.1 $\mu g\,m^{-3}$. The small contribution to PM mass concentrations does however not mean that all these trace elements are unimportant for air quality. There is indication that some trace elements are relevant indicators for air quality that can be linked to negative health impacts.[3] Some trace elements show clear site type gradients with increasing concentrations from rural to urban and roadside environments (subsection 3.4). This allows drawing conclusions about sources of corresponding trace elements which is also of importance

for the identification of sources of PM_{10} and the determination of their contributions (section 5).

In order to provide an overview of the distribution of trace elements and main constituents between $PM_{2.5}$ and the coarse particle fraction $PM_{2.5-10}$, their mean percentage contribution of $PM_{2.5}$ to PM_{10} is shown in Figure A.7. Table A.2 lists the measured mean concentration of trace elements in $PM_{2.5-10}$.

Table 9 – Mean concentration of elements in PM_{10} for the 2018–2019 measurement period. Values are in $ng\,m^{-3}$ and have been rounded to three significant figures and three decimal places. For elements that have been measured by two different methods, both mean values are listed in order to facilitate a comparison of results.

Variable	Method	Bern-Bollwerk	Zürich-Kaserne	Basel-Binningen	Magadino-Cadenazzo	Payerne
Lithium	ICP-MS	0.096	0.054	0.077	0.102	0.055
Sodium	ICP-OES	196	108	150	100	97.8
Sodium	IC	200	109	141	81.2	90.3
Magnesium	ICP-OES	69.3	44.9	42.2	53.2	35.4
Magnesium	IC	42.2	34.2	29.9	24.6	19.5
Aluminium	ICP-OES	181	86.8	106	161	102
Phosphorus	ICP-OES	17.1	13.1	13.3	20.1	13.1
Sulfur	ICP-OES	497	504	512	417	408
Potassium	ICP-OES	276	214	250	182	188
Potassium	IC	252	202	225	149	168
Calcium	ICP-OES	537	317	212	202	173
Calcium	IC	541	321	231	206	187
Scandium	ICP-MS	0.049	0.028	0.025	0.066	
Titanium	ICP-MS	10.8	7.1	5.27	8.87	5.25
Vanadium	ICP-MS	0.522	0.312	0.287	0.479	0.269
Chromium	ICP-MS	3.66	1.72	0.976	1.78	
Manganese	ICP-MS	11.2	5.79	3.65	4.77	2.82
Iron	ICP-OES	1080	478	236	341	152
Cobalt	ICP-MS	0.132	0.089	0.085	0.108	0.04
Nickel	ICP-MS	0.571				
Copper	ICP-MS	46.5	18.4	7.38	8.2	4.66
Zinc	ICP-MS	27.5	18.4	13.6	11.4	10.1
Gallium	ICP-MS	0.064	0.033	0.045	0.052	0.027
Arsenic	ICP-MS	0.288	0.242	0.282	0.325	0.539
Selenium	ICP-MS	0.022			0.031	0.029
Rubidium	ICP-MS	0.785	0.515	0.635	0.681	0.586
Strontium	ICP-MS	3.33	2.32		0.917	0.828
Yttrium	ICP-MS	0.059			0.044	
Zirconium	ICP-MS	2.95	2.44	1.8	2.16	
Niobium	ICP-MS	0.053	0.06	0.097		
Cadmium	ICP-MS	0.069	0.066	0.064	0.072	0.048
Tin	ICP-MS	6.19	2.66	1.25	1.63	1.06
Antimony	ICP-MS	4.82	1.63	0.835	0.952	0.58
Cesium	ICP-MS	0.008		0.02	0.004	0.05
Barium	ICP-MS	15.4	5.93		3.31	1.58
Lanthanum	ICP-MS	0.227	0.104	0.09	0.09	0.066
Cerium	ICP-MS	0.492	0.193	0.156	0.163	0.121
Praseodymium	ICP-MS	0.026	0.01	0.013	0.017	0.011
Neodymium	ICP-MS	0.103	0.041	0.047	0.052	0.042
Samarium	ICP-MS	0.021		0.01	0.01	0.01
Europium	ICP-MS	0.003	0.003			
Gadolinium	ICP-MS	0.011			0.006	
Terbium	ICP-MS	0.009				
Dysprosium	ICP-MS	0.01				
Erbium	ICP-MS				0.005	
Ytterbium	ICP-MS	0.007			0.003	
Hafnium	ICP-MS	0.123	0.086	0.072	0.102	
Tungsten	ICP-MS	0.054	0.022		0.059	
Thallium	ICP-MS					0.023
Lead	ICP-MS	3.61	2.82	2.87	2.54	2.23
Bismuth	ICP-MS	0.473	0.62		0.149	0.152
Thorium	ICP-MS	0.027			0.015	
Uranium	ICP-MS	0.029			0.01	
Chloride	IC	179	39.9	55.4	35.4	27.3
Ammonium	IC	856	1080	1040	804	1130
Nitrate	IC	2390	2530	2310	1480	2610
Sulfate	IC	1310	1440	1460	1170	1180

Table 10 – Mean concentrations of elements in $PM_{2.5}$ for the 2018–2019 measurement period. Values are in $ng\,m^{-3}$ and have been rounded to three significant figures and three decimal places. For elements that have been measured by two different methods, both mean values are listed in order to facilitate a comparison of results.

Variable	Method	Bern-Bollwerk	Zürich-Kaserne	Basel-Binningen	Magadino-Cadenazzo	Payerne
Lithium	ICP-MS	0.016	0.017	0.021	0.014	
Sodium	ICP-OES	55.1	31.4	72.8	31.1	38.7
Sodium	IC	53.3	38.4	65.3	25.3	37
Magnesium	ICP-OES	18.2	12.4	14	12.8	9.21
Magnesium	IC	15.3	10.6	12.7	6.44	6.37
Aluminium	ICP-OES	48.5	28.1	19.9	48.1	26.9
Phosphorus	ICP-OES	4.32	5.93	5.44	1	1.35
Sulfur	ICP-OES	421	438	461	368	345
Potassium	ICP-OES	235	183	217	128	133
Potassium	IC	230	179	203	116	140
Calcium	ICP-OES	118	63.4	43.1	43.2	32.2
Calcium	IC	140	84.1	73.6	80.5	69.3
Scandium	ICP-MS	0.03	0.024	0.035		
Titanium	ICP-MS	2.88	1.97	1.47	1.9	0.895
Vanadium	ICP-MS	0.198	0.157	0.178	0.241	0.144
Chromium	ICP-MS	1.38	0.969		0.625	0.825
Manganese	ICP-MS	3.61	2.1	1.71	1.59	1.11
Iron	ICP-OES	232	108	66.3	88.3	41.7
Cobalt	ICP-MS	0.058	0.026	0.032	0.042	
Copper	ICP-MS	10.2	5.56	3.76	2.63	1.74
Zinc	ICP-MS	15.8	14.8	13.1	9.38	7.31
Gallium	ICP-MS	0.039	0.011	0.025		0.01
Arsenic	ICP-MS	0.265	0.229	0.243	0.235	0.496
Selenium	ICP-MS		0.016	0.034	0.018	
Rubidium	ICP-MS	0.602	0.407	0.514	0.441	0.464
Strontium	ICP-MS	1.84			0.342	0.441
Yttrium	ICP-MS				0.06	
Zirconium	ICP-MS	2.3	1.86	4.13	4.18	1.23
Niobium	ICP-MS	0.031		0.061	0.063	0.039
Cadmium	ICP-MS	0.071	0.057	0.064	0.065	0.019
Tin	ICP-MS	1.21	0.724	0.542	0.651	0.489
Antimony	ICP-MS	1.58	0.695	0.512	0.499	0.305
Cesium	ICP-MS					0.041
Barium	ICP-MS	2.08	2.53			
Lanthanum	ICP-MS	0.087	0.054	0.02	0.044	0.023
Cerium	ICP-MS	0.209	0.113	0.019	0.066	0.044
Neodymium	ICP-MS	0.024			0.031	0.012
Samarium	ICP-MS	0.005			0.018	
Gadolinium	ICP-MS				0.013	
Terbium	ICP-MS	0.005			0.011	
Dysprosium	ICP-MS				0.019	
Holmium	ICP-MS				0.023	
Ytterbium	ICP-MS				0.009	
Hafnium	ICP-MS	0.087	0.081	0.194	0.208	0.052
Tungsten	ICP-MS			0.034		
Thallium	ICP-MS					0.018
Lead	ICP-MS	2.63	2.36	2.29	2.1	1.85
Bismuth	ICP-MS	0.173	0.364		0.067	0.081
Chloride	IC	28.7	14.7	21.2	10.1	11.8
Ammonium	IC	1040	1140	1060	804	1040
Nitrate	IC	2300	2290	1940	1190	2110
Sulfate	IC	1200	1290	1380	1070	1030

3.4 Urban and roadside increments of PM_{10} and $PM_{2.5}$

Pollutant concentrations in an urban area can be conceptualised of as a combination of pollutants sourced directly from the urban area, added to a regional background component.[44] Regional background concentrations can be further split into non-anthropogenically enhanced concentrations (a true "natural" component), and an enhanced amount from direct emissions and secondary generation from precursors outside the immediate urban area.[45] Urban and roadside increments refer to increases in concentrations which reflect increased emissions from more intensive resource consumption in these specific environments. The urban and roadside increments can be very variable and are subjected to complex atmospheric dispersion processes as well as variable emission processes, however, they also feedback, especially in the case of PM, to the regional background component. Following this concept, the urban and roadside increments of PM_{10} and $PM_{2.5}$ as well as of constituents of PM can be calculated from mean concentration differences at representative sites. In particular, the urban increment can be calculated as the difference from measurements in Zürich-Kaserne and Payerne[46] and the roadside increment can be expressed as the difference in concentrations at Bern-Bollwerk and Zürich-Kaserne. Figure 13 and Figure 14 show the calculated absolute and relative urban and roadside increments of mass concentrations and the concentrations of the main constituents of PM_{10} and $PM_{2.5}$. For calculation of the relative urban and roadside increments denoted as urban enrichment (UE) and roadside enrichment (RE), the concentration differences were divided by the mean concentrations at the urban site (Zürich-Kaserne) and the urban roadside site (Bern-Bollwerk), respectively.[15,47]

As already outlined in subsection 3.1, the concentrations of secondary inorganic aerosols (ammonium, sulfate and nitrate) are homogeneous on the regional scale and and their concentrations are not higher in urban environments. The urban increment of PM_{10} mass concentration is almost exclusively due to urban emissions of primary particulate matter such as primary organic matter, trace elements, elemental carbon and for mineral dust (only roadside increment). Their marked enrichment in urban roadside environments demonstrates that road traffic is an important source of these chemical components. For $PM_{2.5}$, it can be seen that both urban and roadside increments of trace elements and mineral dust are much smaller, urban emissions of these constituents are predominantly in the coarse PM fraction.

It is interesting to look at urban and roadside increments and the enrichment of a selection of elements in PM_{10} and $PM_{2.5}$ (Figure 15 and Figure 16). Almost all elements measured with a good signal to noise ratio show an enrichment in urban environments. In agreement with the evaluation of element concentrations for the 2008–2009 measurement period in Gianini et al.
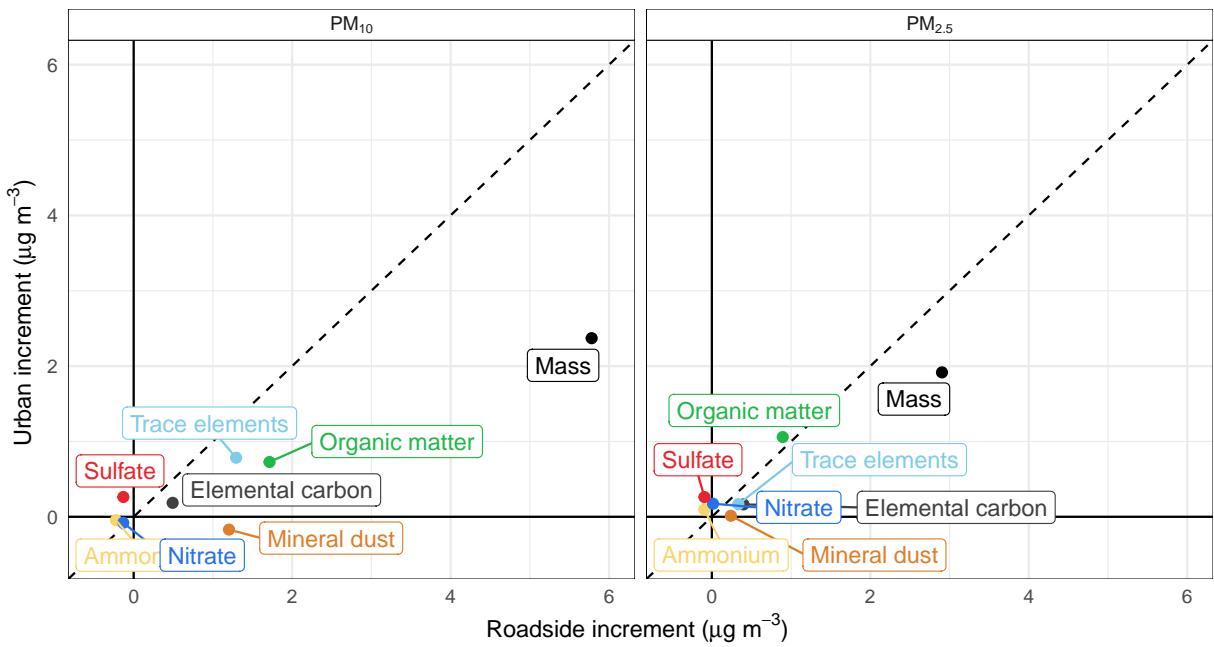
Figure 13 – Urban increment versus roadside increment of the mass concentration and the concentration of main chemical constituents in PM_{10} (left) and $PM_{2.5}$ (right) for the 2018–2019 measurement periods. The urban increment was calculated from the concentration differences at the urban site Zürich-Kaserne and the rural site Payerne, whereas the roadside increment has been derived from the concentration differences at the urban roadside site Bern-Bollwerk and the urban site Zürich-Kaserne.
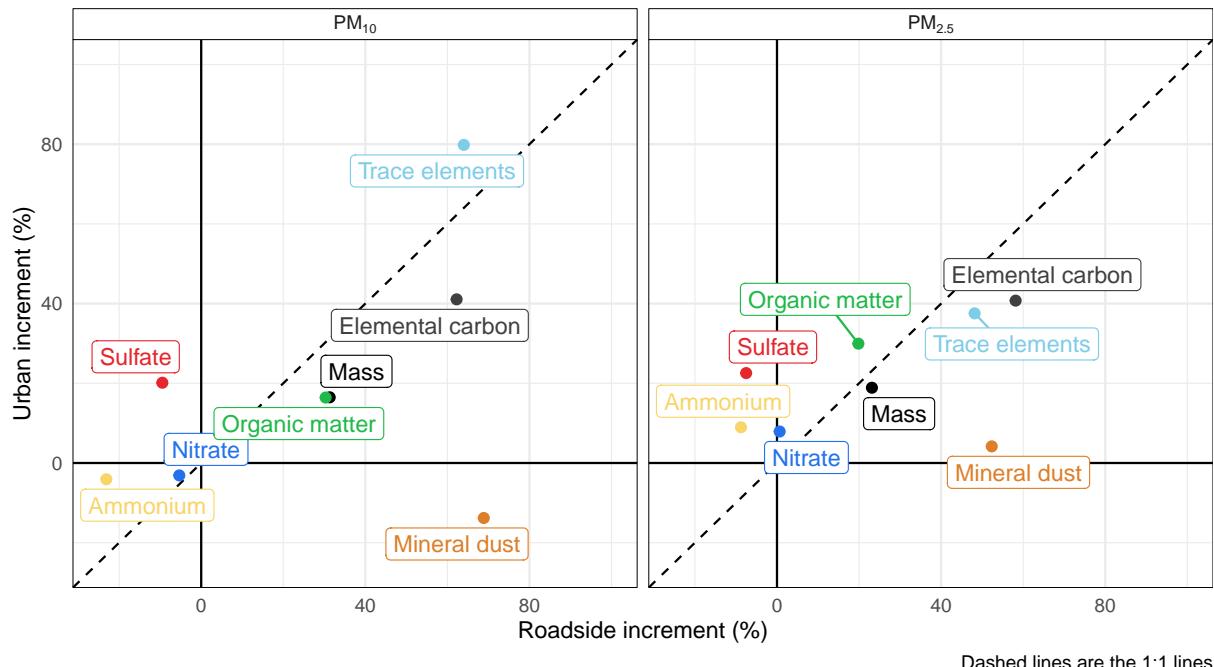
Figure 14 – Urban enrichment versus roadside enrichment of the mass concentration and the concentration of main chemical constituents in PM_{10} (left) and $PM_{2.5}$ (right) for the 2018–2019 measurement period.
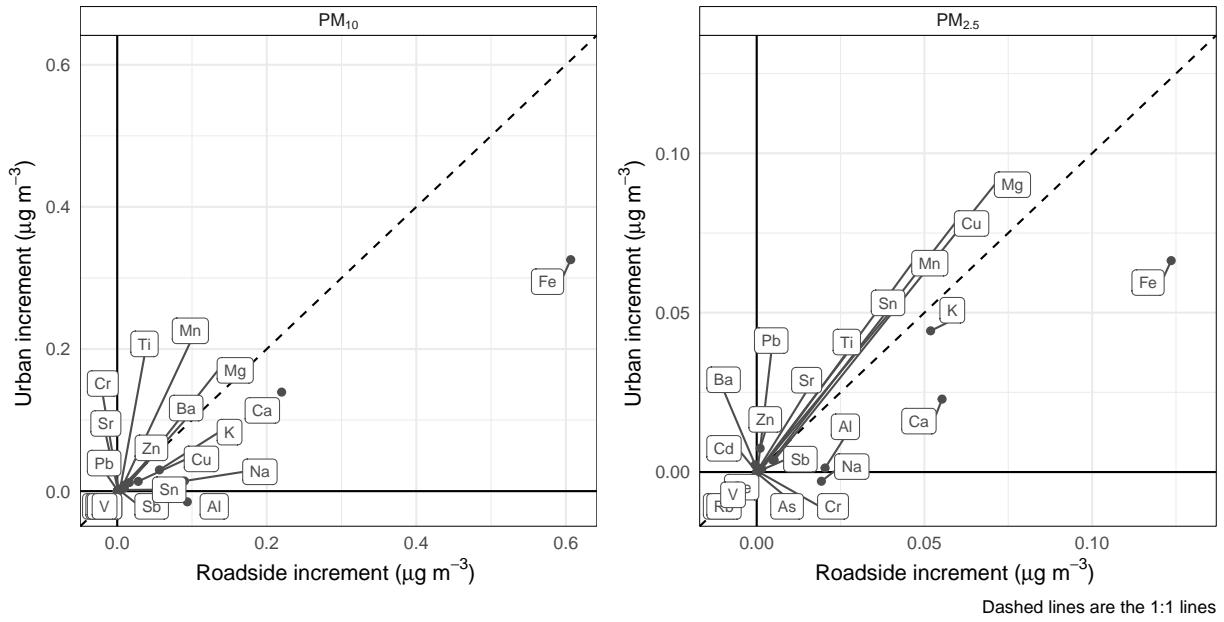
Figure 15 – Urban increment versus roadside increment of a selection of elements in PM$_{10}$ (left) and PM$_{2.5}$ (right) for the 2018–2019 measurement periods. Note the different scales of the y-axes.
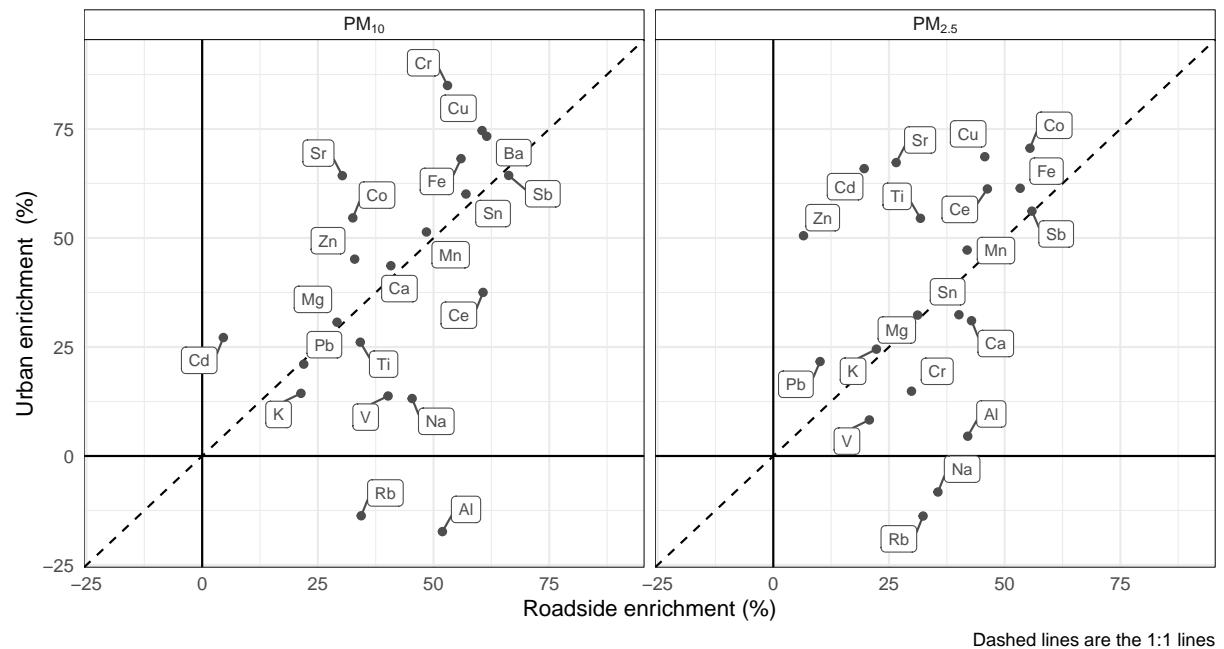
Figure 16 – Urban enrichment versus roadside enrichment of a selection of elements in PM$_{10}$ (left) and PM$_{2.5}$ (right) for the 2018–2019 measurement periods.

[15], a group of elements with high urban and roadside enrichment in PM$_{10}$ (UE and RE > 35 %) can be identified. This group of elements includes Ba, Cr, Cu, Fe, Sb, Sn, Ca, Mn, Co, Sr, Ce and Zn, elements that are associated with non-exhaust road traffic emissions from resuspension of road dust as well as road and vehicle wear.[5,48] Except iron, these elements do not play a role for total PM mass concentration, there are, however, indications that they are important for health

impacts of PM.[3] Further elements with clear roadside enrichment (RE > 35 %) but small urban enrichement (UE < 35 %) are Al, Na, and V. In contrast to the first group, these elements show no clear urban enrichment. Finally, there is a third group of elements that show only a small or moderate urban and roadside enrichment (Cd, K, Mg, Pb, Ti, Rb). These elements appear to result predominantly from long-range transport or from sources that are similarly active in rural environments outside the cities. Urban and roadside increments and enrichments in $PM_{2.5}$ are similar to those in PM_{10}, although the concentration of most elements is much lower. It should be noted that the shown urban and roadside enrichments of element have rather large uncertainties as the calculation often involves the division of small numbers. Nevertheless, Figure 15 and Figure 16 allow an unambiguous identification of elements that are characteristic for non-exhaust emissions from road traffic, facilitating the interpretation of source profiles calculated in section 5.
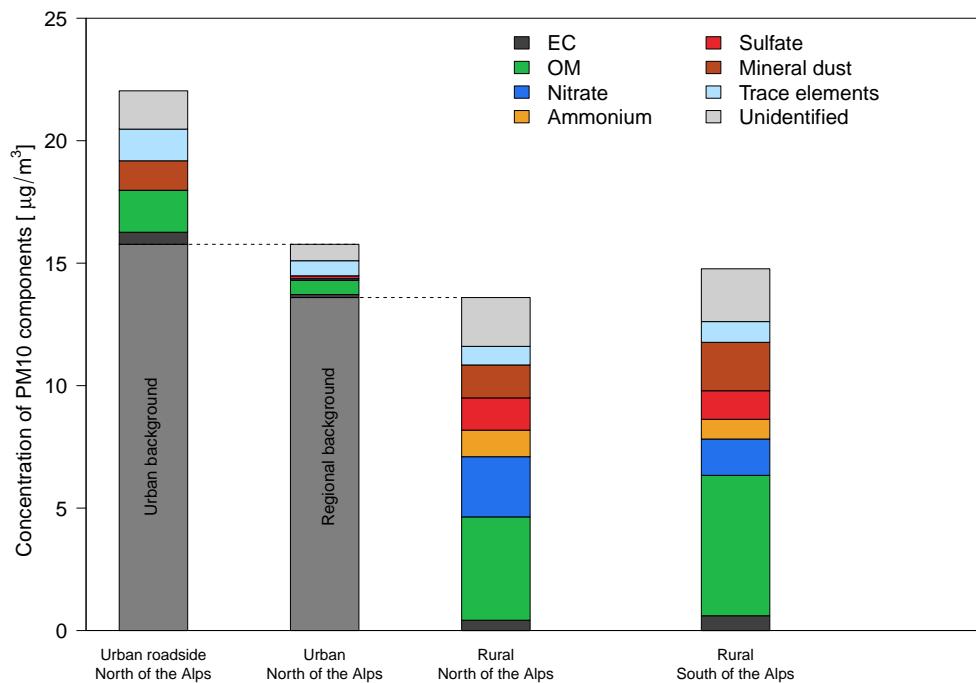
Figure 17 – Summary of mean chemical composition of PM_{10} for the 2018–2019 measurement period at a rural site south of the Alps (Magadino-Cadenazzo) and at regional background sites north of the Alps (mean of suburban site Basel-Binningen and rural site Payerne). The composition of the urban increment and the roadside increment as derived from the chemical composition data from Zürich-Kaserne and Bern-Bollwerk respectively is also shown.

Figure 17 and Figure 18 provide an overview and comparison of the chemical composition of PM_{10} and $PM_{2.5}$ for typical environments in Switzerland as derived from the chemical characterization at the five representative sites. This approach of comparing typical composition
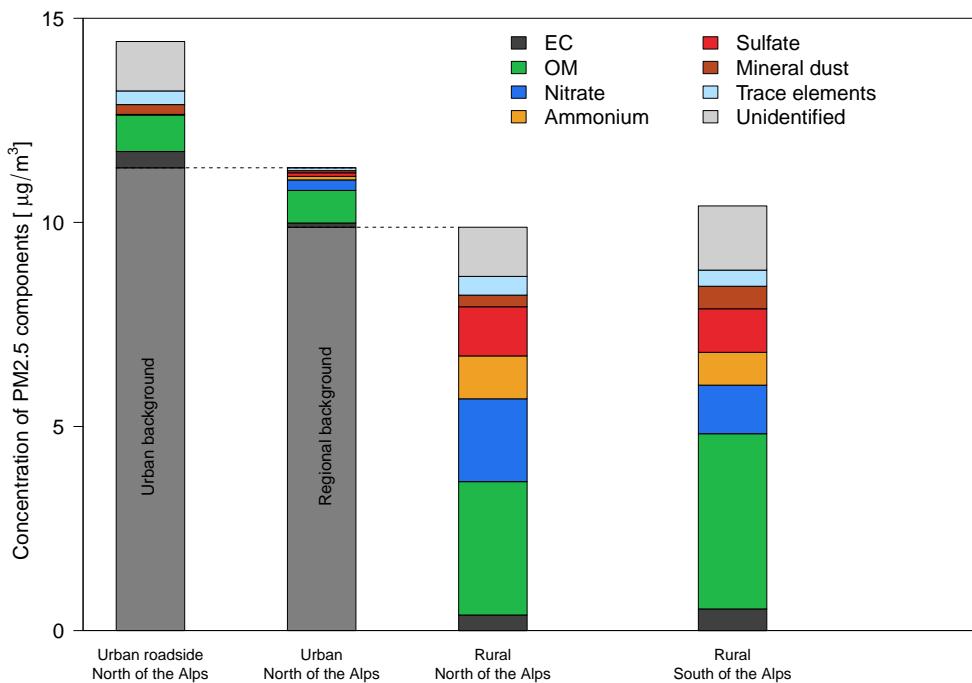
Figure 18 – Summary of mean chemical composition of PM$_{2.5}$ for the 2018–2019 measurement period at a rural site south of the Alps (Magadino-Cadenazzo) and at regional background sites north of the Alps (mean of suburban site Basel-Binningen and rural site Payerne). The composition of the urban increment and the roadside increment as derived from the chemical composition data from Zürich-Kaserne and Bern-Bollwerk respectively is also shown.

in rural, urban and urban roadside environments incorporates large uncertainties due to the relatively small number of samples analysed. However, Figure 17 and Figure 18 illustrate that atmospheric particulate matter (PM$_{10}$ and PM$_{2.5}$) in rural environments can generally be understood as a homogeneously distributed regional background predominantly consisting of secondary PM. In urban environments, as well as in rural locations in the vicinity of sources, emissions of primary PM add to this background concentration leading to higher PM mass concentrations. The urban increment of PM is mainly due to higher concentrations of OM, EC, mineral dust and trace elements.

4   Trends in chemical composition of PM_{10} and $PM_{2.5}$

During the three intensive PM measurement periods in Switzerland (1998–1999, 2008–2009, and 2018–2019; Figure 7), PM_{10} and $PM_{2.5}$ concentrations consistently and progressively decreased over time (Figure 19). The decreases observed are consistent with continuous and routine ambient PM_{10} and $PM_{2.5}$ monitoring data (Figure 5 and Figure 20). Notably, it can be seen from Figure 20 that the average PM concentrations during the intensive measurement periods where representative for the considered time periods and not markedly affected by factors such as unusual weather conditions leading to untypical air pollutant levels.
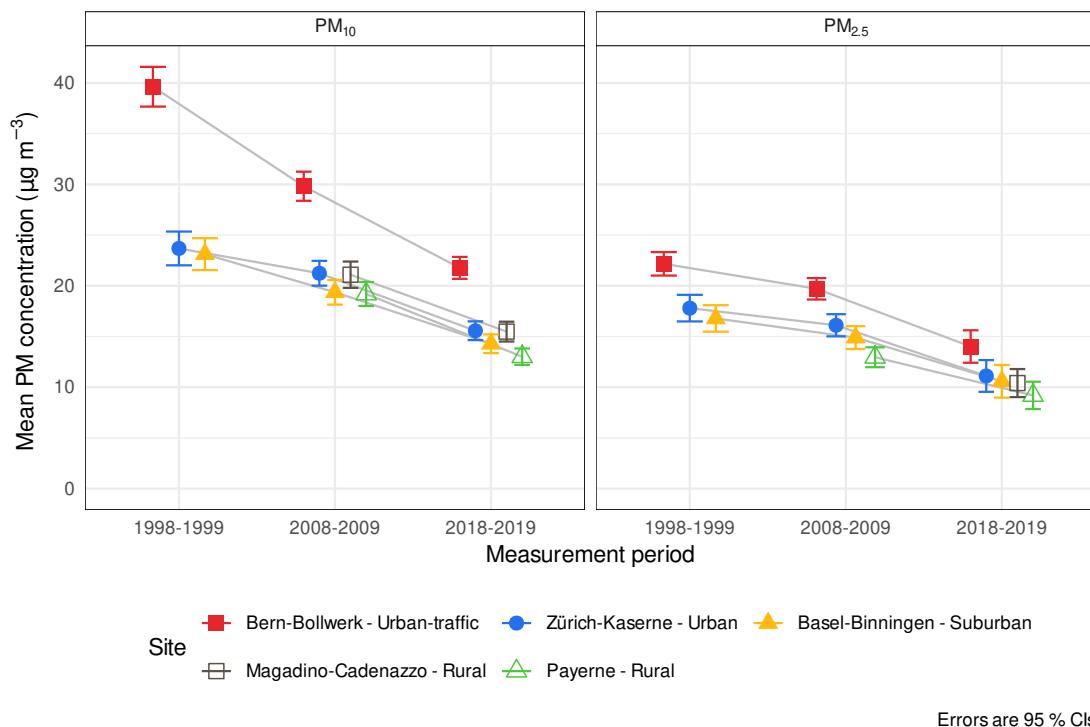
Figure 19 – Mean PM_{10} and $PM_{2.5}$ for five monitoring sites in Switzerland for the duration of the three field campaigns between 1998 and 2019. The measurement periods lasted 12 months but were not aligned with calendar years and therefore are not strictly equivalent to annual means.

As shown in Figure 21 as well as in Figure 3 and Figure A.8, the absolute concentration of most of the major chemical constituents in PM_{10} and $PM_{2.5}$ progressively decreased over the course of the three measurement periods between 1998 and 2019. With the exception of elemental carbon and mineral dust, the rate of decline of the main chemical constituents is similar to the decline rates of PM_{10} and $PM_{2.5}$, resulting in small and on the first sight less pronounced changes in the relative composition of PM (see Figure A.3 and Figure A.4 in the Annex). However, looking at the constituents forming secondary inorganic aerosols (sulfate, nitrate and ammonium), it can be seen that sulfate shows the largest decline within

these constituents and the relative contribution of sulfate is decreasing in PM_{10} and $PM_{2.5}$ for all monitoring locations. In contrast, the decline of ammonium and nitrate was in absolute concentrations lower and their relative abundance in PM_{10} and $PM_{2.5}$ remained about constant, overall resulting in a slightly decreasing percentage of secondary inorganic aerosols in PM_{10} and $PM_{2.5}$ since 1998. The percentage of the sum of sulfate, nitrate in PM_{10} ranges for the 2018–2019 period from 21.4 % in Bern-Bollwerk to 37.2 % in Payerne, and in $PM_{2.5}$ from 29.4 % in Magadino-Cadenazzo to 45.5 % in Payerne.
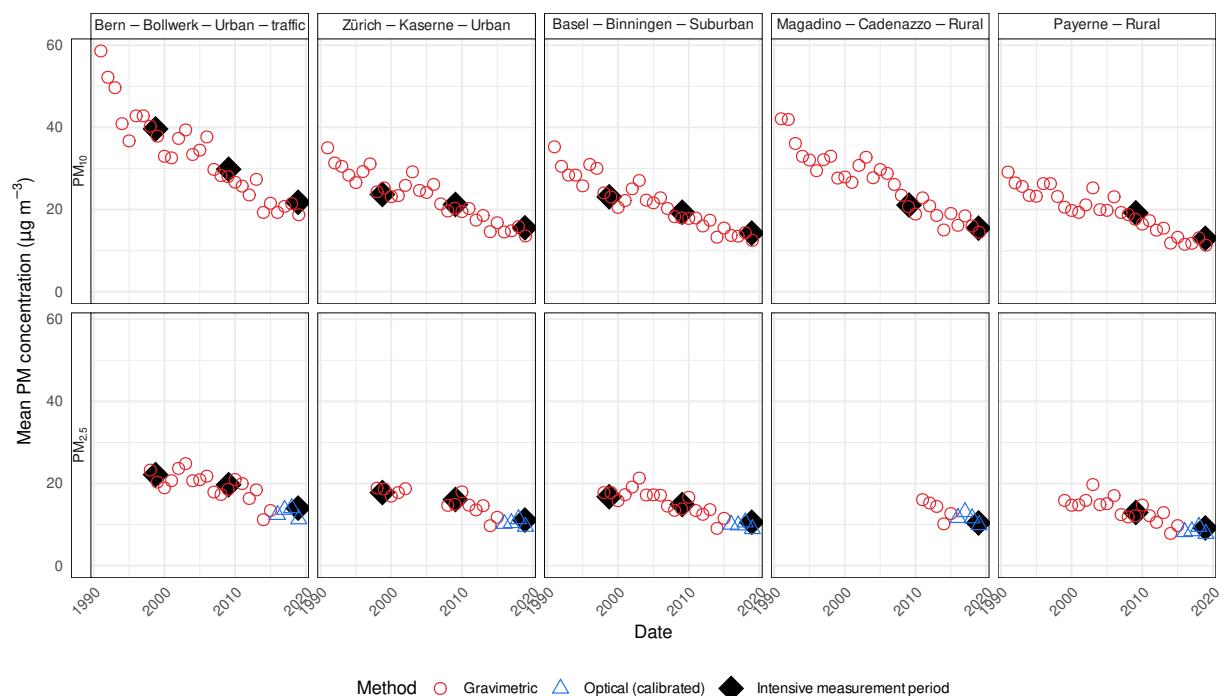
Figure 20 – Annual PM_{10} and $PM_{2.5}$ means for five monitoring sites in Switzerland between 1991 and 2019. The different open symbols indicate a change in measurement method from gravimetric to an optical method that is corrected based on regular parallel measurements with the gravimetric method.

Steadily decreasing absolute concentrations of organic matter can also be observed. However, the rate of decrease is somewhat smaller than that of total PM_{10} and $PM_{2.5}$ leading to an increasing percentage of OM in 2018–2019 compared to the earlier measurement periods. An exception is Magadino-Cadenazzo, where the percentage of OM in PM_{10} slightly declined in the past ten years. Elemental carbon shows large reductions for all monitoring locations and particularly at the urban roadside site Bern-Bollwerk. This demonstrates the effectiveness of the policies for the abatement of elemental carbon emissions, notably the implementation of particle filter systems for diesel engines. These results are inline with what has been reported previously.[17–19,49]

Trace element concentrations did show a decrease since 1998 but were about constant for

the measurement periods 2008–2009 and 2018-2019. An exception is the urban traffic site Bern-Bollwerk, where trace element concentrations in PM_{10} strongly decreased from 7.4 $\mu g\,m^{-3}$ in 1998–1999 to 4.1 $\mu g\,m^{-3}$ in 2008-2009 and 2.7 $\mu g\,m^{-3}$ in 2018–2019. This is a remarkable change and must be explained to be largely due to reduced emissions of non-exhaust PM from road traffic (mostly resuspension of vehicle and road wear as well as road dust) nearby the measurement site. There has been a decline in the traffic activity on the road next to the Bern-Bollwerk site (from 25'000 vehicles per day in 1998–1999 to 17'000 vehicles per day in 2008–2009 to about 15'000 vehicles per day during the 2018–2019 measurement period), a development that certainly had an influence on the observed temporal changes of trace element concentrations at Bern-Bollwerk. In addition, the pavement of the road next to the Bern-Bollwerk site has been renewed just before the start of the measurement campaign 2008–2009,[15] the effect on the concentration of trace elements at Bern-Bollwerk is, however, unknown. It is interesting to note that a few elements dominate the total mass concentration of trace elements. These are sodium, chloride and the anthropogenic fraction of iron and potassium as well as calcium for the site south of the Alps (see subsection 2.5). Since the concentration of potassium was constant over the three measurement periods, the declining trace element concentration observed at Bern-Bollwerk is mainly due to lower concentrations of iron in 2008–2009 and 2018–2019 and the low concentrations of sodium and chloride in the 2018–2019 (Figure 22). The latter is most likely due to the mild winter 2018/2019 and the reduced utilisation of de-icing salt on the road nearby the Bern-Bollwerk site.

Finally, the mineral dust concentration in PM_{10} remained about constant over the three measurement periods. This is not surprising because mineral dust calculated as described in subsection 2.5 is expected to mainly represent natural crustal dust with possibly some contributions from anthropogenic sources such as construction work, re-suspension of mineral dust by agricultural activities and (in particular in urban environments) road dust. The constant absolute mineral dust concentration in PM_{10} had the effect that the relative contribution of natural mineral dust in PM_{10} increased since 1998 at all monitoring locations.

Despite the large decline in total concentration of PM_{10} and $PM_{2.5}$, the change in relative contributions of major constituents to PM_{10} and $PM_{2.5}$ is moderate. The measures to control the emissions of PM and its precursors as implemented in Switzerland and Europe successfully reduced the percentage of PM from anthropogenic sources. As a consequence, the relative share of PM from natural sources is increasing. Another positive consequence of the achieved reductions in emissions of PM from anthropogenic sources are the decreasing urban and roadside increments over time.
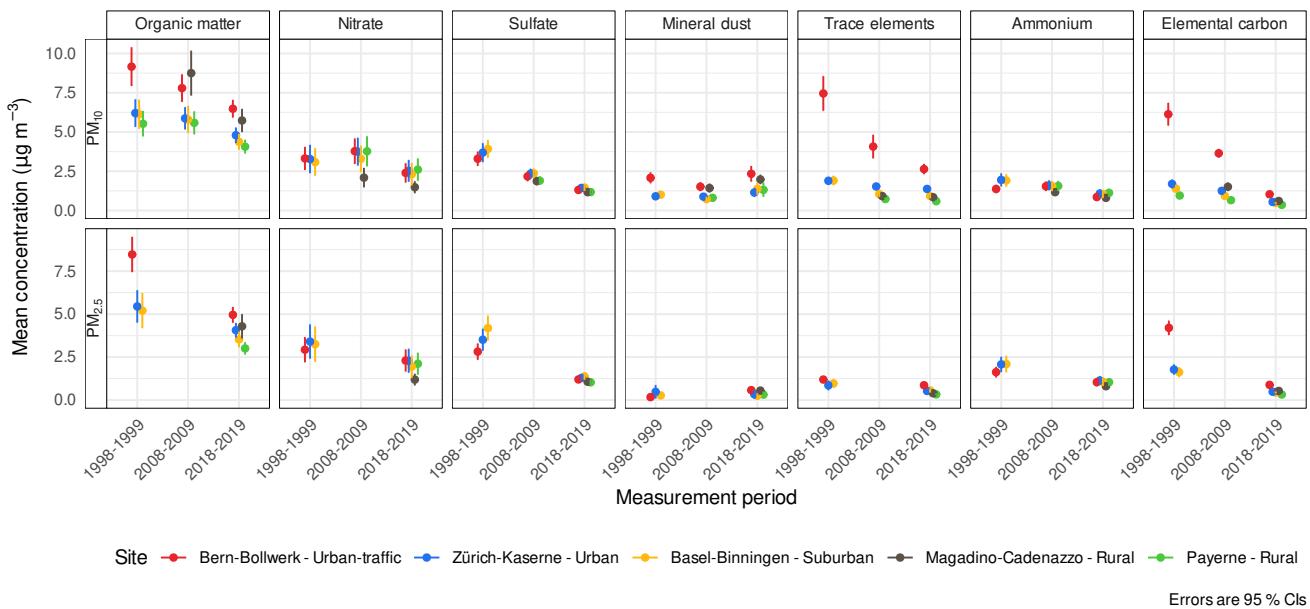
Figure 21 – Mean mass concentrations of seven major constituents in PM_{10} and $PM_{2.5}$ in Switzerland between 1998 and 2019.

The temporal changes of individual trace elements are divers (Figure 22). Trace elements in PM_{10} that are mainly associated with crustal material show no or only moderate changes during the three measurement periods. These elements include Mg, Al, Ca, La and Nd. Similarly, K and Rb, elements that are typically associated with wood combustion emissions, remained rather constant during the three measurement periods. Some of the elements attributed to resuspension of road dust and vehicle wear remained fairly constant (Sb, Ba), others were fairly constant except at the roadside site Bern-Bollwerk were concentrations markedly declined (Ca, Cu, Fe, Mn, Zn; decline of Ca, Fe and Mn in Bern-Bollwerk between first and second measurement period). Finally, there is a class of elements with steadily declining concentrations, probably due to the implementation of policies for the abatement of emissions and the availability of cleaner technologies. Elements with steadily decreasing concentrations include V, Ni, Cd, Th and Pb. For $PM_{2.5}$, element concentrations are available for three sites during the 1998-1999 measurement period and the five sites of the 2018–2019 measurement period. The concentration of most trace elements is much lower in $PM_{2.5}$ than in PM_{10}, it is referred to Table 10 for the mean concentrations of individual elements.

All of the discussed changes in absolute and relative contributions to PM above show that Switzerland's PM load has become progressively less loaded with anthropogenically sourced components between 1998 and 2019. These reductions can be viewed as successes of PM control and abatement strategies both within Switzerland, and in the surrounding European countries. Although such results represent policy successes, it is important to mention that the reductions in PM concentrations have to a large extend been made with combustion process control.
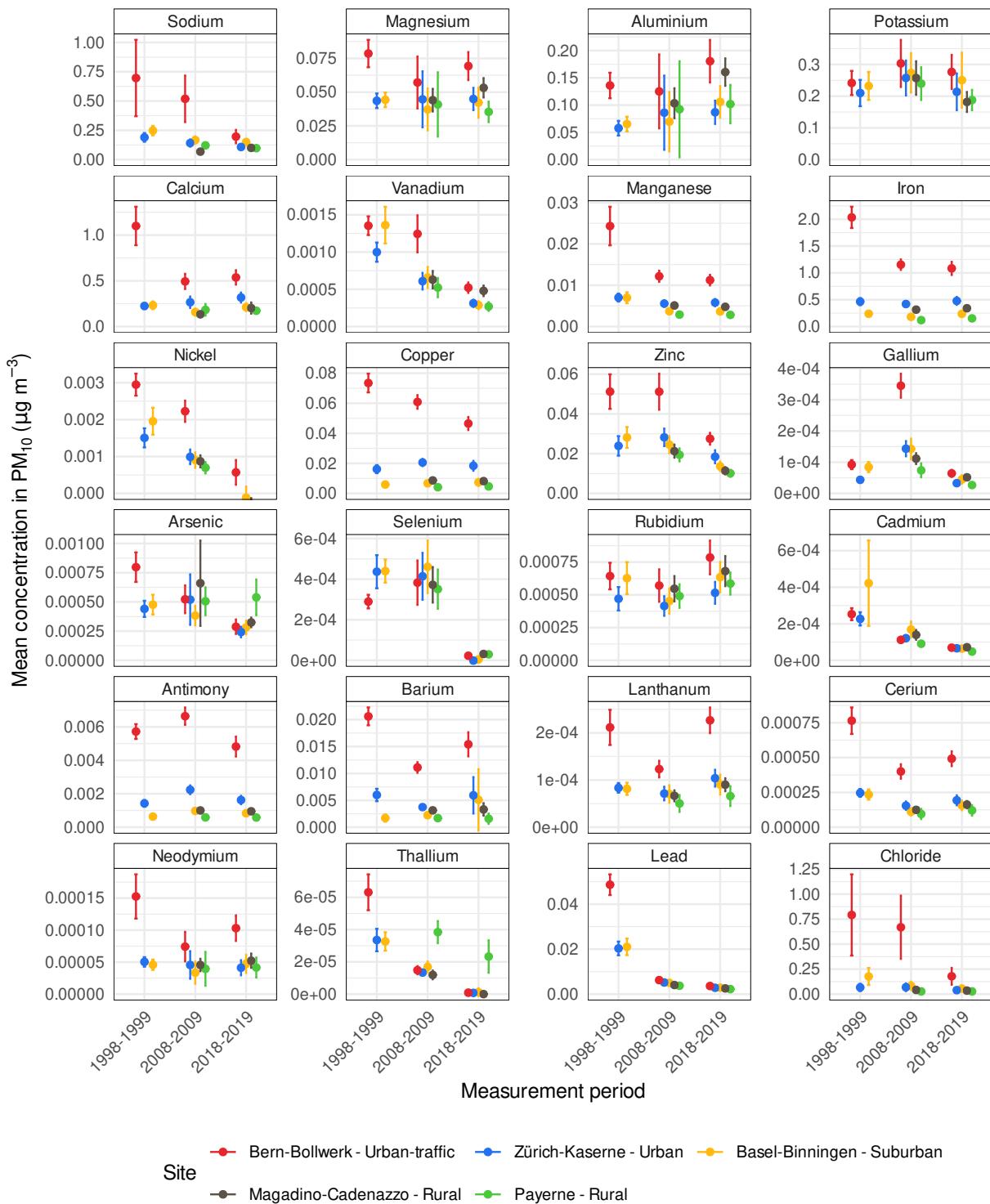
Figure 22 – Measurement period means for selected elements in PM_{10} between 1998 and 2019.

The desirable further decline in PM mass concentration will require additional management strategies in the future, targeting on non-combustion sources such as non-exhaust emissions from traffic [50].

5 Source apportionment with PMF

5.1 Identified PM$_{10}$ sources

Up to six PM$_{10}$ sources were identified for the five monitoring sites in Switzerland by receptor modelling with PMF between 2018 and 2019. The six sources were, in increasing order of mean contribution: vehicle wear, mineral dust, wood combustion, nitrate-rich, road traffic, and sulfate-rich. The vehicle wear source was identified at Bern-Bollwerk and Basel-Binningen, but not at the other three sampling sites.

For the analysis, the vehicle wear (if present) and road traffic sources were combined to form a consistent road traffic source. The identified vehicle wear sources have higher contributions from iron and lower contributions from elemental and organic carbon (Figure A.9 and Figure A.10). However, the two identified sources should not quantitatively be interpreted as representing non-exhaust and exhaust emissions from road traffic. It is unlikely that the source profiles of these two highly correlated emission processes are properly separated. Nevertheless, the identified vehicle wear and road traffic sources contributed on average 2.0 $\mu g\,m^{-3}$ and 5.3 $\mu g\,m^{-3}$ in Bern Bollwerk, and 0.7 $\mu g\,m^{-3}$ and 3.2 $\mu g\,m^{-3}$ in Basel-Binningen.

The mean contributions of the final five sources and all PMF diagnostic plots can be found in the Annex (Table A.3 and Figure A.9 to Figure A.16). Unlike the past observations in 1998–1999 and 2008–2009, neither the road salt nor sodium and magnesium-rich[16] (reclassified as aged marine aerosol by Pandolfi et al. [46]) sources were identified in the 2018–2019 measurement period.

To ensure the labelled sources were consistent among the 13 PM model runs, the sources for each measurement period and each site were aggregated and similarity identity distances (SID) were calculated. The SID statistic offers a robust method to compare different factor profiles.[51] Across the three measurement periods and five sampling locations, SID remained below one which indicates the sources identified were comparable for the different sampling locations and for each measurement period and can be thought of as the same identified source (Figure A.17).

For the interpretation of source factors and estimated source contributions, it should be kept in mind that the identification of source profiles in PMF models is based on the chemical composition and the temporal variation of PM$_{10}$ sources and formation processes. Consequently, the separation of sources with either chemically similar profiles or similar temporal variation

68

is difficult.[33] This can lead to somewhat mixed source profiles or imperfect separation of source contributions. These limitations are especially important to acknowledge in this analysis because the signal to noise ratios are relatively low. This is due to the low absolute concentrations of PM_{10} across Switzerland in the 2018–2019 measurement period (Figure 19).

Two identified sources represent secondary aerosols: sulfate- and nitrate-rich aerosol. These two sources were consistently identified in all sampling locations in Switzerland and for all three measurement periods. Sulfate- and nitrate-rich aerosol explain large parts of sulfate and nitrate mass in PM_{10} and were both accompanied by significant amounts of ammonium. The two sources therefore represented the secondary inorganic aerosol sourced from the oxidation of precursors such as SO_2 and NO_x and subsequent reaction of these oxidation products with ammonia (NH_3) to form ammonium sulfate and ammonium nitrate. The sulfate-rich and nitrate-rich aerosols were the sources with the greatest and third greatest average contributions to PM_{10} mass in the latest 2018–2019 measurement period respectively (**??**).

A large fraction of OC was assigned to the sulfate-rich aerosol (from 21.5 % in Bern-Bollwerk to 51.3 % in Payerne; Figure 23). The sulfate-rich aerosol therefore, represents a major source of OM which shows similar temporal variability as ammonium sulfate. The sulfate-rich aerosol appears to predominantly describe the variation of ammonium sulfate plus secondary organic aerosol. This can be seen when the average contributions of the sulfate-rich aerosol for the three measurement periods are compared to the mass concentration of ammonium sulfate ($(NH_4)_2SO_4$), as calculated from the measured sulfate concentration assuming that all of the sulfate is present as $(NH_4)_2SO_4$. The average contributions from the sulfate-rich aerosol for most sites across all measurement periods are 1–3 $\mu g\,m^{-3}$ larger than the calculated ammonium sulfate concentrations. For the 1998–1999 measurement period, there was at the three studied sites (Basel-Binningen, Bern-Bollwerk, Zürich-Kaserne) a good match between the PMF derived sulfate-rich aerosol and the calculated ammonium sulfate concentration and much smaller contribution from organic carbon than for the two other measurement periods (Figure A.14). This indicates for the 1998–1999 measurement period sulfate-rich source factors that almost exclusively represent ammonium sulfate.

The nitrate-rich source was very seasonal with higher concentrations during the winter. This cycle was driven by the transfer between the particulate and the gas phase of this source which is based on temperature, and to a lesser extent, relative humidity.[52] The nitrate-rich aerosol represented almost exclusively secondary ammonium nitrate because there is generally a good agreement between the average contribution from the nitrate-rich source, and the calculated concentration of ammonium nitrate (NH_4NO_3), assuming that nitrate is entirely

69
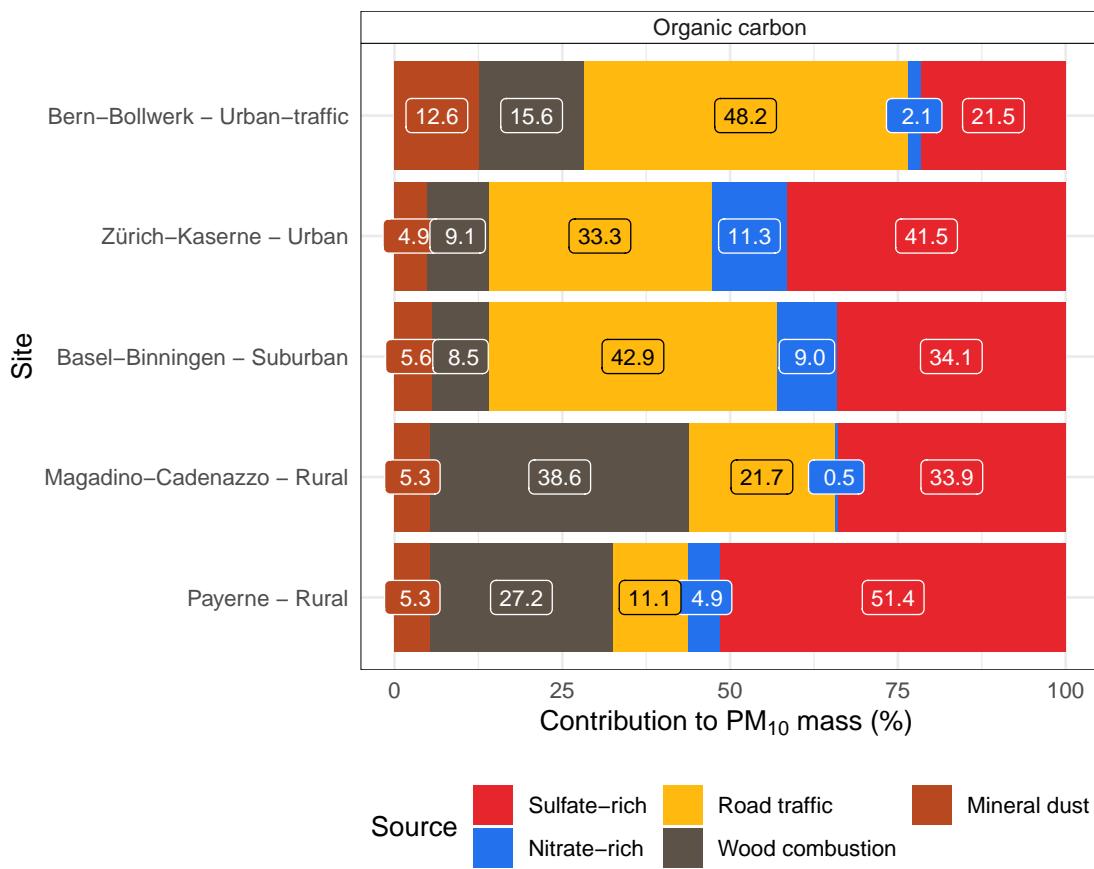
Figure 23 – Percentage of the mass of organic carbon explained by the PMF-identified sources at the five sampling locations between 2018 and 2019. The high percentage of organic carbon explained by the sulfate-rich aerosol is notable (see text). Noticeable is also the high percentage of organic carbon explained by the wood combustion source in Magadino-Cadenazzo, indicating the strongest influence of imperfect combustion of wood fuel at this site. The shown numbers also apply to the mass of organic matter.

present as NH_4NO_3. However, there were two measurement series where the contribution of the nitrate-rich aerosol clearly deviated from the calculated concentration of ammonium nitrate: At Bern-Bollwerk during the 2008–2009 measurement period the contribution from the nitrate-rich source was on average $1.6\,\mu g\,m^{-3}$ larger than the calculated concentration of ammonium nitrate. This indicated that the PMF derived factor was enriched by contributions from other sources or processes. In contrast, the contribution of nitrate-rich aerosol at Basel-Binningen for the 2008–2009 measurement period was on average $2.1\,\mu g\,m^{-3}$ lower than the calculated concentration of ammonium nitrate, thus suggesting that the PMF model attributed a significant part of secondary ammonium nitrate to other sources. Although PMF is a powerful tool for disentangling contributions from different sources and processes at receptor sites, the latter two examples show the limitations of PMF and illustrate that there can be significant uncertainty and bias in the source contribution estimates. The interpretation of the PMF model based sources and source contributions must therefore be done with care.

Two other sources which were identified in all sampling locations and all three measurement periods were road traffic and wood combustion. The road traffic source(s) were composed of a collection of metals such as copper, antimony, iron, barium, manganese, and zinc which are primarily emitted by abrasion processes from mechanical wear, the combustion of gasoline and diesel, and emissions of lubricating oils. These metals are in Switzerland rather specific for traffic sources as can be seen from the large site-type dependence and the elevated concentrations at the urban traffic site Bern-Bollwerk (see Figure 22 and subsection 3.4). The wood combustion sources were highly seasonal and were clearly identified by the presence of potassium, rubidium, OC, and EC. Levoglucosan, a widely utilised tracer for biomass burning[53] observations were available for the five monitoring sites and generally showed good agreement with the PMF-identified wood combustion source (Figure 24 and Figure 25). In particular at Magadino-Cadenazzo where peak levoglucosan concentrations were much higher than at the other locations, the calculated contribution of wood combustion and the concentration of levoglucosan where highly correlated. The relationship between PMF-identified wood combustion contributions and Levoglucosan concentrations are very similar to those found for the measurement period in 2008–2009.[16] Like in 2008–2009, the contents of Levoglucosan and of organic carbon (see Figure 23) in the PMF-identified wood combustion emissions are highest in Magadino-Cadenazzo, indicating a higher influence of imperfect combustion of wood fuel at this site compared to the other studied locations.

The wavelength-depended measurements of $PM_{2.5}$ light absorption performed within the NABEL air quality monitoring network can be used to calculate the contribution of wood combustion to black carbon in $PM_{2.5}$.[49] Similar to levoglucosan, a reasonably good correlation between calculated black carbon from wood combustion and PMF-identified wood combustion source contributions were found (Figure A.18). PMF-identified wood combustion contribution and levoglucosan concentrations differ in Payerne during the warm season, where the calculated contribution from wood burning is suspiciously high (Figure 24). In contrast, the calculated road traffic contribution in Payerne is unexpectedly low (Figure 27), potentially indicating a reallocation of road traffic related PM_{10} to the wood combustion contribution. Again, there are limitations for the separation of sources of PM_{10} when PMF is applied to daily chemical speciation data. Nevertheless, the application of this source apportionment technique applied to multiple sites and for multiple measurement campaigns is capable of providing consistent insight into the contributions of main sources and processes of PM_{10} even though the individual source estimations might have some bias and a higher uncertainty.

Finally, the mineral dust sources were somewhat intermittent and was represented by 'spiky'
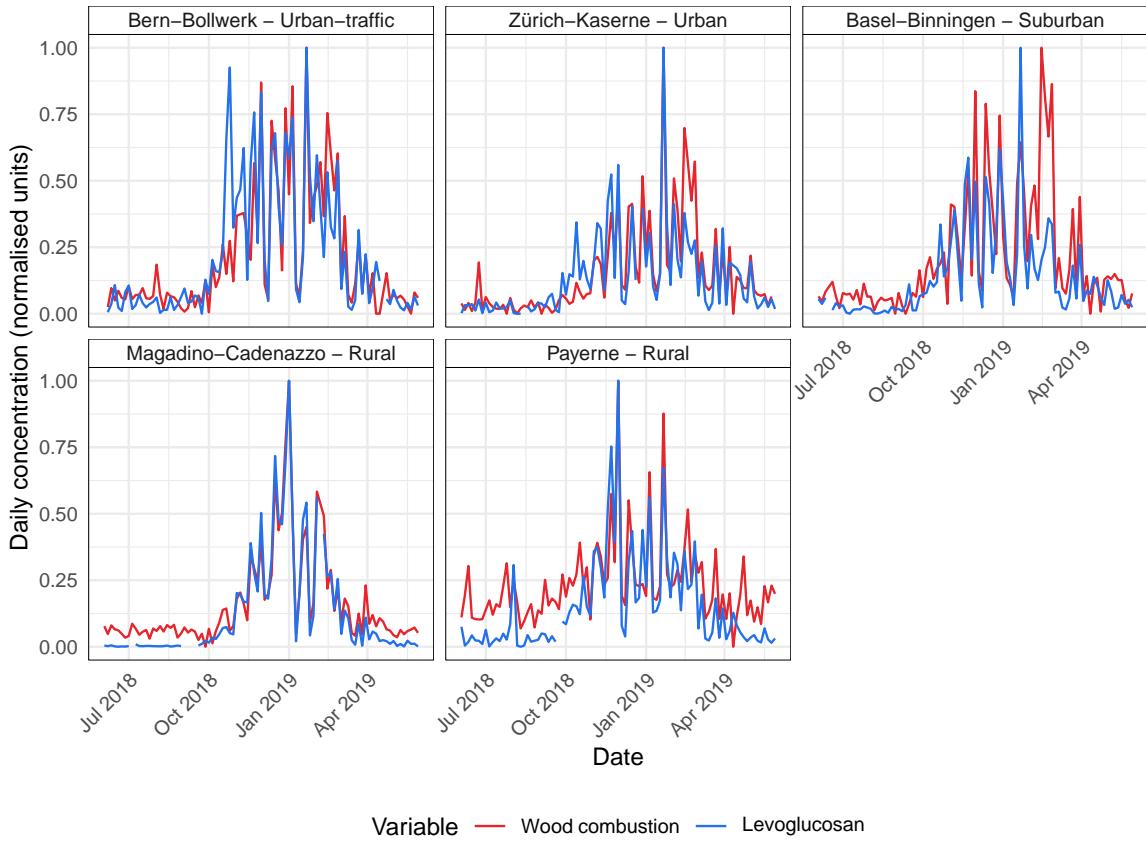
Figure 24 – Normalised time series of the wood combustion sources and levoglucosan for five sites in Switzerland between 2018 and 2019.

time series and were composed of common crustal elements such as aluminium, calcium, iron, magnesium, and titanium. However, about the half of the mass of calcium in PM_{10} is at the sampling locations Basel-Binningen and Zürich-Kaserne represented by the road traffic source. The chemical profile of road dust and mineral dust is very similar, making a perfect separation of the road traffic and mineral dust sources difficult. As a consequence, the contributions of road traffic and mineral dust sources may have been over- or underestimated by the PMF models depending on the sampling location.

For the 2018–2019 measurement period, there was a good agreement between the average contribution of the mineral dust sources and the concentrations as calculated from the chemical composition of PM_{10} (Figure 21). An exception was observed at Bern-Bollwerk, the urban-traffic site where the estimated contribution for the PMF mineral dust factor for the 2018–2019 measurement period was much higher than at the other sites, and also 1.5 $\mu g\,m^{-3}$ higher than the concentration of mineral dust as calculated by the mass closure calculations. This indicated that the mineral dust source identified by PMF at Bern-Bollwerk included contributions from other sources, most likely road traffic, and perhaps minor emissions from construction and demolition activities. Interestingly, a discrepancy between the average contributions from the PMF-derived
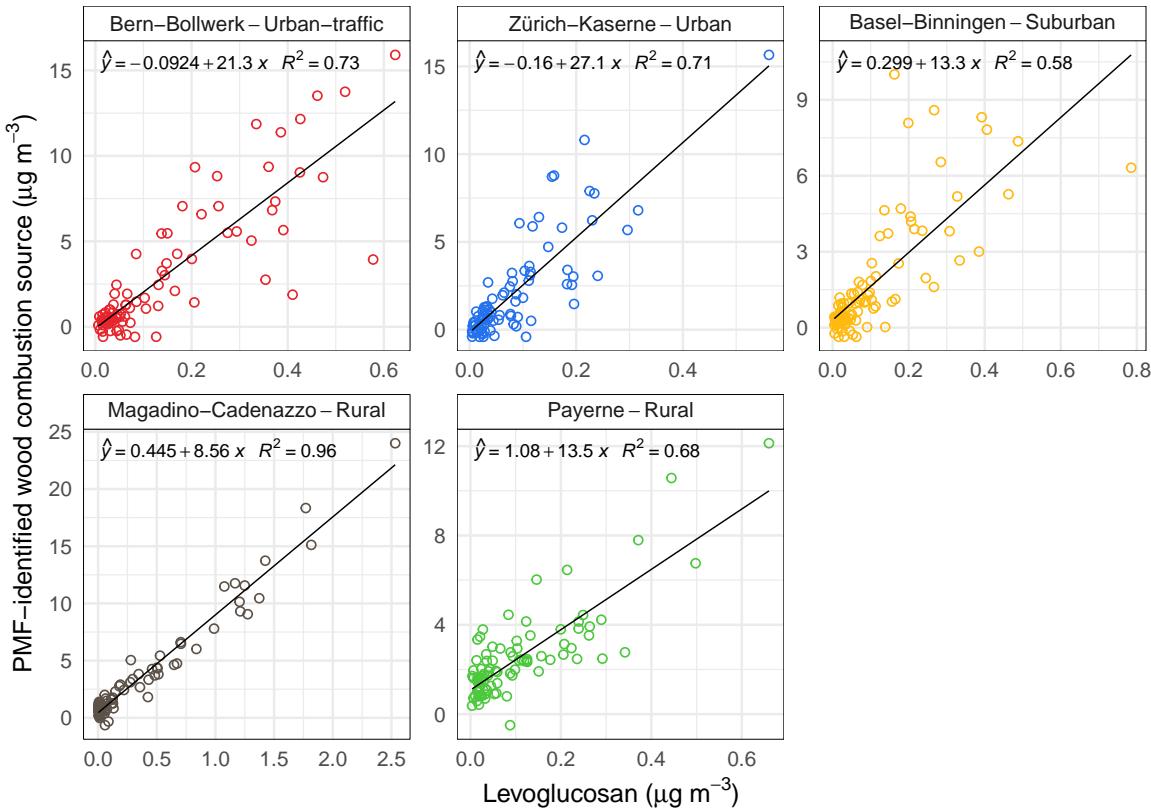
Figure 25 – Contribution of the wood combustion sources to PM_{10} versus levoglucosan for five sites in Switzerland between 2018 and 2019.

mineral dust factors and mineral dust calculated from the chemical composition was apparent in most sampling locations for the 1998–1999 and 2008–2009 measurement periods. It seems that for unknown reasons, mineral dust sources as identified by PMF represent not only natural mineral dust, but include at least parts of PM_{10} from other sources. Understandably, the partially imperfect separation of the mineral dust sources by PMF hampers the evaluation of the changes of the contribution of this source of PM_{10} over time.

5.1.1 Environmental increments

Figure 26 shows the rural to urban (Zürich-Kaserne minus Payerne), urban to roadside (Bern-Bollwerk minus Zürich-Kaserne), and rural to roadside (Bern-Bollwerk minus Payerne) increments of the PM_{10} sources for the most recent measurement period in 2018–2019. The sulfate-rich and the nitrate-rich sources were not enriched in Switzerland's urban environments, indicating that these sources represent regional, homogeneous sources and atmospheric processes such as long-range transport and secondary aerosol formation. The positive rural to urban increment of 0.9 µg m^{-3} for the nitrate-rich source is likely to be within the uncertainty of the PMF models, and results from the high average contribution of the nitrate-rich source in Zürich-Kaserne. Zürich-Kaserne is the only sampling location during the 2018–2019 mea-

surement period where the average contribution of the nitrate-rich source was clearly greater ($0.8\,\mu g\,m^{-3}$) than the concentration of ammonium nitrate in PM_{10}, suggesting the PMF model has overestimated the nitrate-rich source in this location.
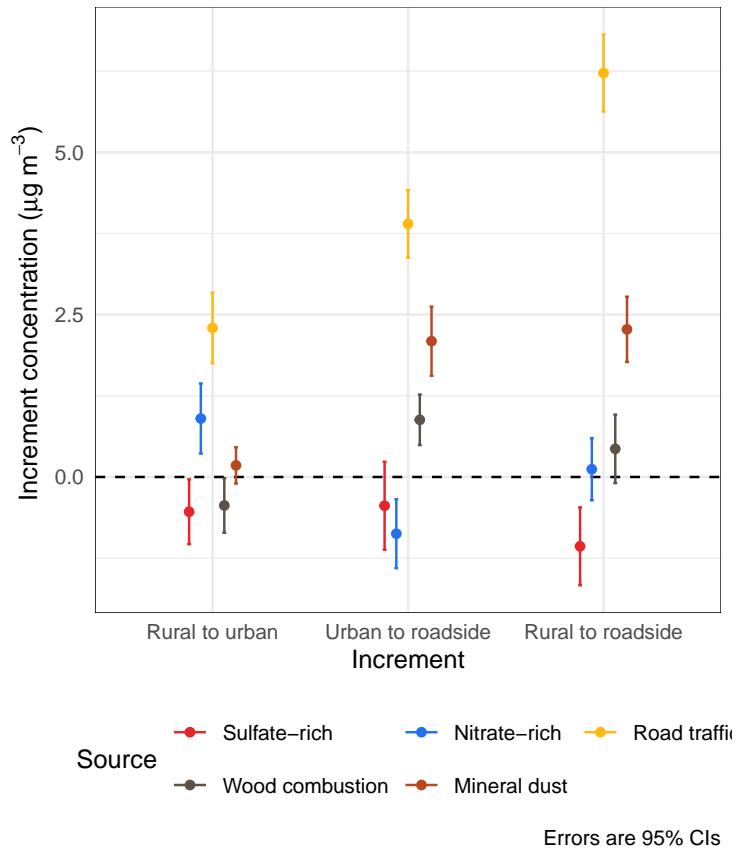
Figure 26 – PM_{10} environmental increments for five PMF-identified sources between 2018 and 2019 in Switzerland.

Similarly, the wood combustion source and mineral dust showed no enrichment from rural to urban environments. However, there was a roadside increment of mineral dust of $2.1\,\mu g\,m^{-3}$. As mentioned in subsection 3.4, most of this increment is likely due to road dust resuspended from the traffic in the immediate vicinity of the sampling location. Most of the roadside increment due to the PMF model based mineral dust source should therefore, be attributed to road traffic emissions.

The PMF-identified road traffic source was the only source that showed a clear and progressive environmental increment enhancement. The average rural to urban increment of the PMF road traffic source's contribution was $2.3\,\mu g\,m^{-3}$, which agree well with the average urban increment of $2.4\,\mu g\,m^{-3}$ as calculated from the difference of PM_{10} at Zürich-Kaserne and Payerne (Table 5). Similarly, the urban to roadside increment of the road traffic source was found to be $3.9\,\mu g\,m^{-3}$. When adding the roadside increments of the PMF model based

road traffic and mineral dust factors (see above), the total average roadside increment due to emissions of PM_{10} from very local road traffic including resuspended road dust was quantified to 6.0 µg m^{-3}, a value that is slightly higher than the roadside increment as calculated from the difference of PM_{10} at Bern-Bollwerk and Zürich-Kaserne (5.7 µg m^{-3}, see Figure 13). It should be noted that there is still some uncertainty about the role of primary emissions of PM_{10} from the railway traffic at the Bern-Bollwerk site. The site is next to Bern main station, albeit protected from the railway tracks by high buildings. It was not possible in this study and not in the partner project using SEM/EDX analysis to identify and quantify an impact of railway traffic on PM_{10} at the Bern-Bollwerk site. Despite this uncertainty, we can conclude that the observed urban increment PM_{10} can mostly be explained by road traffic emissions, indicating that in Switzerland road traffic is an important source and largely responsible for the generally higher PM_{10} concentrations in urban environments. This is also visualised in Figure A.22 where the PMF based source contribution calculations for the 2018–2019 measurement period are compiled for typical environments in Switzerland as derived from source apportionment models at the five representative sites. For comparison, the same illustration of the results for the measurement period 2008–2009 is provided in Figure A.23.

5.1.2 Comparisons of source contributions over time

A goal of this analysis was to investigate how the PM sources across Switzerland changed over time. Using PMF for this purpose offers some challenges because the number and sources identified were not always conserved in time and space. Despite this challenge, this entire data has the interesting advantage that the previous measurement periods' observations have been analysed with PMF before and the results have been reported by two other studies: Gianini et al. [16] for the 1998–1999 and 2008–2009 periods, and Pandolfi et al. [46] for the 2008–2009 period have been analysed the identical data sets as used again in this study. This offers an opportunity to compare and validate the different PMF solutions determined by three different projects and data users.

The PMF results for PM_{10} for the three measurement periods, for five locations, from three different projects are shown in Figure 27. The most conspicuous pattern in Figure 27 is that most sources have decreased over time, but with the exception of the road traffic source at Bern-Bollwerk, the decreases have been modest. This is interesting because the calculations of major components in the mass closure section (Section 4) generally show clearer decreasing trends.

Figure 27 demonstrates that the mixed anthropogenic, sodium and magnesium-rich, and
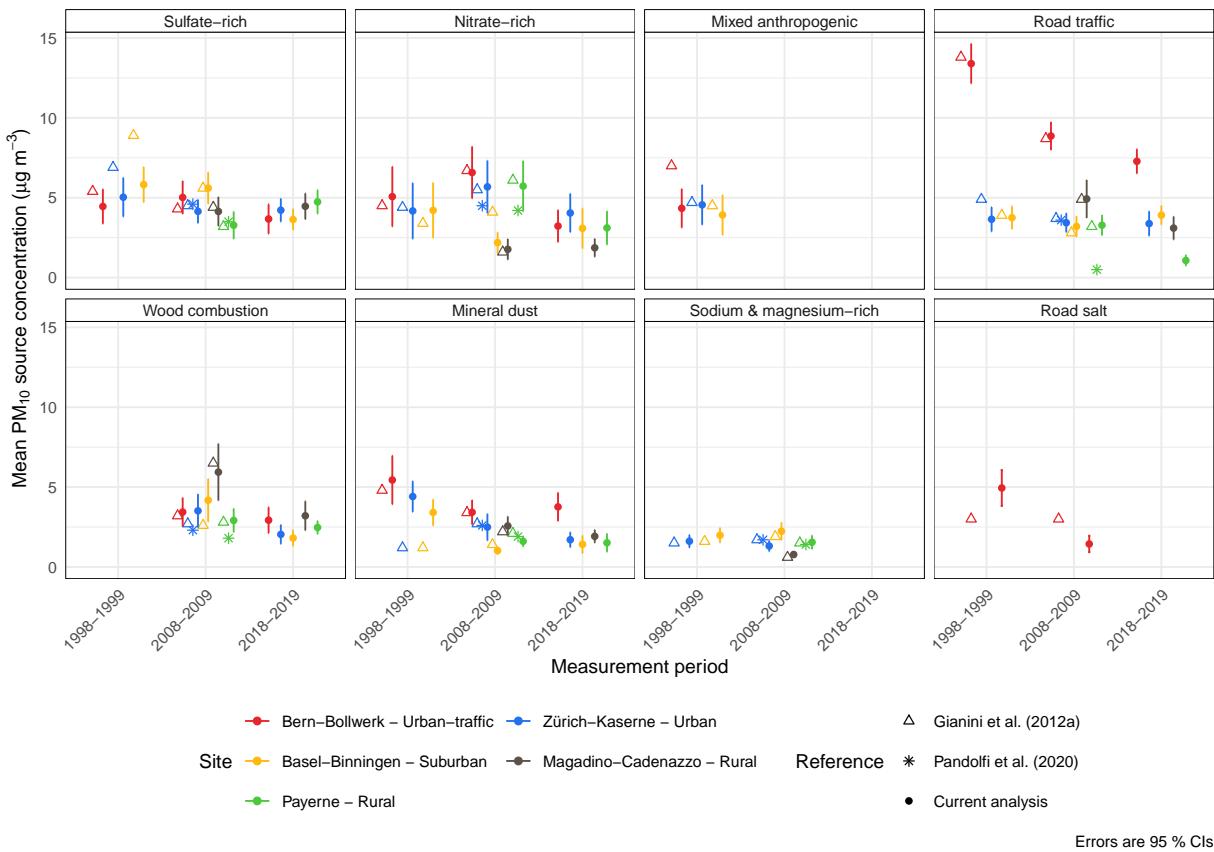
Figure 27 – Mean concentrations for eight, PM_{10} PMF-identified sources for five sites in Switzerland between 1998 and 2019. Two previous studies' results are also displayed.

road salt sources were inconsistently identified among the three measurement periods. The mixed anthropogenic source in the 1998–1999 measurement period could also be interpreted as primarily a wood combustion source, but there were additional elements indicative of vehicular wear (in the form of some metals) and therefore, this source was not representative as a single, pure source. If this source was labelled as a wood combustion source, it would overestimate the contribution of wood burning emissions during this measurement period.

Somewhat curiously, the sodium and magnesium-rich source was absent in all 2018–2019 PMF models (Figure 27). For the previous measurement periods, this source was clearly identifiable, but there was no evidence of this source in the latest measurement period. Pandolfi et al. [46] interpreted this source as aged sea-salt and this long-range process may have been allocated to the sulfate-rich source in 2018–2019. This may explain why ionic sulfate concentrations have decreased over time (??), while the accompanying PMF source does not show the same clear decrease.

The road salt source also failed to be identified at Bern-Bollwerk for the 2018–2019 measurement period (Figure 27). Although there was a clear, albeit minor, sodium and chloride enhancement during the winter months at this roadside location, the additional loading was

much less than the past due to mild temperatures and presumably fewer salting days for the winter which straddled 2018 and 2019. It is likely that the road salt source was incorporated into both of the road traffic and mineral dust sources at Bern-Bollwerk for the 2018–2019 measurement period's PMF models.

The comparison among the three studies utilising PMF generally show good agreement (Figure 27). The sulfate-rich sources in the 1998–1999 measurement period display a systematic bias between Gianini et al. [16]'s results and this work, but this feature is not observed for any other source or time period. When the studies' mean PMF masses diverge, it usually takes the form of a 'drop out', where a particular source contributes a small amount of mass, for example, this study's Basel-Binningen nitrate-rich source in 2008–2009, Gianini et al. [16]'s mineral dust contributions in 1998–1999, and Pandolfi et al. [46]'s road traffic source at Payerne in 2008–2009. In the case of Basel-Binningen's nitrate-rich source for this work, it can be seen that the wood combustion source is higher than what has been reported in the past and the model run has attributed more mass to wood combustion at the expense of the nitrate-rich source. The seasonal cycle of the wood combustion and nitrate-rich sources are similar so it is understandable why some PMF models would conflate these two sources. For other PMF users, it is recommended to investigate such low-mass factors or sources as an additional quality control step.

5.2   Relative contribution of sources

The relative contributions of the various PMF-identified sources of PM_{10} have varied over time and strikingly demonstrate that the secondary generated sources (nitrate- and sulfate-rich) have grown in importance in all locations, with the exception of the roadside Bern-Bollwerk (Figure 28). Wood combustion emissions continue to decrease in relative importance across Switzerland. However, 20 % of Magadino-Cadenazzo's PM_{10} was from wood burning in 2018–2019, and because this source in only active in winter (Figure 24), significant improvements can still be made in this location, and most likely in other areas across Switzerland where residential wood burning in small appliances are common.

Figure 28 clearly demonstrates that the road traffic and mineral dust sources are very important to consider for Switzerland's PM climate. Although this is discussed above in Section 5.1.1, the importance of non-exhaust PM sources are again highlighted because the mineral dust source contains a significant portion of road vehicle-induced resuspension PM. Such non-exhaust emissions will need to be focused on in the future to continue reducing ambient PM concentrations across Switzerland. This issue has also been previously raised across
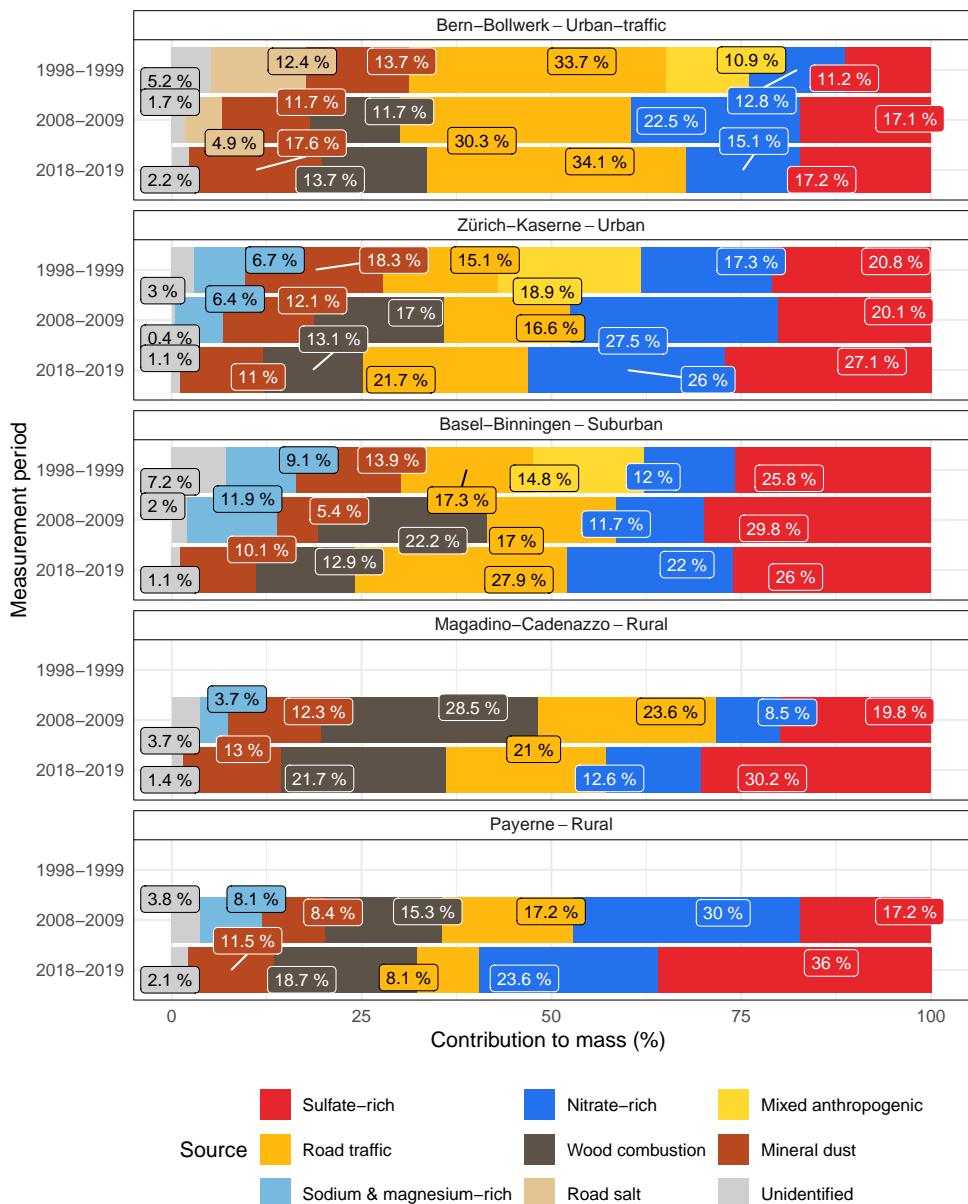
Figure 28 – Relative PM_{10} source contributions determined by PMF for five monitoring sites in Switzerland for three intensive sampling periods between 1998 and 2019.

many other European environments [5, 27, 54].

6   Oxidative potential of PM

Within this report, only a very brief and descriptive overview of the measurements of oxidative potential markers in PM_{10} and $PM_{2.5}$ can be given. Detailed analyses including the linkage of OP to chemical constituents including trace elements and sources of PM_{10} and $PM_{2.5}$ is ongoing and will be made available in a future report or publication.

However, OP from three assays, at five locations in Switzerland demonstrated a clear seasonal cycle between June 1, 2018 and May 31, 2019 (Figure 29). The highest OP signal was experienced during the winter months, and this pattern is consistent with most primary atmospheric pollutants where emissions are higher, and the atmospheric state is less conducive to pollutant transportation and dispersion.
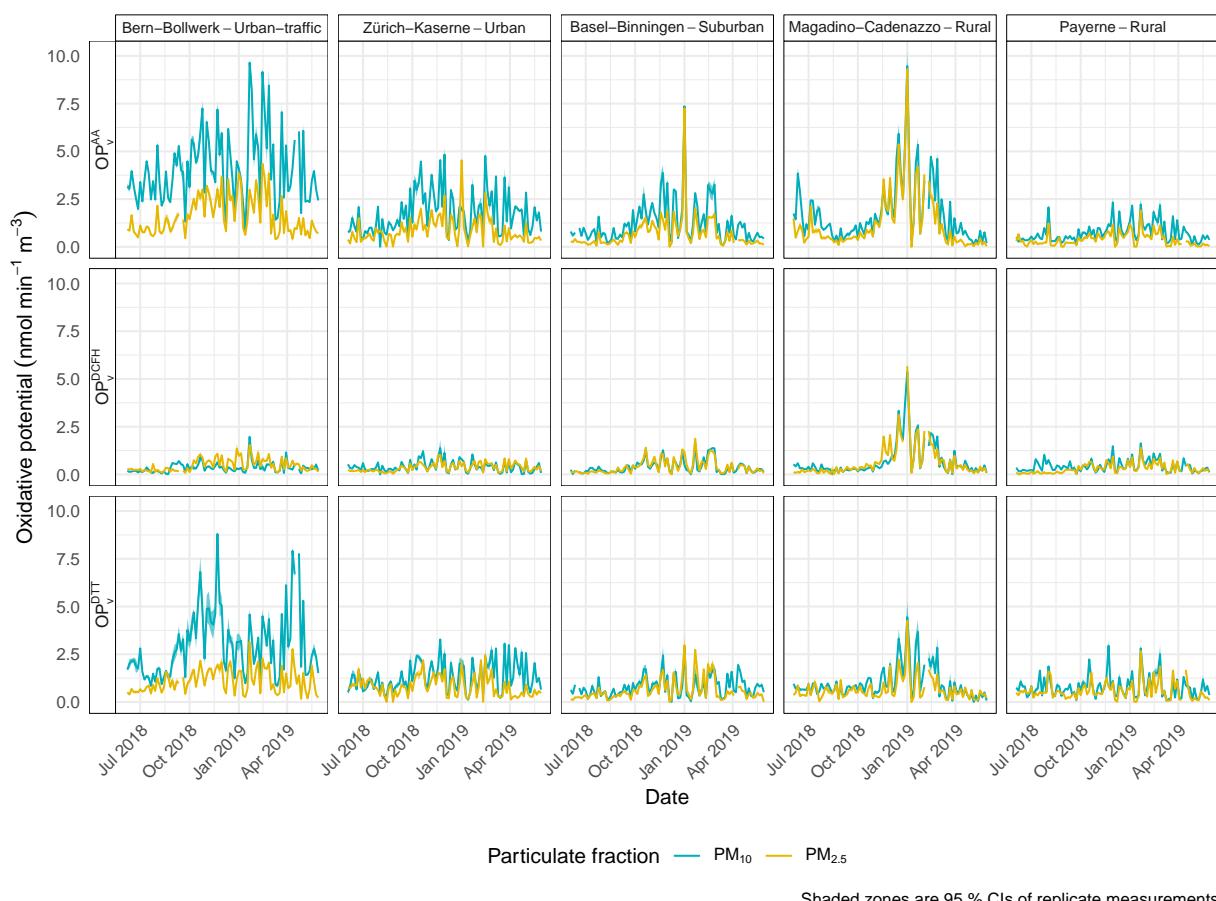
Figure 29 – Time series of oxidative potential from three assays for five sites in Switzerland between June 1, 2018 and May 31, 2019.

Mean OP measures showed a distinct dependence on sampling location in Switzerland between 2018 and 2019 (Table 11). The strong site-type gradient followed the roadside to rural

gradient. This gradient manifested itself where the roadside Bern-Bollwerk location had the highest OP of all sites while Payerne, a rural site on the western Swiss plateau had the lowest OP. However, Magadino-Cadenazzo defied this pattern, especially when considering the DCFH assay where OP was higher than the rural classification would suggest. Magadino-Cadenazzo suffers from high loads of wood smoke during the winter [55] and the high concentrations of carbonaceous species may explain this enhanced OP at this location. Note that the site-type gradient for OP assays AA and DTT is much stronger than for the mass concentrations of $PM_{2.5}$ and PM_{10}.

Table 11 – Mean PM_{10} and $PM_{2.5}$ OP for five locations and three assays in Switzerland between 2018 and 2019. The units are $nmol\,min^{-1}\,m^{-3}$, the ranges indicate the 95 % confidence intervals around the mean, and all values have been rounded to one decimal point.

Assay	Site	PM_{10}	$PM_{2.5}$
OP_v^{AA}	Bern-Bollwerk	4.1 [3.7, 4.4]; $n = 89$	1.6 [1.4, 1.8]; $n = 89$
OP_v^{AA}	Zürich-Kaserne	1.7 [1.5, 2.0]; $n = 90$	0.8 [0.7, 1.0]; $n = 90$
OP_v^{AA}	Basel-Binningen	1.2 [1.0, 1.5]; $n = 90$	0.7 [0.5, 0.9]; $n = 90$
OP_v^{AA}	Magadino-Cadenazzo	1.7 [1.4, 2.0]; $n = 90$	1.2 [0.9, 1.5]; $n = 90$
OP_v^{AA}	Payerne	0.7 [0.6, 0.8]; $n = 91$	0.4 [0.3, 0.5]; $n = 90$
OP_v^{DCFH}	Bern-Bollwerk	0.4 [0.3, 0.4]; $n = 89$	0.5 [0.4, 0.5]; $n = 89$
OP_v^{DCFH}	Zürich-Kaserne	0.4 [0.3, 0.5]; $n = 90$	0.4 [0.3, 0.4]; $n = 90$
OP_v^{DCFH}	Basel-Binningen	0.4 [0.3, 0.5]; $n = 90$	0.4 [0.3, 0.5]; $n = 90$
OP_v^{DCFH}	Magadino-Cadenazzo	0.7 [0.5, 0.9]; $n = 90$	0.7 [0.5, 0.9]; $n = 89$
OP_v^{DCFH}	Payerne	0.4 [0.4, 0.5]; $n = 91$	0.3 [0.3, 0.4]; $n = 90$
OP_v^{DTT}	Bern-Bollwerk	3.0 [2.6, 3.3]; $n = 89$	1.1 [1.0, 1.2]; $n = 89$
OP_v^{DTT}	Zürich-Kaserne	1.3 [1.1, 1.5]; $n = 90$	0.8 [0.7, 0.9]; $n = 90$
OP_v^{DTT}	Basel-Binningen	0.8 [0.7, 0.9]; $n = 90$	0.6 [0.5, 0.7]; $n = 90$
OP_v^{DTT}	Magadino-Cadenazzo	1.0 [0.8, 1.2]; $n = 90$	0.7 [0.5, 0.8]; $n = 90$
OP_v^{DTT}	Payerne	0.8 [0.7, 0.9]; $n = 91$	0.6 [0.5, 0.7]; $n = 90$

When OP is aggregated by season, it is very clear that Magadino-Cadenazzo's enhanced OP was almost exclusively isolated to the winter months (Figure 30). At the urban traffic site Bern-Bollwerk, OP in PM_{10} is substantially higher than in $PM_{2.5}$. This observation is clearly pointing to the importance of the coarse particle fraction for the oxidative potential of PM_{10}.
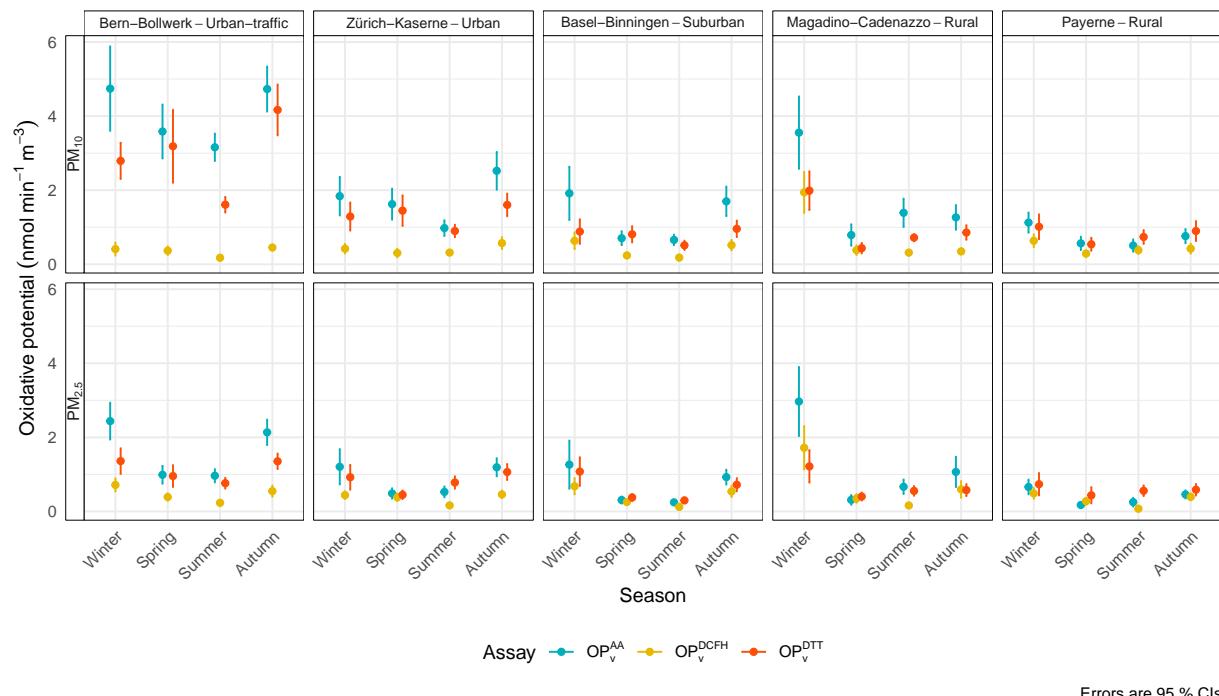
Figure 30 – Seasonal mean air volume oxidative potential for three types of assays and five monitoring sites between June 1 2018 and May 31 2019.

7 References

[1] Hüglin, C., Gianini, M., and Gehrig, R. Chemische Zusammensetzung und Quellen von Feinstaub. Untersuchungen an ausgewählten NABEL-Standorten. Schlussbericht. Im Auftrag des Bundesamtes für Umwelt (BAFU). Empa, Abt. für Luftfremdstoffe und Umwelttechnik. 2012.

[2] Daellenbach, K. R., Stefenelli, G., Bozzetti, C., Vlachou, A., Fermo, P., Gonzalez, R., Piazzalunga, A., Colombi, C., Canonaco, F., Hueglin, C., Kasper-Giebl, A., Jaffrezo, J.-L., Bianchi, F., Slowik, J. G., Baltensperger, U., El-Haddad, I., and Prévôt, A. S. H. Long-term chemical analysis and organic aerosol source apportionment at nine sites in central Europe: source identification and uncertainty assessment. *Atmospheric Chemistry and Physics* 17.21 (2017), pp. 13265–13282. URL: https://acp.copernicus.org/articles/17/13265/2017/.

[3] Daellenbach, K. R., Uzu, G., Jiang, J., Cassagnes, L.-E., Leni, Z., Vlachou, A., Stefenelli, G., Canonaco, F., Weber, S., Segers, A., Kuenen, J. J. P., Schaap, M., Favez, O., Albinet, A., Aksoyoglu, S., Dommen, J., Baltensperger, U., Geiser, M., El Haddad, I., Jaffrezo, J.-L., and Prévôt, A. S. H. Sources of particulate-matter air pollution and its oxidative potential in Europe. *Nature* 587.7834 (2020), pp. 414–419. URL: https://doi.org/10.1038/s41586-020-2902-8.

[4] Bundesamt für Umwelt. Luftqualität 2019 – Messresultate des Nationalen Beobachtungsnetzes für Luftfremdstoffe (NABEL). Umwelt-Zustand Nr. 2020: 28 S. 2020.

[5] Air Quality Expert Group. Non-Exhaust Emissions from Road Traffic. Department for Environment, Food and Rural Affairs. PB14581. 2019.

[6] Rausch, J., Vogel, D. J., and Schnidrig, N. Charakterisierung und Herkunftsbestimmung von Grobstaubpartikeln im PM10. REM/EDX Einzelpartikelanalytik an den NABEL-Standorten Bern Bollwerk und Zürich Kaserne. Schlussbericht über die Messkampagne Juni 2018–Juni 2019. Freiburg, 6.10.2020 Entwurf. Particle Vision GmbH. 2020. URL: https://www.bafu.admin.ch/dam/bafu/de/dokumente/luft/externe-studien-berichte/Schlussbericht_Charakterisierung_und_Herkunftsbestimmung_von%20Grobstaub_im_PM10_2020_30.10.2020_final.pdf.download.pdf/Schlussbericht_Charakterisierung_und_Herkunftsbestimmung_von%20Grobstaub_im_PM10_2020_30.10.2020_final.pdf.

[7] Galvão, E. S., Santos, J. M., Lima, A. T., Reis, N. C., Orlando, M. T. D., and Stuetz, R. M. Trends in analytical techniques applied to particulate matter characterization: A critical review of fundaments and applications. *Chemosphere* 199 (2018), pp. 546–568. URL: http://www.sciencedirect.com/science/article/pii/S0045653518302340.

[8] Van Dingenen, R., Raes, F., Putaud, J.-P., Baltensperger, U., Charron, A., Facchini, M.-C., Decesari, S., Fuzzi, S., Gehrig, R., Hansson, H.-C., Harrison, R. M., Hüglin, C., Jones, A. M., Laj, P., Lorbeer, G., Maenhaut, W., Palmgren, F., Querol, X., Rodriguez, S., Schneider, J., Brink, H. t., Tunved, P., Tørseth, K., Wehner, B., Weingartner, E., Wiedensohler, A., and Wåhlin, P. A European aerosol phenomenology – 1: physical characteristics of particulate matter at kerbside, urban, rural and

background sites in Europe. *Atmospheric Environment* 38.16 (2004), pp. 2561–2577. URL: http://www.sciencedirect.com/science/article/pii/S1352231004000937.

[9] Sapkota, A., Symons, J. M., Kleissl, J., Wang, L., Parlange, M. B., Ondov, J., Breysse, P. N., Diette, G. B., Eggleston, P. A., and Buckley, T. J. Impact of the 2002 Canadian Forest Fires on Particulate Matter Air Quality in Baltimore City. *Environmental Science & Technology* 39.1 (2005), pp. 24–32. URL: https://doi.org/10.1021/es035311z.

[10] Ivey, C. E., Holmes, H. A., Hu, Y., Mulholland, J. A., and Russell, A. G. A method for quantifying bias in modeled concentrations and source impacts for secondary particulate matter. *Frontiers of Environmental Science & Engineering* 10.5 (2016), p. 14. URL: https://doi.org/10.1007/s11783-016-0866-6.

[11] Viana, M., Kuhlbusch, T., Querol, X., Alastuey, A., Harrison, R., Hopke, P., Winiwarter, W., Vallius, M., Szidat, S., Prvt, A., Hueglin, C., Bloemen, H., Whlin, P., Vecchi, R., Miranda, A., Kasper-Giebl, A., Maenhaut, W., and Hitzenberger, R. Source apportionment of particulate matter in Europe: A review of methods and results. *Journal of Aerosol Science* 39.10 (2008), pp. 827–849. URL: https://www.sciencedirect.com/science/article/pii/S0021850208001018?via%3Dihub.

[12] Zhang, H., Hu, J., Kleeman, M., and Ying, Q. Source apportionment of sulfate and nitrate particulate matter in the Eastern United States and effectiveness of emission control programs. *Science of The Total Environment* 490 (2014), pp. 171–181. URL: http://www.sciencedirect.com/science/article/pii/S0048969714005749.

[13] Putaud, J.-P., Van Dingenen, R., Alastuey, A., Bauer, H., Birmili, W., Cyrys, J., Flentje, H., Fuzzi, S., Gehrig, R., Hansson, H., Harrison, R., Herrmann, H., Hitzenberger, R., Hüglin, C., Jones, A., Kasper-Giebl, A., Kiss, G., Kousa, A., Kuhlbusch, T., Löschau, G., Maenhaut, W., Molnar, A., Moreno, T., Pekkanen, J., Perrino, C., Pitz, M., Puxbaum, H., Querol, X., Rodriguez, S., Salma, I., Schwarz, J., Smolik, J., Schneider, J., Spindler, G., ten Brink, H., Tursic, J., Viana, M., Wiedensohler, A., and Raes, F. A European aerosol phenomenology – 3: Physical and chemical characteristics of particulate matter from 60 rural, urban, and kerbside sites across Europe. *Atmospheric Environment* 44.10 (2010), pp. 1308–1320. URL: http://www.sciencedirect.com/science/article/pii/S1352231009010358.

[14] Hueglin, C., Gehrig, R., Baltensperger, U., Gysel, M., Monn, C., and Vonmont, H. Chemical characterisation of PM2.5, PM10 and coarse particles at urban, near-city and rural sites in Switzerland. *Atmospheric Environment* 39.4 (2005), pp. 637–651. URL: http://www.sciencedirect.com/science/article/pii/S1352231004010131.

[15] Gianini, M. F. D., Gehrig, R., Fischer, A., Ulrich, A., Wichser, A., and Hueglin, C. Chemical composition of PM10 in Switzerland: An analysis for 2008/2009 and changes since 1998/1999. *Atmospheric Environment* 54 (2012), pp. 97–106. URL: http://www.sciencedirect.com/science/article/pii/S1352231012001525.

[16]   Gianini, M. F. D., Fischer, A., Gehrig, R., Ulrich, A., Wichser, A., Piot, C., Besombes, J.-L., and Hueglin, C. Comparative source apportionment of PM10 in Switzerland for 2008/2009 and 1998/1999 by Positive Matrix Factorisation. *Atmospheric Environment* 54 (2012), pp. 149–158. URL: http://www.sciencedirect.com/science/article/pii/S1352231012001513.

[17]   Barmpadimos, I., Hueglin, C., Keller, J., Henne, S., and Prévôt, A. S. H. Influence of meteorology on PM_{10} trends and variability in Switzerland from 1991 to 2008. *Atmospheric Chemistry and Physics* 11.4 (2011), pp. 1813–1835. URL: http://www.atmos-chem-phys.net/11/1813/2011/.

[18]   Grange, S. K., Carslaw, D. C., Lewis, A. C., Boleti, E., and Hueglin, C. Random forest meteorological normalisation models for Swiss PM_{10} trend analysis. *Atmospheric Chemistry and Physics* 18.9 (2018), pp. 6223–6239. URL: https://www.atmos-chem-phys.net/18/6223/2018/.

[19]   Grange, S. K., Lötscher, H., Fischer, A., Emmenegger, L., and Hueglin, C. Evaluation of equivalent black carbon source apportionment using observations from Switzerland between 2008 and 2018. *Atmospheric Measurement Techniques* 13.4 (2020), pp. 1867–1885. URL: https://www.atmos-meas-tech.net/13/1867/2020/.

[20]   European Committee for Standardization. Ambient air – Standard gravimetric measurement method for the determination of the PM_{10} or $PM_{2.5}$ mass concentration of suspended particulate matter. Ref Nr.: SN EN 12341:2014 en. Prepared by Technical Committee CEN/TC 264 "Air quality". 2014.

[21]   European Committee for Standardization (CEN). CEN EN 16909: Ambient air – Measurement of elemental carbon (EC) and organic carbon (OC) collected on filters. 2017.

[22]   Pérez, N., Pey, J., Querol, X., Alastuey, A., López, J. M., and Viana, M. Partitioning of major and trace components in PM_{10}-$PM_{2.5}$-PM_1 at an urban site in Southern Europe. *Atmospheric Environment* 42.8 (2008), pp. 1677–1691. URL: http://www.sciencedirect.com/science/article/pii/S1352231007010874.

[23]   Deutsches Institut für Normung. DIN - VDI 2465 BLATT 1: Measurement of soot (immission) - Chemical analysis of elemental carbon by extraction and thermal desorption of the organic carbon. 1996. URL: https://standards.globalspec.com/std/51449/vdi-2465-blatt-1.

[24]   Chow, J. C., Watson, J. G., Fujita, E. M., Lu, Z., Lawson, D. R., and Ashbaugh, L. L. Temporal and spatial variations of $PM_{2.5}$ and PM_{10} aerosol in the Southern California air quality study. *Atmospheric Environment* 28.12 (1994), pp. 2061–2080. URL: http://www.sciencedirect.com/science/article/pii/135223109490474X.

[25]   Hans Wedepohl, K. The composition of the continental crust. *Geochimica et Cosmochimica Acta* 59.7 (1995), pp. 1217–1232. URL: http://www.sciencedirect.com/science/article/pii/0016703795000382.

[26] Kreider, M. L., Panko, J. M., McAtee, B. L., Sweet, L. I., and Finley, B. L. Physical and chemical characterization of tire-related particles: Comparison of particles generated using different methodologies. *Science of The Total Environment* 408.3 (2010), pp. 652–659. URL: http://www.sciencedirect.com/science/article/pii/S0048969709009590.

[27] Amato, F., Alastuey, A., Rosa, J. de la, Gonzalez Castanedo, Y., Sánchez de la Campa, A. M., Pandolfi, M., Lozano, A., Contreras González, J., and Querol, X. Trends of road dust emissions contributions on ambient air particulate levels at rural, urban and industrial sites in southern Spain. *Atmospheric Chemistry and Physics* 14.7 (2014), pp. 3533–3544. URL: https://acp.copernicus.org/articles/14/3533/2014/.

[28] Janssen, N. A. H., Yang, A., Strak, M., Steenhof, M., Hellack, B., Gerlofs-Nijland, M. E., Kuhlbusch, T., Kelly, F., Harrison, R., Brunekreef, B., Hoek, G., and Cassee, F. Oxidative potential of particulate matter collected at sites with different source characteristics. *Science of The Total Environment* 472 (2014), pp. 572–581. URL: http://www.sciencedirect.com/science/article/pii/S0048969713014022.

[29] Calas, A., Uzu, G., Besombes, J.-L., Martins, J. M. F., Redaelli, M., Weber, S., Charron, A., Albinet, A., Chevrier, F., Brulfert, G., Mesbah, B., Favez, O., and Jaffrezo, J.-L. Seasonal Variations and Chemical Predictors of Oxidative Potential (OP) of Particulate Matter (PM), for Seven Urban French Sites. *Atmosphere* 10.11 (2019), p. 698. URL: https://www.mdpi.com/2073-4433/10/11/698.

[30] Hopke, P. K. Review of receptor modeling methods for source apportionment. *Journal of the Air & Waste Management Association* 66.3 (2016). PMID: 26756961, pp. 237–259. URL: https://doi.org/10.1080/10962247.2016.1140693.

[31] Paatero, P. The Multilinear Engine – A Table-Driven, Least Squares Program for Solving Multilinear Problems, Including the *n*-Way Parallel Factor Analysis Model. *Journal of Computational and Graphical Statistics* 8.4 (1999), pp. 854–888. URL: https://doi.org/10.1080/10618600.1999.10474853.

[32] Comero, S., Capitani, L., and Gawlik, B. M. Positive Matrix Factorisation (PMF). An introduction to the chemometric evaluation of environmental monitoring data using PMF. EUR 23946 EN - 2009. 2009. URL: https://publications.jrc.ec.europa.eu/repository/handle/JRC52754.

[33] Olivier, F., Belis, C. A., Amato, F., Decesari, S., Diapouli, E., Haddad, I. E., Gilardoni, S., Harrison, R., Hopke, P. K., Larsen, B. R., Manousakas, M.-I., Mocnik, G., Mooibroek, D., Nava, S., Paatero, P., Paglione, M., Prévôt, A., Quass, U., Salvador, P., Takahama, S., Vecchi, R., Viana, M., and Vratolis, S. European Guide on Air Pollution Source Apportionment with Receptor Models REVISION 2019. 2019. URL: https://source-apportionment.jrc.ec.europa.eu/Docu/european%20_guide_SA_RMs_revision_2019.pdf.

[34] Weber, S., Salameh, D., Albinet, A., Alleman, L. Y., Waked, A., Besombes, J.-L., Jacob, V., Guillaud, G., Meshbah, B., Rocq, B., Hulin, A., Chrétien, M. D.-S. E., Jaffrezo, J.-L., and Favez, O. Comparison

of PM_{10} Sources Profiles at 15 French Sites Using a Harmonized Constrained Positive Matrix Factorization Approach. *Atmosphere* 10.6 (2019), p. 310.

[35] Norris, G., Duvall, R., Brown, S., and Bai, S. EPA Positive Matrix Factorization (PMF) 5.0 Fundamentals and User Guide. U.S. Environmental Protection Agency, EPA/600/R-14/108, April 2014. 2014. URL: https://www.epa.gov/air-research/epa-positive-matrix-factorization-50-fundamentals-and-user-guide.

[36] Brown, S. G., Eberly, S., Paatero, P., and Norris, G. A. Methods for estimating uncertainty in PMF solutions: Examples with ambient air and water quality data and guidance on reporting PMF results. *Science of The Total Environment* 518-519 (2015), pp. 626–635. URL: http://www.sciencedirect.com/science/article/pii/S004896971500025X.

[37] Belis, C. A., Larsen, B. R., Amato, F., Haddad, I. E., Favez, O., M.Harrison, R., Hopke, P. K., Nava, S., Paatero, P., Prévôt, A., Quass, U., Vecchi, R., and Viana, M. European Guide on Air Pollution Source Apportionment with Receptor Models. Reference Report by the Joint Research Centreof the European Commission. Report EUR 26080 EN. 2014. URL: https://ec.europa.eu/jrc/en/publication/reference-reports/european-guide-air-pollution-source-apportionment-receptor-models.

[38] Grange, S. K. *pmfr: Interact With Data Generated by the EPA PMF Tool*. R package. 2020. URL: https://github.com/skgrange/pmfr.

[39] Bozzetti, C., Daellenbach, K. R., Hueglin, C., Fermo, P., Sciare, J., Kasper-Giebl, A., Mazar, Y., Abbaszade, G., El Kazzi, M., Gonzalez, R., Shuster-Meiseles, T., Flasch, M., Wolf, R., Křepelová, A., Canonaco, F., Schnelle-Kreis, J., Slowik, J. G., Zimmermann, R., Rudich, Y., Baltensperger, U., El Haddad, I., and Prévôt, A. Size-Resolved Identification, Characterization, and Quantification of Primary Biological Organic Aerosol at a European Rural Site. *Environmental Science and Technology* 50.7 (2016), pp. 3425–3434. URL: https://doi.org/10.1021/acs.est.5b05960.

[40] Cavalli, F., Viana, M., Yttri, K. E., Genberg, J., and Putaud, J.-P. Toward a standardised thermal-optical protocol for measuring atmospheric organic and elemental carbon: the EUSAAR protocol. *Atmospheric Measurement Techniques* 3.1 (2010), pp. 79–89. URL: https://amt.copernicus.org/articles/3/79/2010/.

[41] Hodzic, A., Bessagnet, B., and Vautard, R. A model evaluation of coarse-mode nitrate heterogeneous formation on dust particles. *Atmospheric Environment* 40.22 (2006), pp. 4158–4171. URL: http://www.sciencedirect.com/science/article/pii/S1352231006002081.

[42] Beuth Publishing DIN. Ambient air measurements – Sampling of atmospheric particles > 2.5 mum on an acceptor surface using the Sigma-2 passive sampler - Characterisation by optical microscopy and calculation of number settling rate and mass concentration. VDI 2119:2013-06. 2013.

[43] Seinfeld, J. H. and Pandis, S. N. *Atmospheric Chemistry and Physics: From Air Pollution to Climate Change*. John Wiley & Sons, 1998.

[44] Harrison, R. M. Urban atmospheric chemistry: a very special case for study. *npj Climate and Atmospheric Science* 1.1 (2018), p. 20175. URL: https://doi.org/10.1038/s41612-017-0010-8.

[45] Thunis, P., Degraeuwe, B., Pisoni, E., Trombetti, M., Peduzzi, E., Belis, C. A., Wilson, J., Clappier, A., and Vignati, E. PM$_{2.5}$ source allocation in European cities: A SHERPA modelling study. *Atmospheric Environment* 187 (2018), pp. 93–106. URL: http://www.sciencedirect.com/science/article/pii/S1352231018303728.

[46] Pandolfi, M., Mooibroek, D., Hopke, P., Pinxteren, D. van, Querol, X., Herrmann, H., Alastuey, A., Favez, O., Hüglin, C., Perdrix, E., Riffault, V., Sauvage, S., Swaluw, E. van der, Tarasova, O., and Colette, A. Long-range and local air pollution: what can we learn from chemical speciation of particulate matter at paired sites? *Atmospheric Chemistry and Physics* 20.1 (2020), pp. 409–429. URL: https://www.atmos-chem-phys.net/20/409/2020/.

[47] Amato, F., Viana, M., Richard, A., Furger, M., Prévôt, A. S. H., Nava, S., Lucarelli, F., Bukowiecki, N., Alastuey, A., Reche, C., Moreno, T., Pandolfi, M., Pey, J., and Querol, X. Size and time-resolved roadside enrichment of atmospheric particulate pollutants. *Atmospheric Chemistry and Physics* 11.6 (2011), pp. 2917–2931. URL: https://acp.copernicus.org/articles/11/2917/2011/.

[48] Denier van der Gon Hugo AC Gerlofs-Nijland, M. E., Gehrig, R., Gustafsson, M., Janssen, N., Harrison, R. M., Hulskotte, J., Johansson, C., Jozwicka, M., Keuken, M., Krijgsheld, K., Ntziachristos, L., Riediker, M., and Cassee, F. R. The Policy Relevance of Wear Emissions from Road Transport, Now and in the Future—An International Workshop Report and Consensus Statement. *Journal of the Air & Waste Management Association* 63.2 (2013), pp. 136–149. eprint: https://doi.org/10.1080/10962247.2012.741055. URL: ://doi.org/10.1080/10962247.2012.741055.

[49] Grange, S. K. and Carslaw, D. C. Using meteorological normalisation to detect interventions in air quality time series. *Science of the Total Environment* 653 (2019), pp. 578–588. URL: http://www.sciencedirect.com/science/article/pii/S004896971834244X.

[50] Wu, T., Lo, K., and Stafford, J. Vehicle non-exhaust emissions – Revealing the pathways from source to environmental exposure. *Environmental Pollution* 268 (2021), p. 115654. URL: http://www.sciencedirect.com/science/article/pii/S0269749120363429.

[51] Belis, C. A., Pernigotti, D., Karagulian, F., Pirovano, G., Larsen, B. R., Gerboles, M., and Hopke, P. K. A new methodology to assess the performance and uncertainty of source apportionment models in intercomparison exercises. *Atmospheric Environment* 119 (2015), pp. 35–44. URL: http://www.sciencedirect.com/science/article/pii/S1352231015302478.

[52] Matsumoto, K. and Tanaka, H. Formation and dissociation of atmospheric particulate nitrate and chloride: An approach based on phase equilibrium. *Atmospheric Environment* 30.4 (1996), pp. 639–648. URL: http://www.sciencedirect.com/science/article/pii/1352231095002901.

[53] Bhattarai, H., Saikawa, E., Wan, X., Zhu, H., Ram, K., Gao, S., Kang, S., Zhang, Q., Zhang, Y., Wu, G., Wang, X., Kawamura, K., Fu, P., and Cong, Z. Levoglucosan as a tracer of biomass burning:

Recent progress and perspectives. *Atmospheric Research* 220 (2019), pp. 20–33. URL: http://www.sciencedirect.com/science/article/pii/S0169809518311098.

[54] Achten, P. A. J., Amato, F., Leeuw, F. de, Miguel, E. de, Denby, B. R., Gon, H. D. van der, Faustini, A., Filip, P., Gramstat, S., Grigoratos, T., Gustafsson, M., Harrison, R. M., Holman, C., Hopke, P. K., Hulskotte, J., Jozwicka, M., Kranenburg, R., Kreider, M., Kuenen, J., Kukutschová, J., Kupiainen, K. J., Martins, V., Minguillón, M. C., Moreno, T., Padoan, E., Panko, J., Querol, X., Reche, C., Robusté, F., Stafoggia, M., Timmers, V. R. J. H., Unice, K., and Visschedijk, A. *Non-exhaust emissions: an urban air quality problem for public health; impact and mitigation measures*. Ed. by F. Amato. Academic Press, 2018. URL: https://www.sciencedirect.com/book/9780128117705/non-exhaust-emissions.

[55] Grange, S. K. and Hüglin, C. Horizontal visibility across Switzerland between 1980 and 2018. A report prepared by Empa, Swiss Federal Laboratories for Materials Science and Technology, Air Pollution/Environmental Technology Laboratory commissioned by the Federal Office for the Environment (FOEN). 2020. URL: https://www.bafu.admin.ch/dam/bafu/en/dokumente/luft/externe-studien-berichte/swiss_visibility_note.pdf.download.pdf/swiss_visibility_note.pdf.

8 Appendix

8.1 Figures
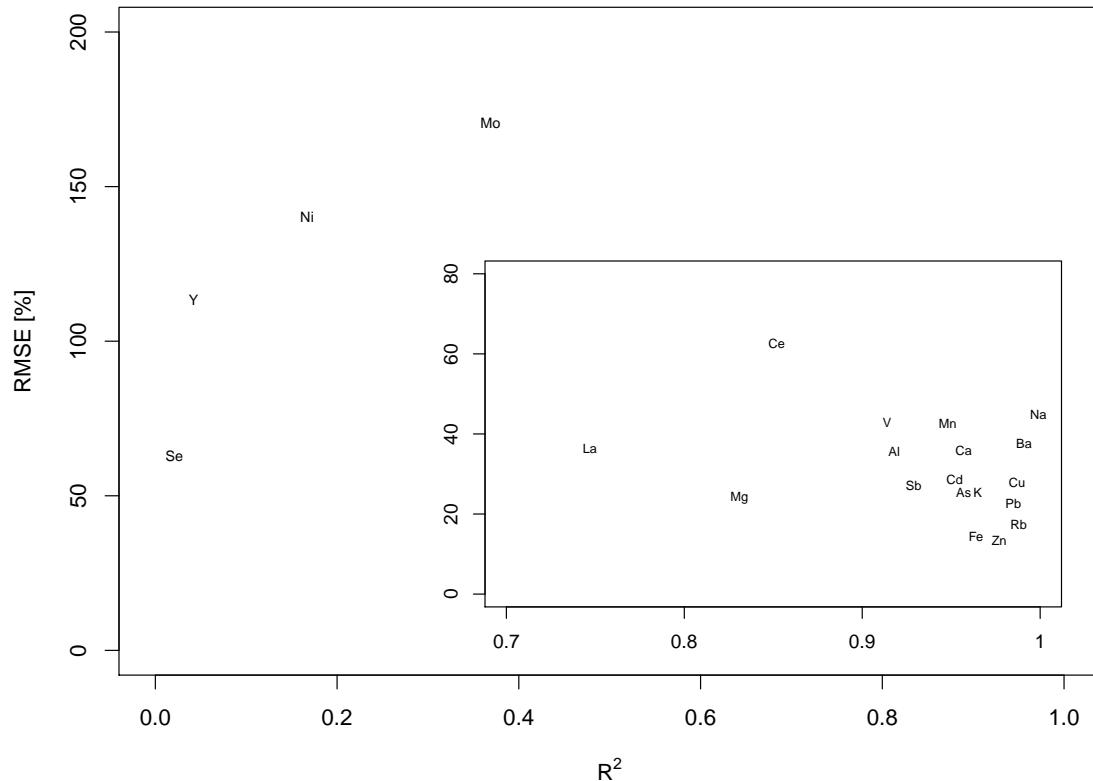
Figure A.1 – Comparison of the results of two different analytical procedures for determination of element concentrations in PM. PM_{10} filter samples from Zürich-Kaserne and Payerne from 04.02.2009, 28.02.2009, 09.04.2009 and 02.07.2009 were analysed by Empa and IDAEA-CSIC using the analytical procedures as for the measurement periods 1998–1999 and 2008–2009 (Empa) and the recent measurement period 2018–2019 (IDAEA-CSIC). Shown is the root mean squared error (RMSE) divided by the mean element concentration versus the coefficient of determination (R^2) for all elements in this method comparison. Few elements show a poor agreement with $R^2 < 0.4$, however, most of the elements show a high correlation as shown by the inserted subplot.
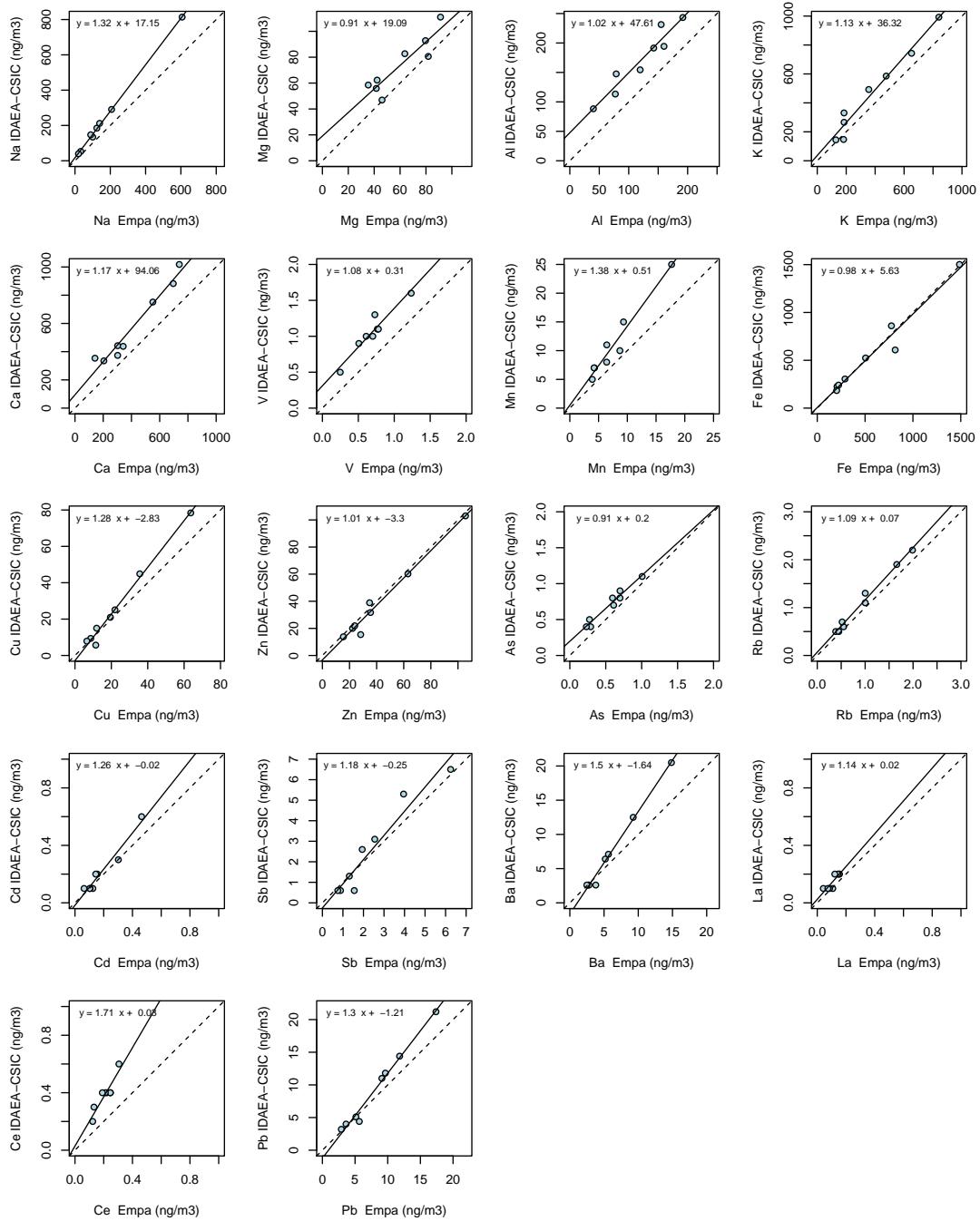
Figure A.2 – Comparison of element concentrations as obtained by IDAEA-CSIC and Empa. PM_{10} filter samples from Zürich-Kaserne and Payerne from 04.02.2009, 28.02.2009, 09.04.2009 and 02.07.2009 were analysed using the analytical procedures as for the measurement periods 1998–1999 and 2008–2009 (Empa) and the recent measurement period 2018–2019 (IDAEA-CSIC). Shown are scatter plots for all elements with $R^2 > 0.7$, see Figure A.1. For most elements, the procedure applied by IDAEA-CSIC results in systematically higher element concentrations compared to the milder acid digestion method applied by Empa.
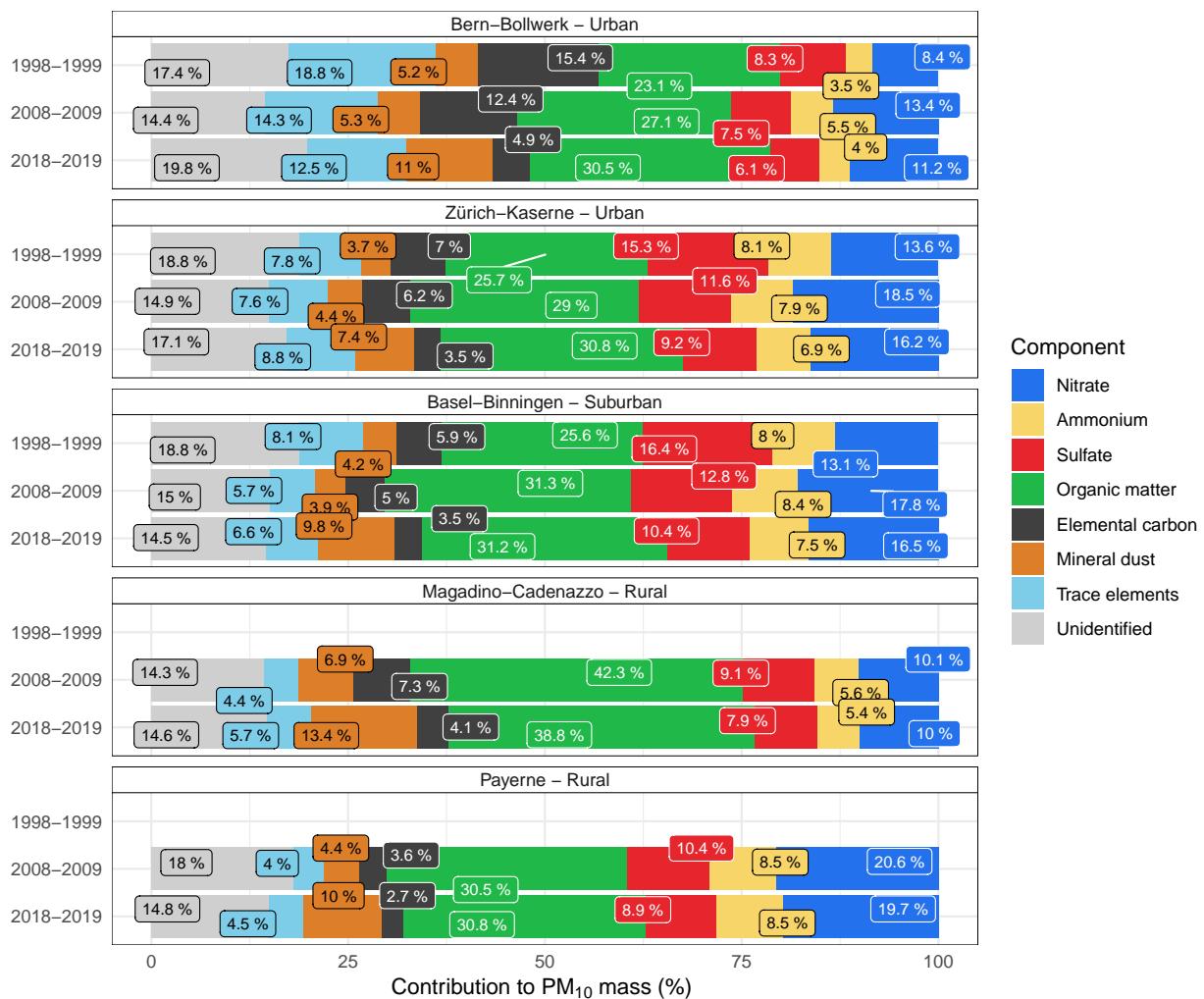
Figure A.3 – Relative contribution of main PM_{10} components for five sites between 1998 and 2019.
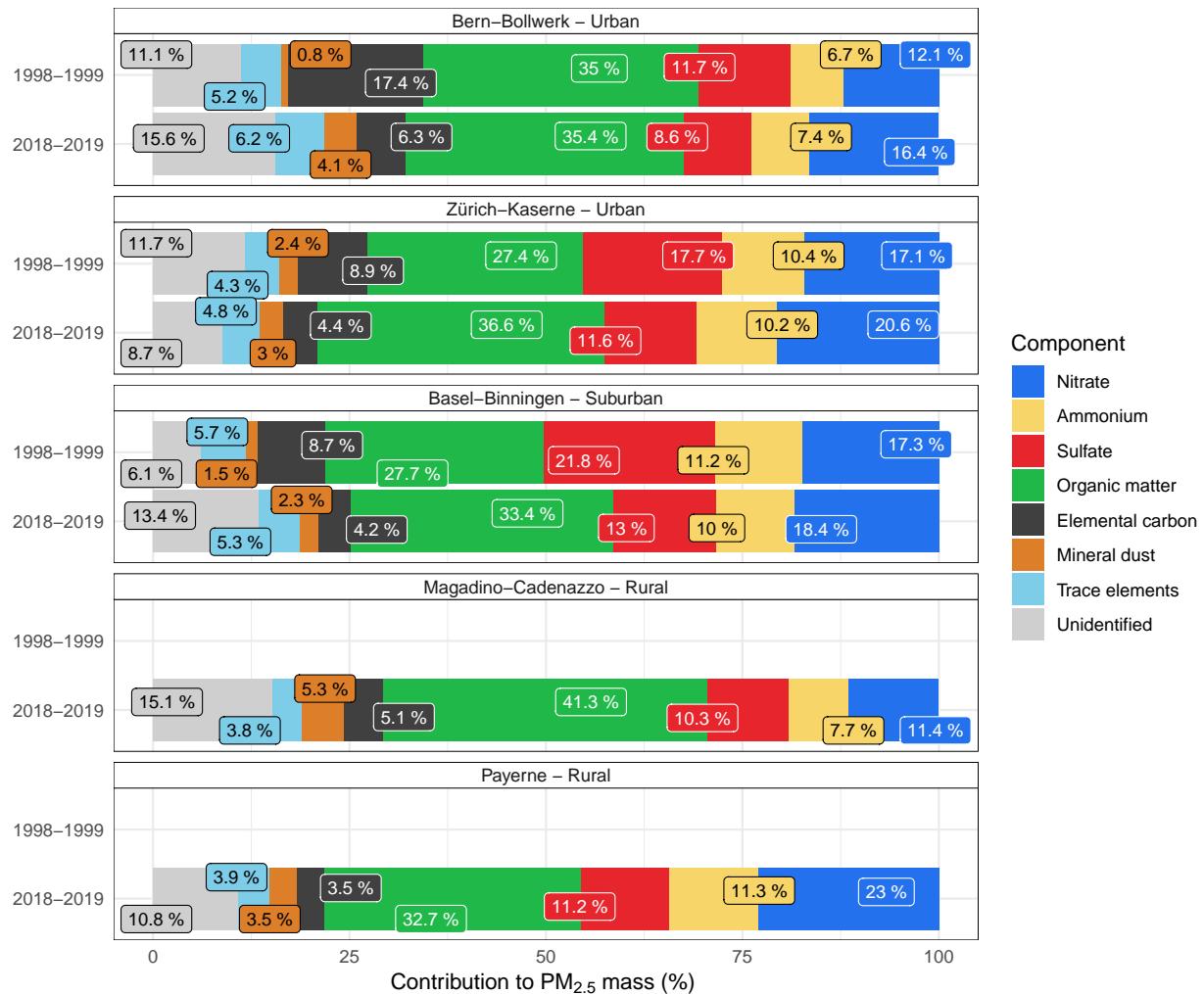
Figure A.4 – Relative contribution of main PM$_{2.5}$ components for five sites between 1998 and 2019.
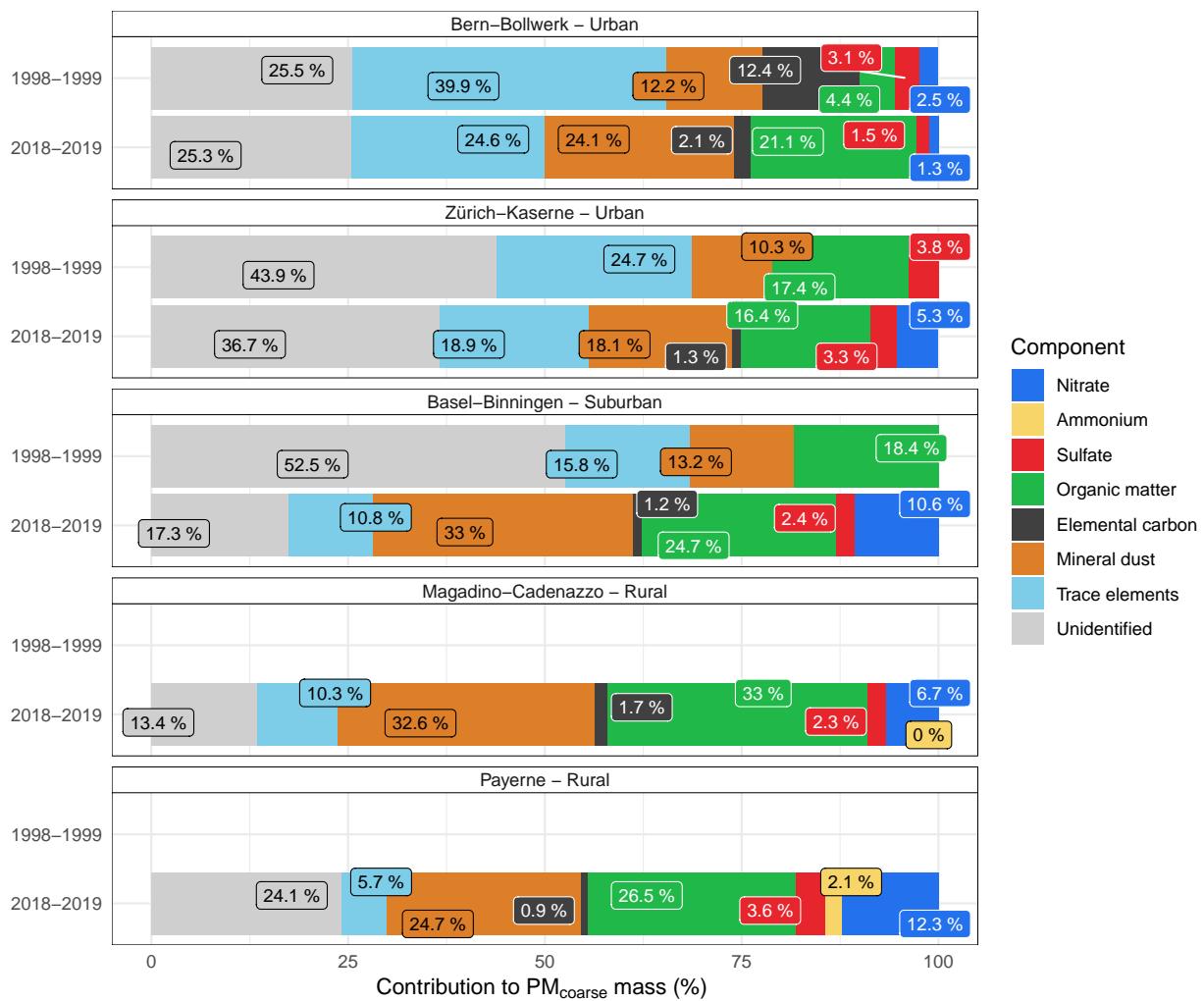
Figure A.5 – Relative contribution of main $PM_{2.5-10}$ components for five sites between 1998 and 2019.
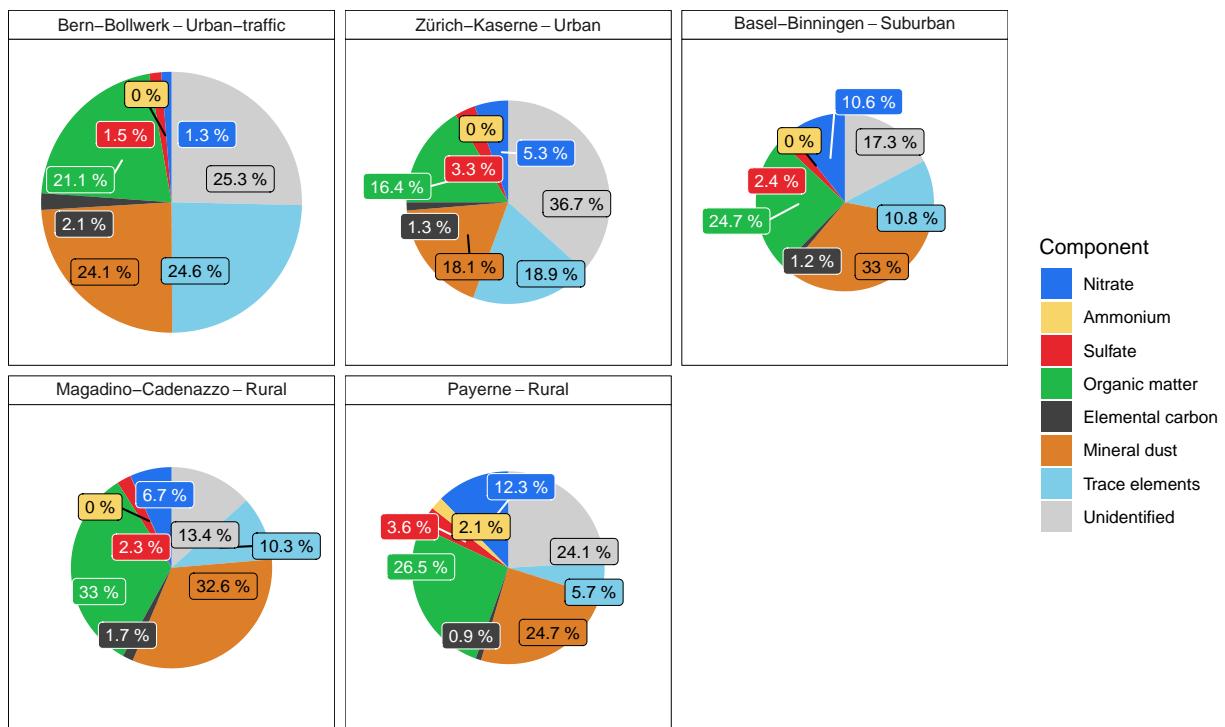
Figure A.6 – Pie charts of the relative contribution of the main PM$_{2.5-10}$ components for five sites the 2018–2019 measurement period. The area of the shown circles is proportional to the PM$_{2.5-10}$ concentration at the different sites (Bern-Bollwerk: 7.3 μg m^{-3}, Zürich-Kaserne: 4.5 μg m^{-3}, Basel-Binningen: 3.4 μg m^{-3}, Magadino-Cadenazzo: 4.4 μg m^{-3}, Payerne: 4.0 μg m^{-3}).
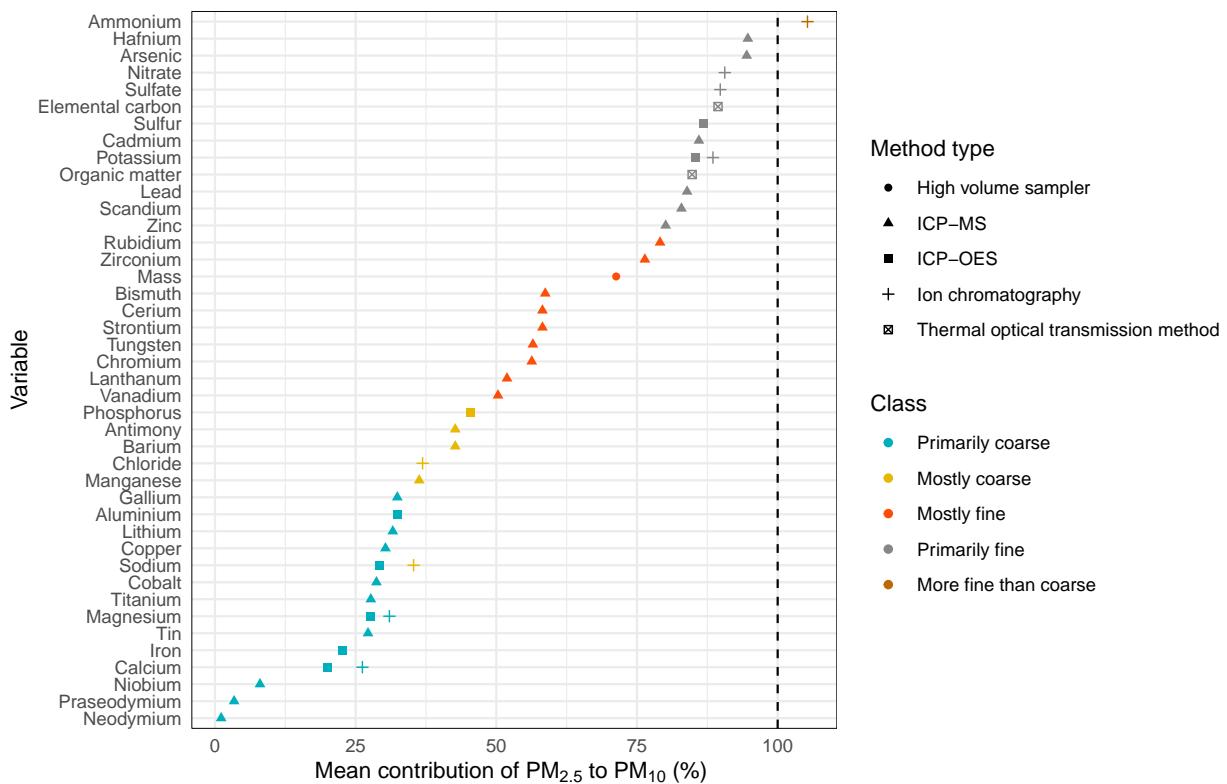
Figure A.7 – Mean percentage of the concentration of main constituents and trace elements in $PM_{2.5}$ compared to the concentrations determined in PM_{10} for all five studied sampling locations. The percentages have been calculated on daily basis and averaged over the measurement period 2018-2019 and across all sites. Note that the shown percentages can have a significant uncertainty. The slightly higher concentration of ammonium found in $PM_{2.5}$ compared to PM_{10} is an example and a result of concentration differences in PM_{10} and $PM_{2.5}$ that are often below the measurement uncertainty. Nevertheless, it can be concluded that ammonium is overwhelmingly associated with $PM_{2.5}$ and virtually not present in $PM_{2.5-10}$ (see Figure A.6). Used classification: primarily coarse 0-33 %, mostly coarse 33-50 %, mostly fine 50-80 %, primarily fine 80-100 %.
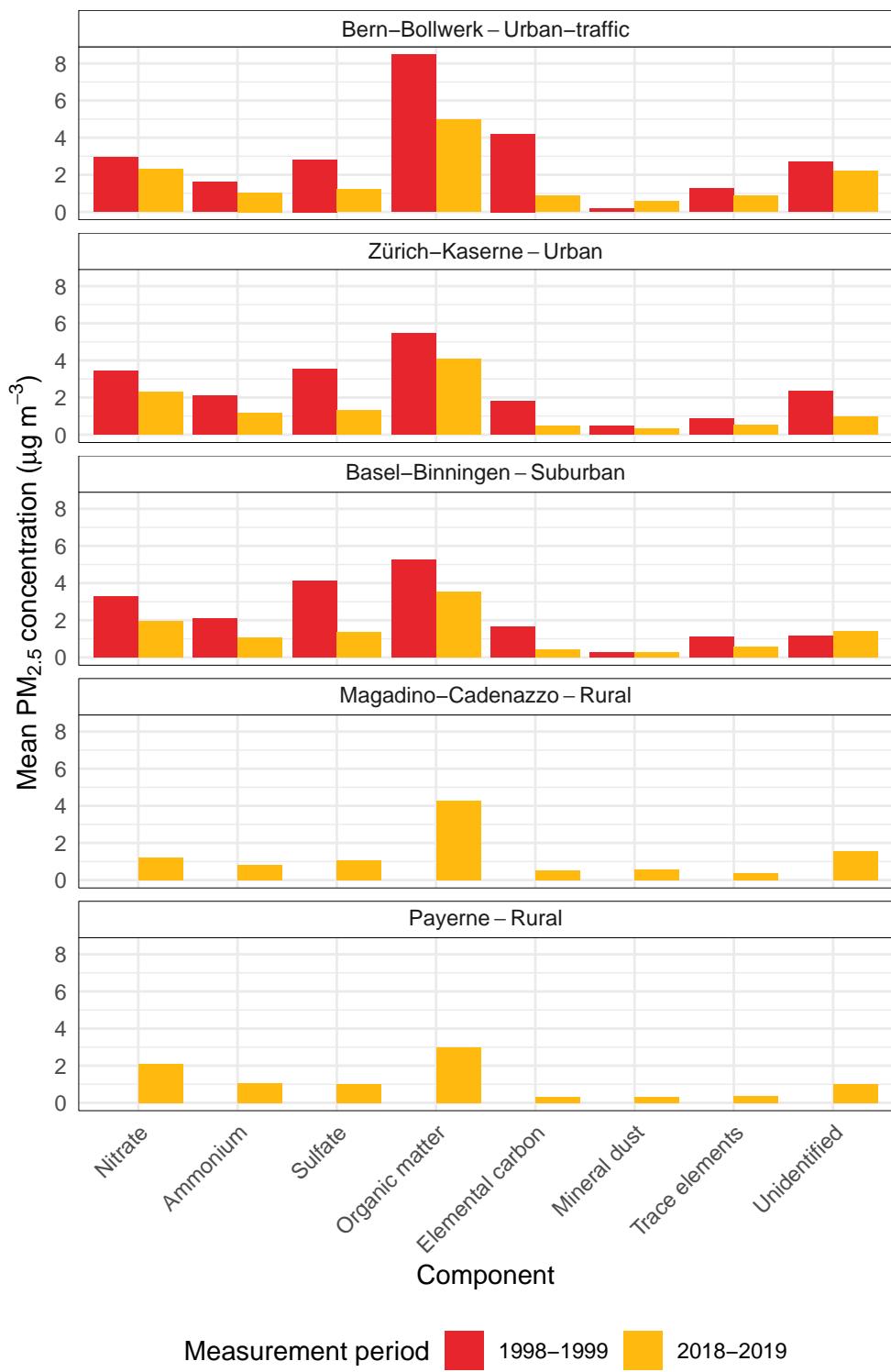
Figure A.8 – Mean concentrations of major constituents in $PM_{2.5}$ for the the 1998–1999 and 2018–2019 measurement periods.
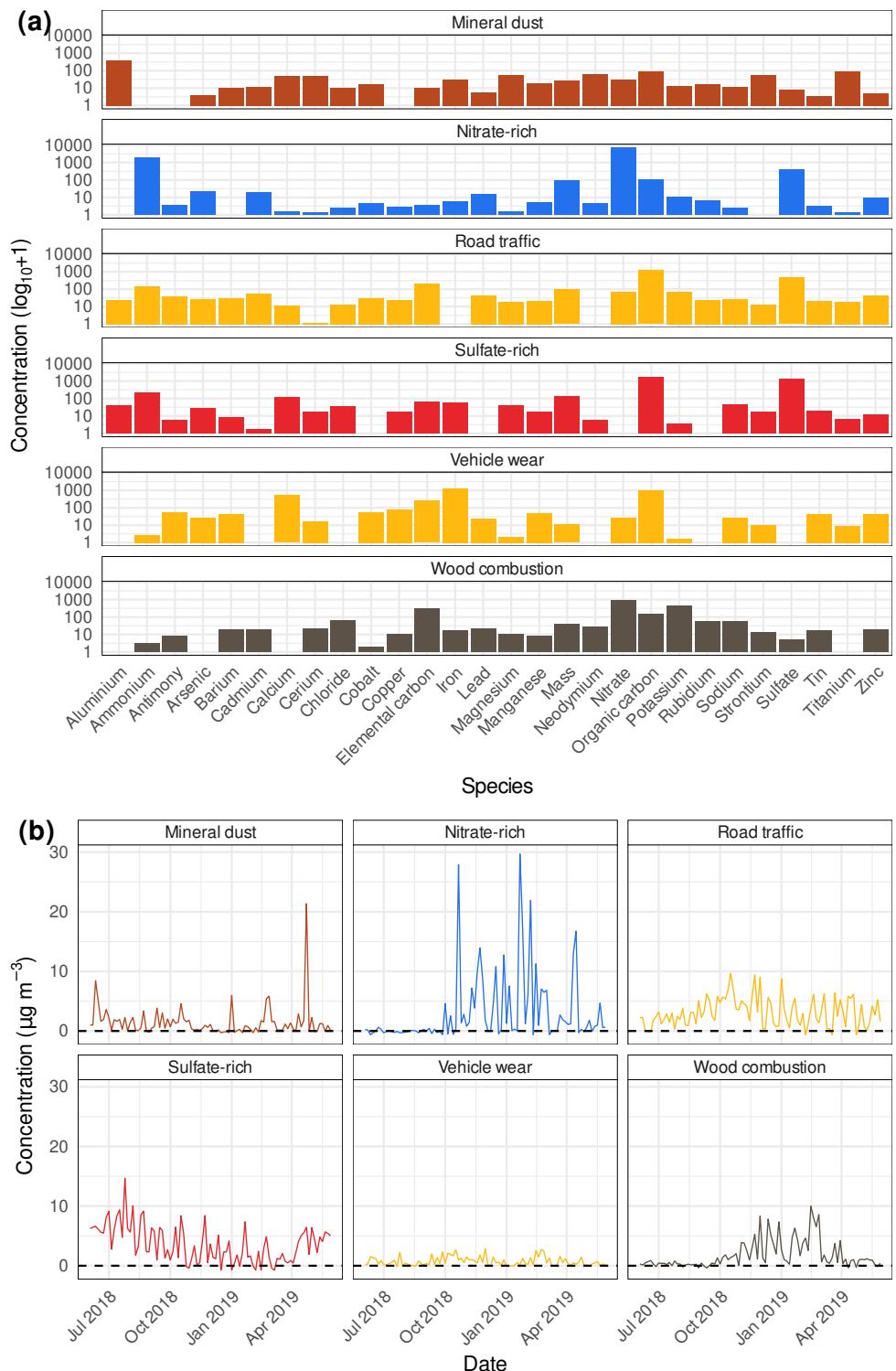
Figure A.9 – Basel-Binningen PM_{10} source contributions (a) and time series (b) between June 1, 2018 and May 31, 2019 identified by positive matrix factorisation (PMF).
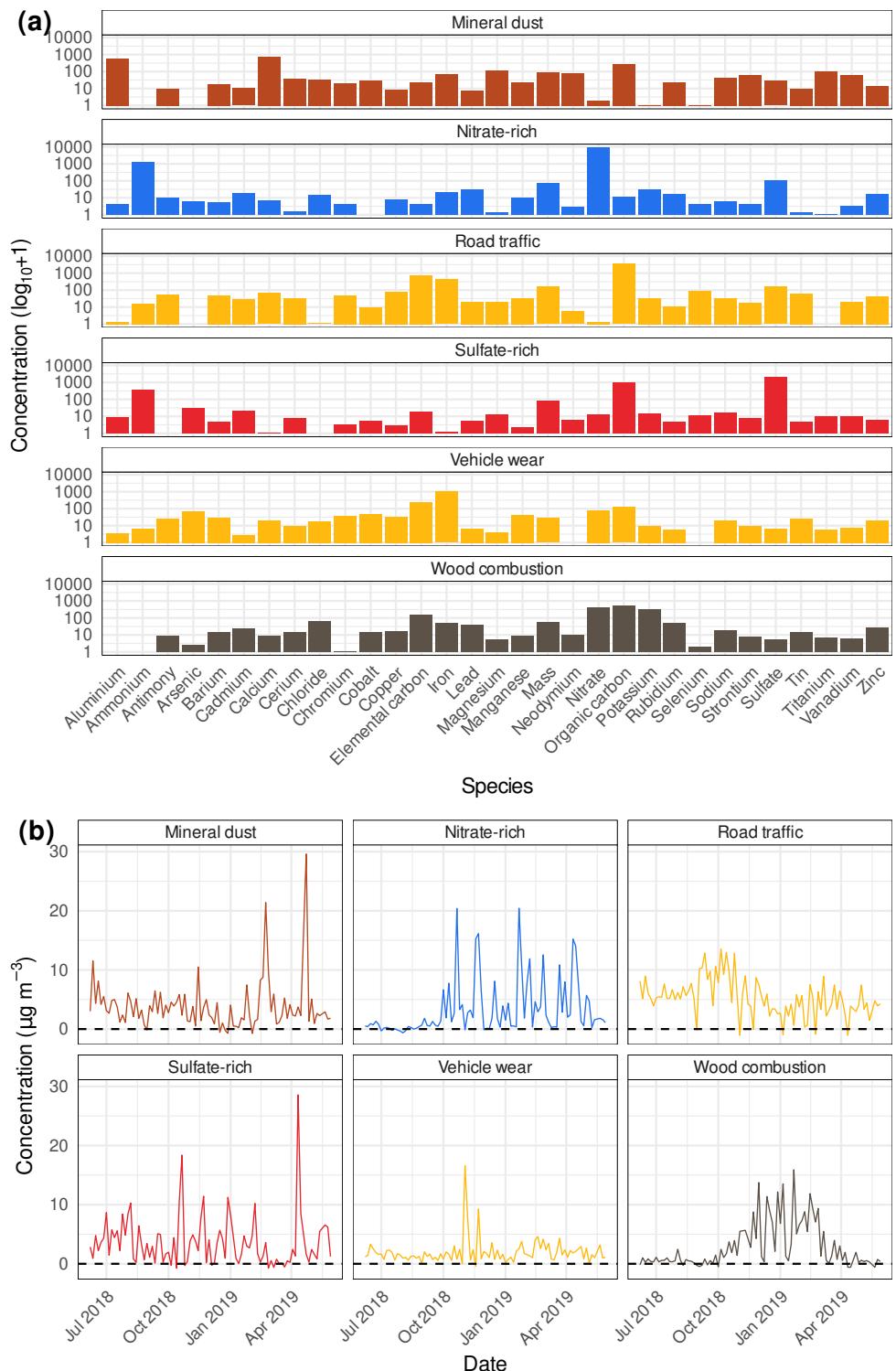
Figure A.10 – Bern-Bollwerk PM$_{10}$ source contributions (a) and time series (b) between June 1, 2018 and May 31, 2019 identified by positive matrix factorisation (PMF).
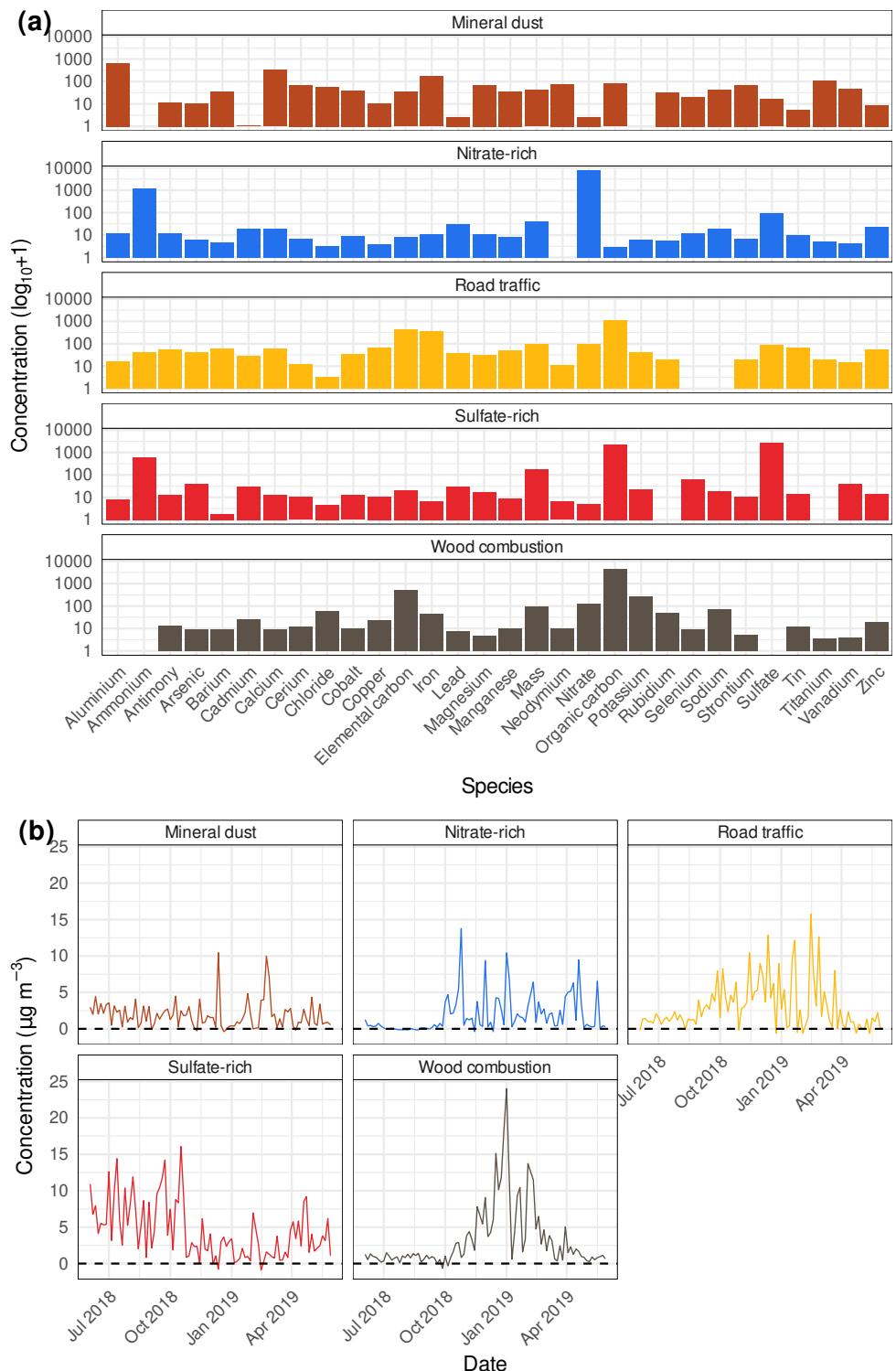
Figure A.11 – Magadino-Cadenazzo PM$_{10}$ source contributions (a) and time series (b) between June 1, 2018 and May 31, 2019 identified by positive matrix factorisation (PMF).
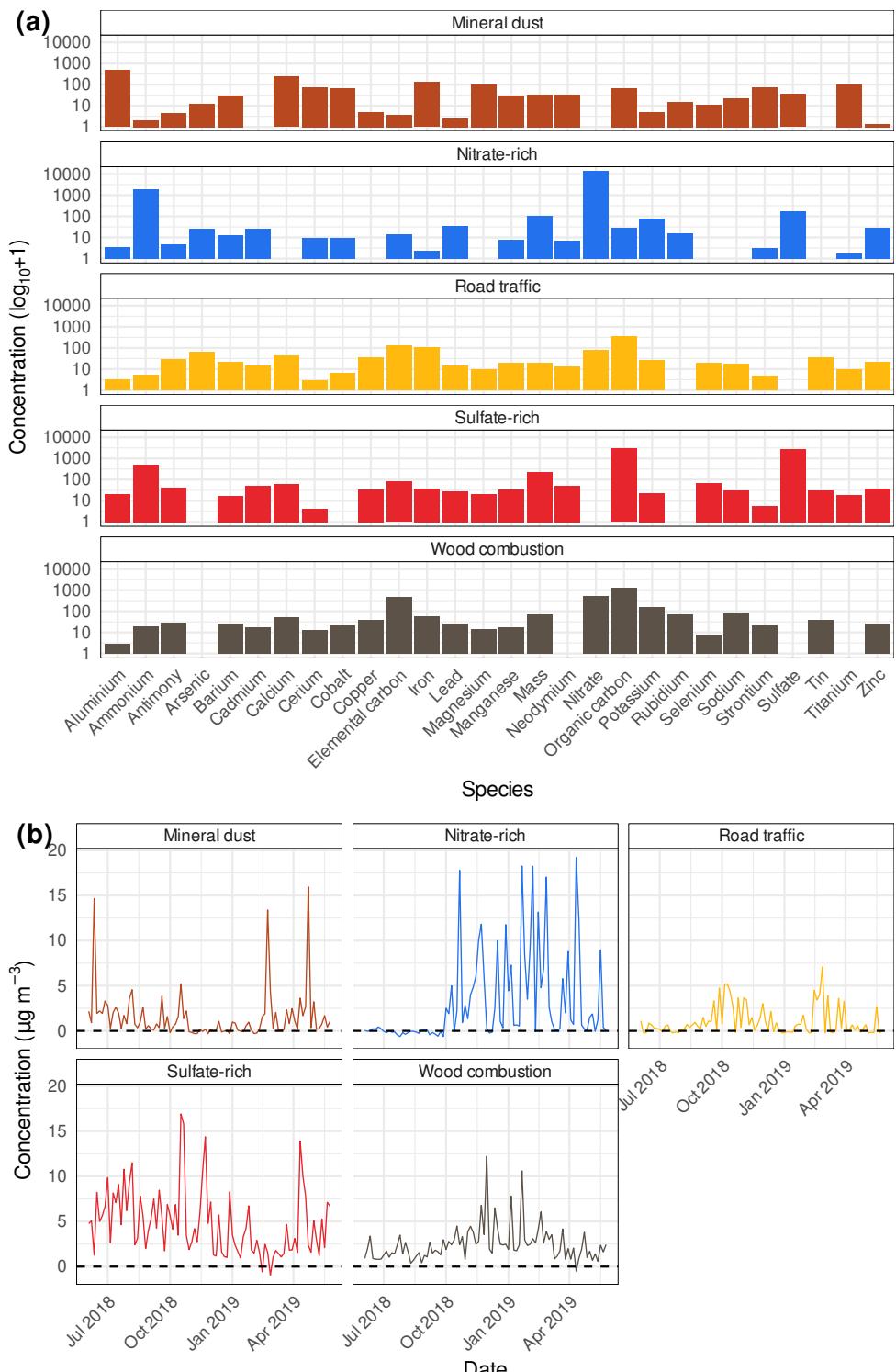
Figure A.12 – Payerne PM$_{10}$ source contributions (a) and time series (b) between June 1, 2018 and May 31, 2019 identified by positive matrix factorisation (PMF).
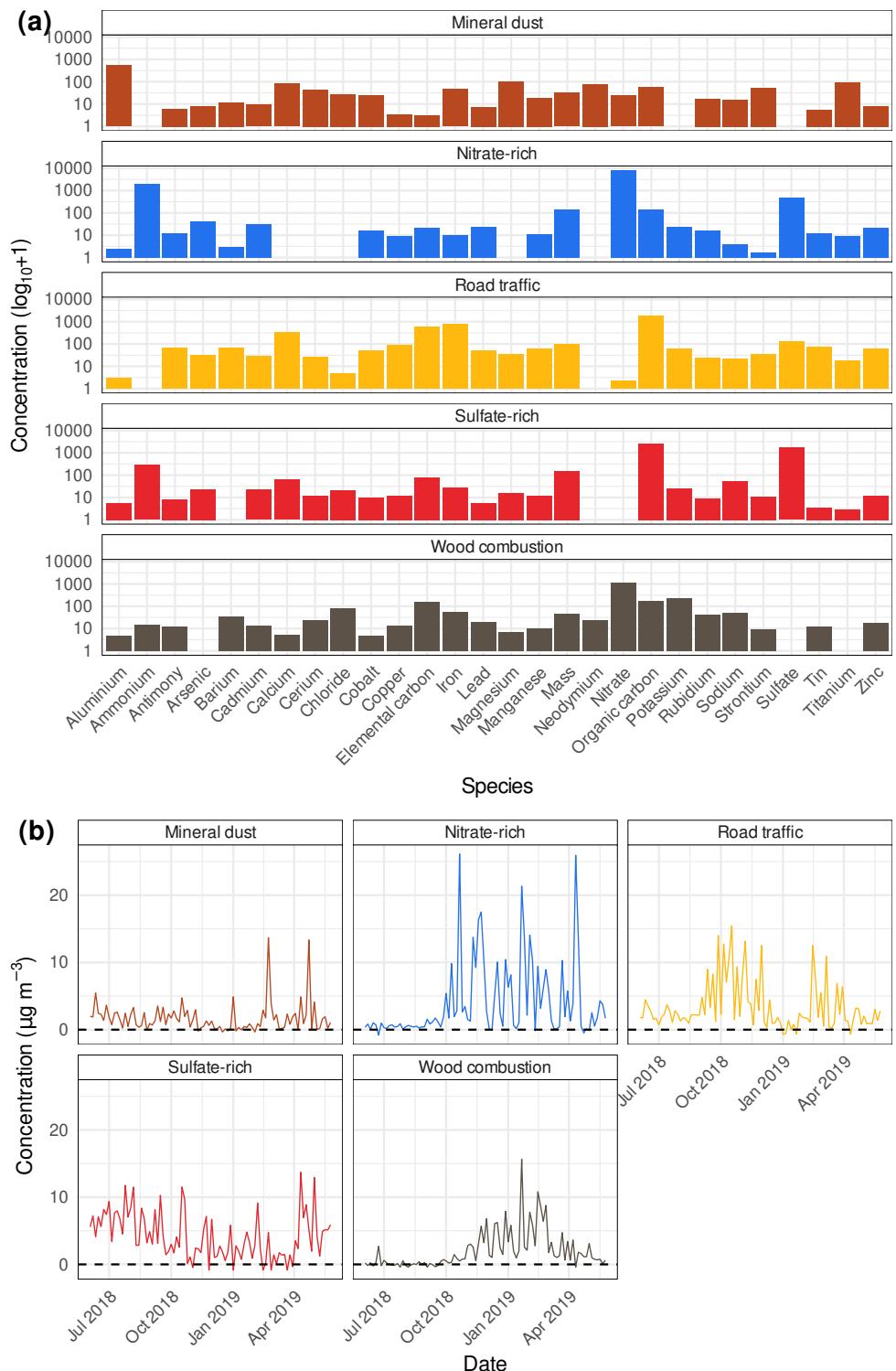
Figure A.13 – Zürich-Kaserne PM$_{10}$ source contributions (a) and time series (b) between June 1, 2018 and May 31, 2019 identified by positive matrix factorisation (PMF).
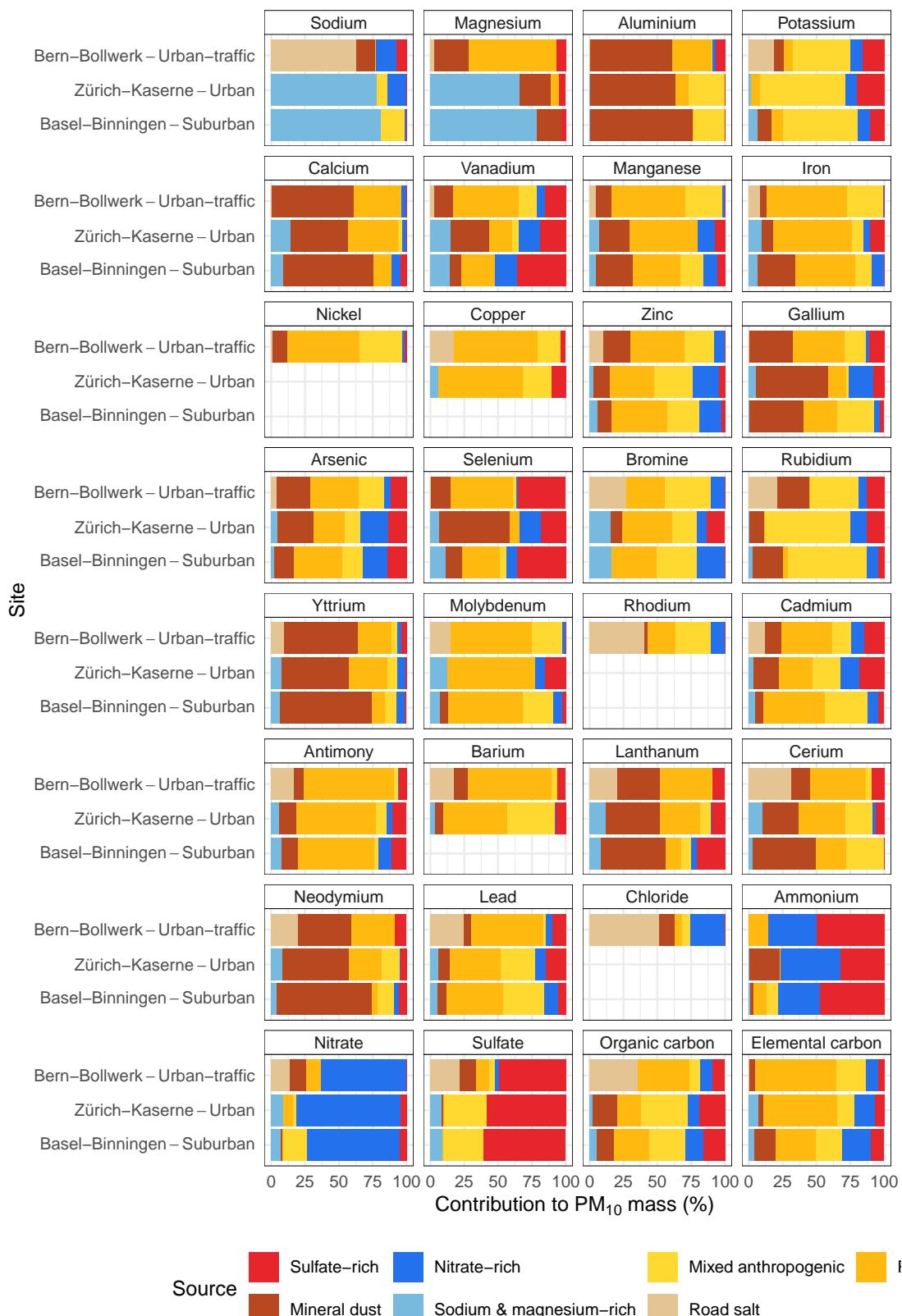
Figure A.14 – Percentage of the mass of constituents of PM$_{10}$ explained by the PMF-identified sources at three sampling locations between April 1, 1998 and March 31, 1999.
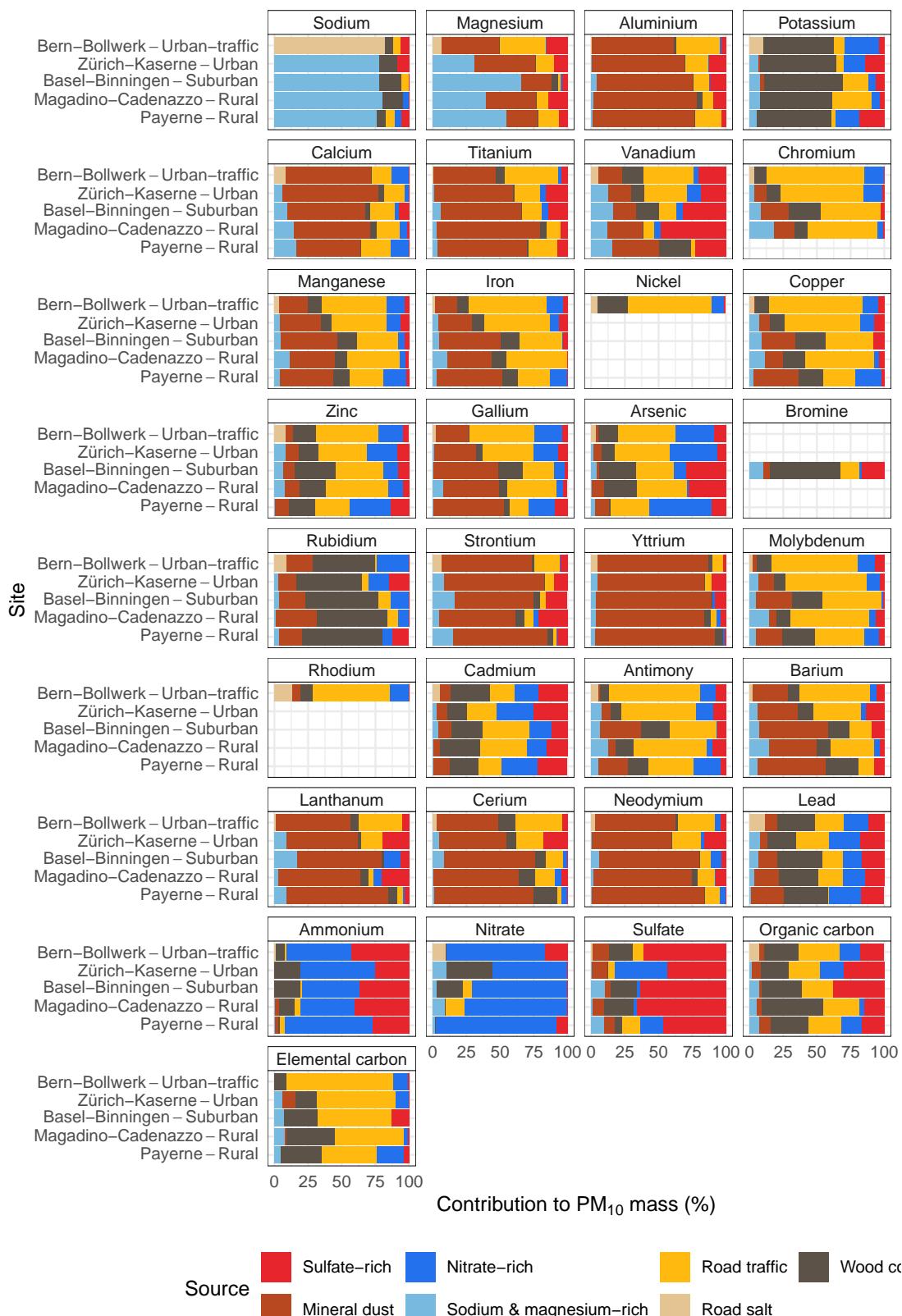
Figure A.15 – Percentage of the mass of constituents of PM_{10} explained by the PMF-identified sources at the five sampling locations between August 1, 2008 and July 31, 2009.
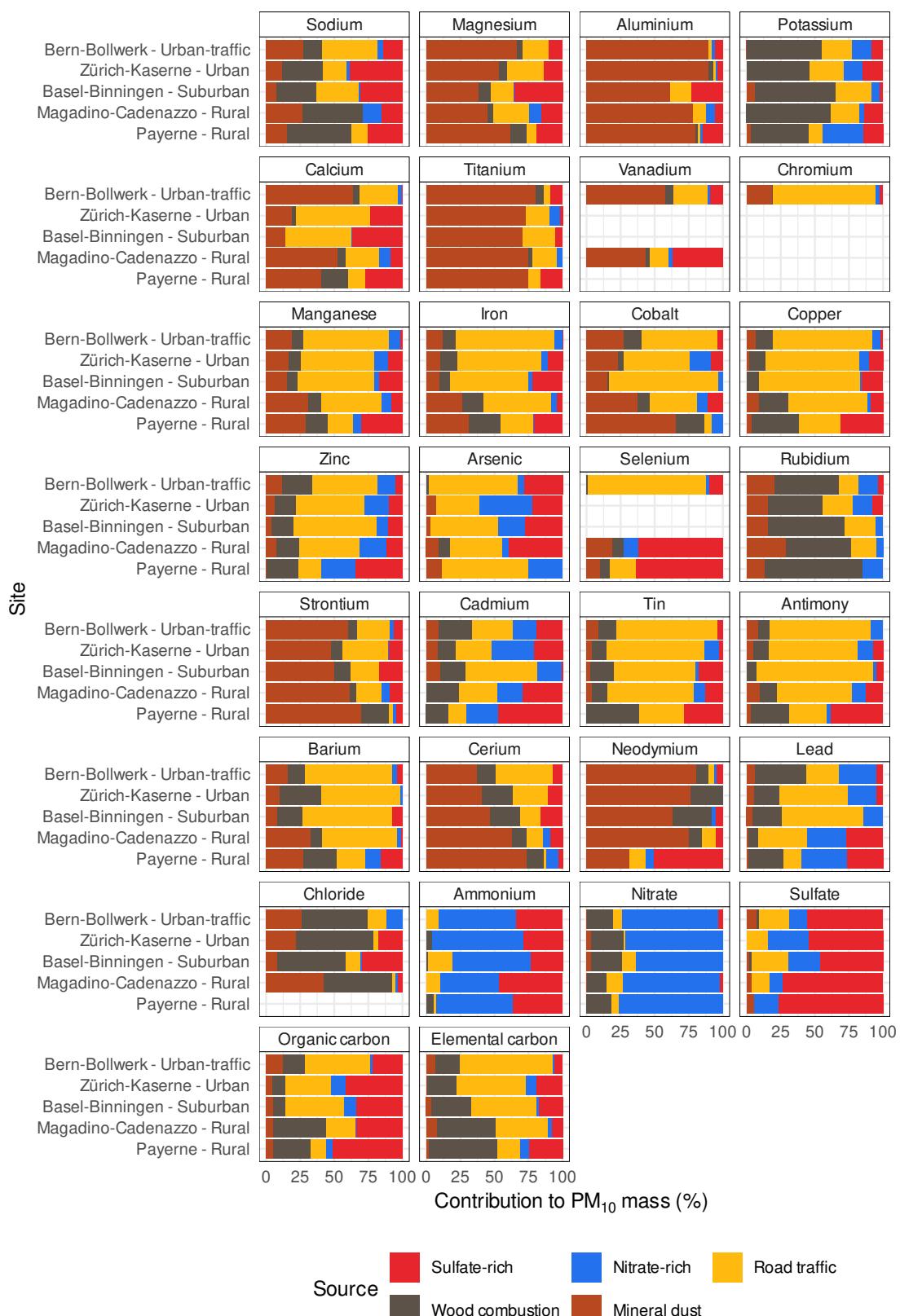
Figure A.16 – Percentage of the mass of constituents of PM_{10} explained by the PMF-identified sources at the five sampling locations between June 1, 2018 and May 31, 2019.
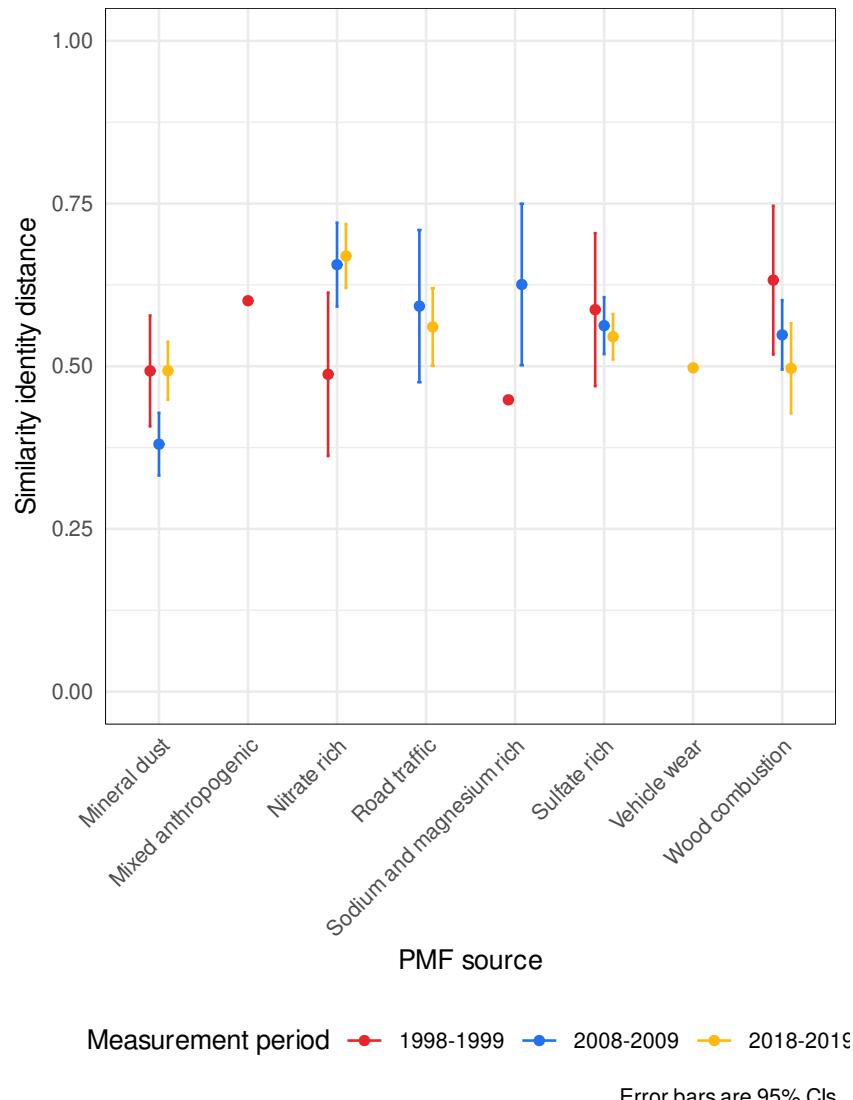
Figure A.17 – Similarity identity distances (SID) of the sites' sources for the three measurement periods in Switzerland between 1998 and 2019.
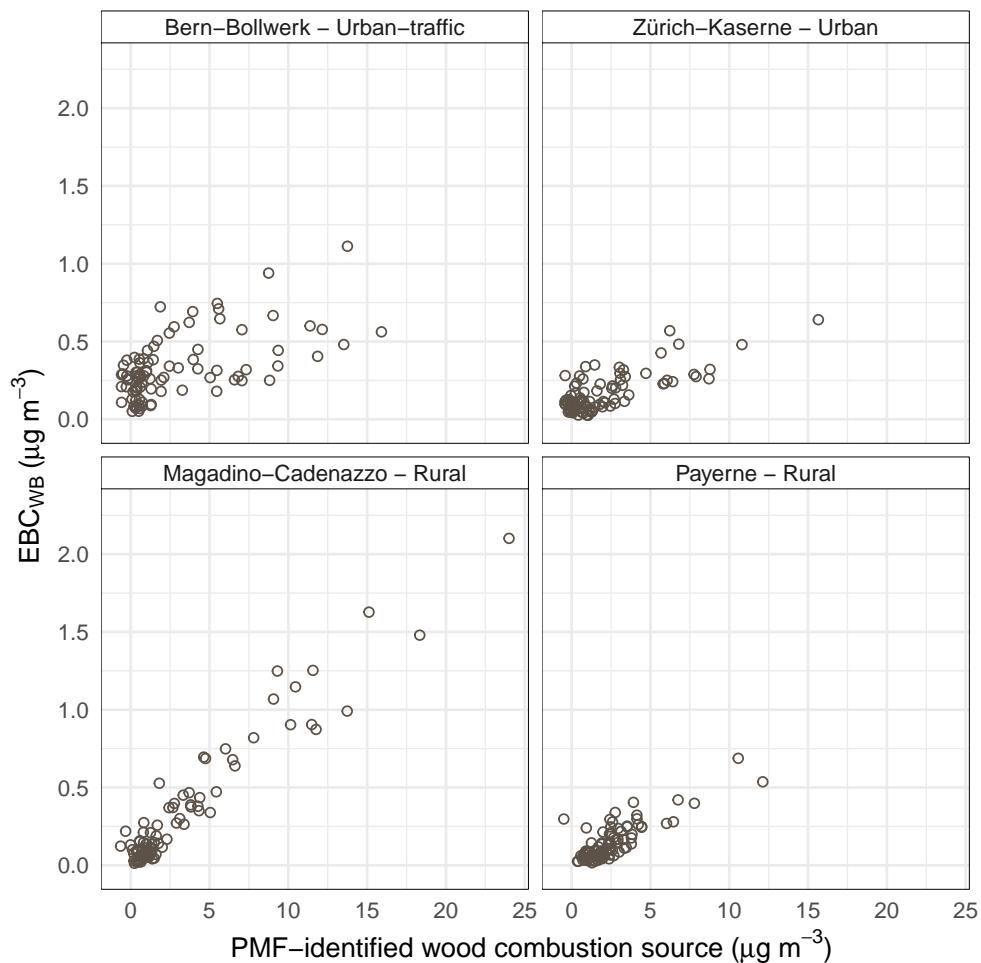
Figure A.18 – Scatterplots of wood burning equivalent black carbon (EBC_{WB}) and the PMF-identified wood combustion sources at four Swiss sites between 2018 and 2019.
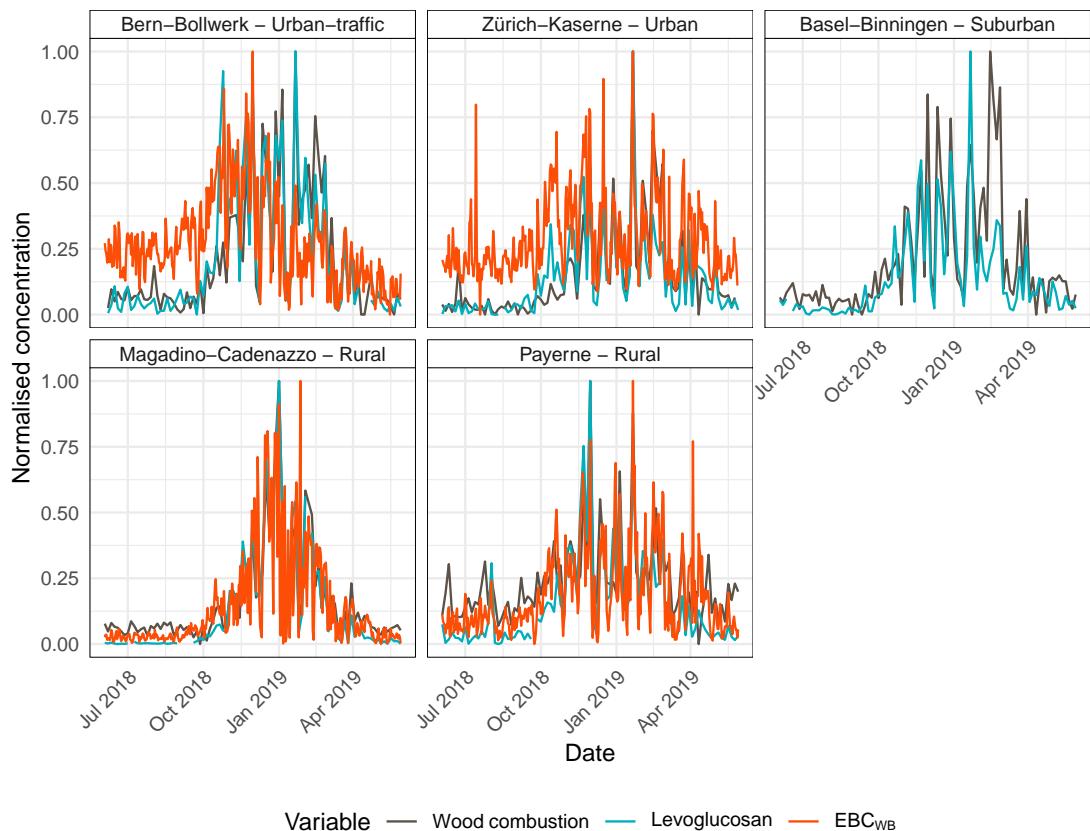
Figure A.19 – Wood burning equivalent black carbon (EBC$_{TR}$), the PMF-identified wood combustion sources, and levoglucosan time series between 2018 and 2019 at four Swiss sites.
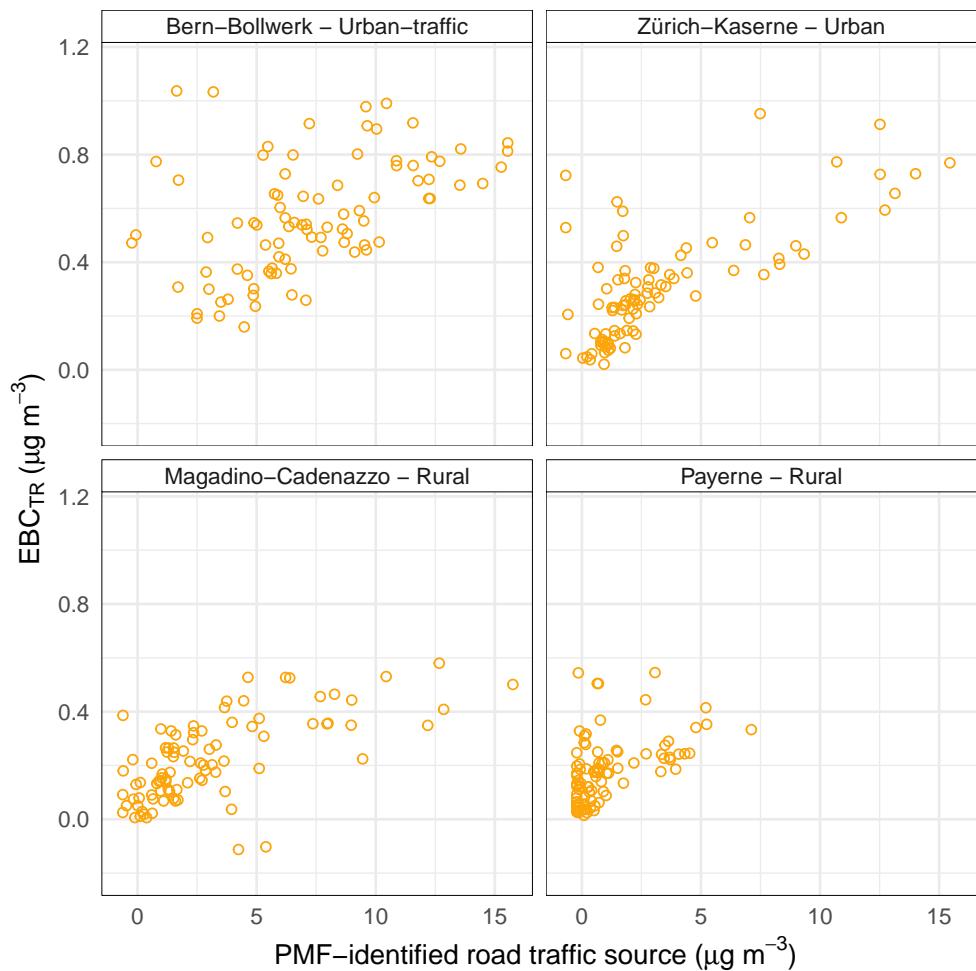
Figure A.20 – Scatterplots of traffic equivalent black carbon (EBC$_{TR}$) and the PMF-identified road traffic sources at four Swiss sites between 2018 and 2019.
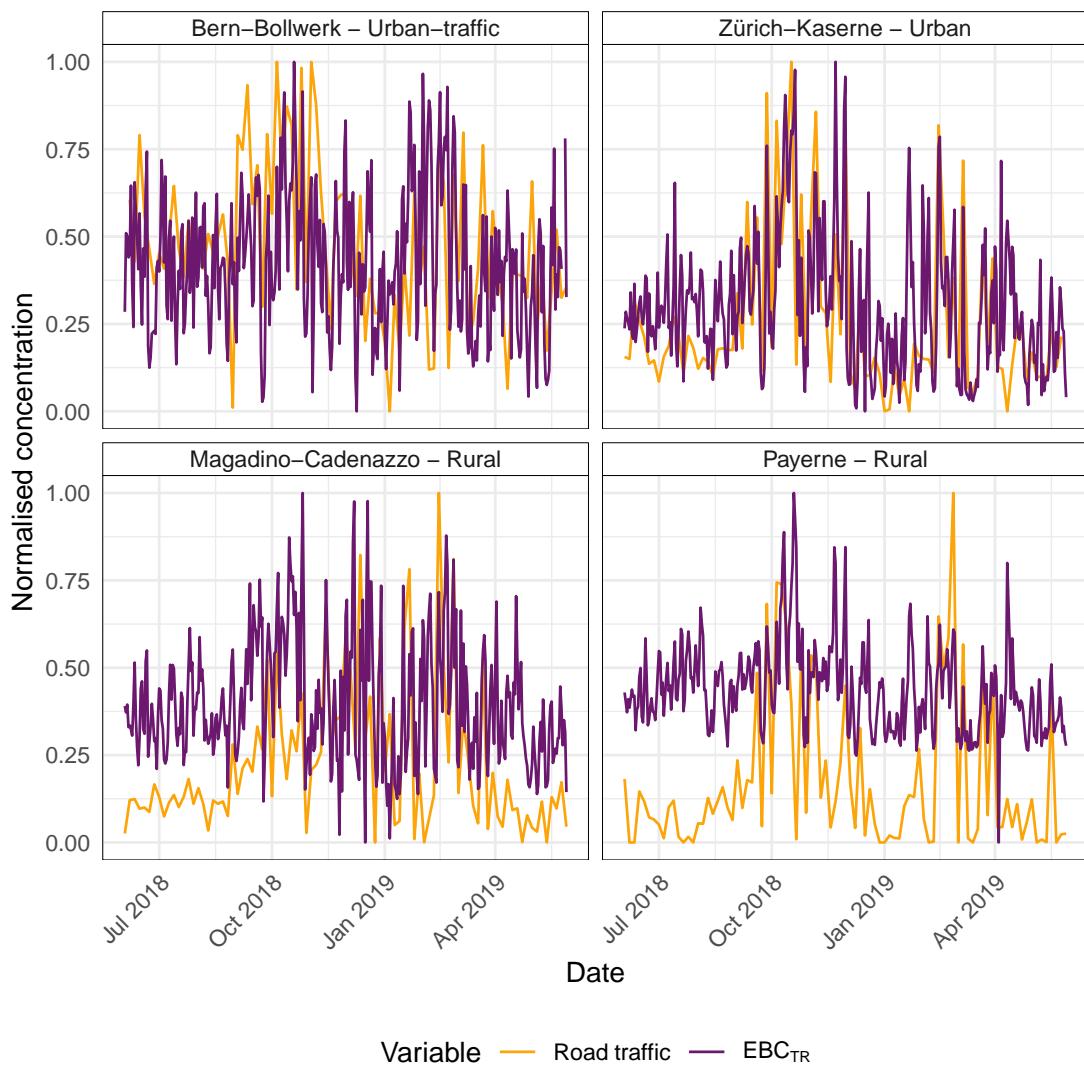
Figure A.21 – Traffic equivalent black carbon (EBC$_{\text{TR}}$) and the PMF-identified road traffic sources time series between 2018 and 2019 at four Swiss sites.
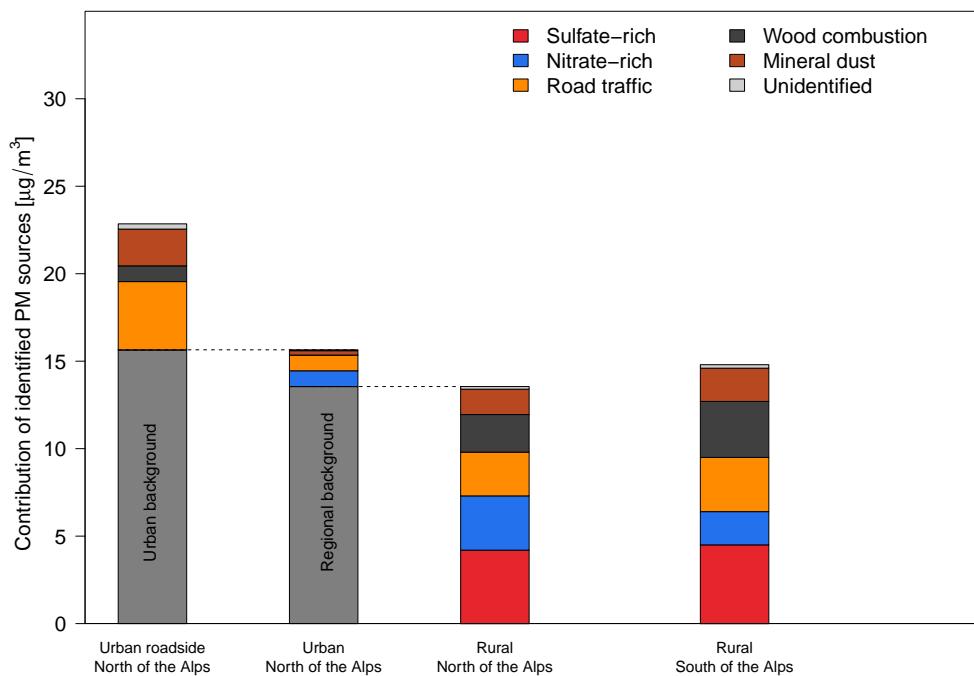
Figure A.22 – Summary of PM_{10} source apportionment for the 2018–2019 measurement period. The estimated mean annual source contributions at Magadino-Cadenazzo are considered to be representative for rural sites south of the Alps, the regional background north of the Alps is represented as the average source contributions at the suburban site Basel-Binningen and the rural site Payerne. The source contributions to the urban and roadside increments are calculated from the PMF derived sources at Zürich-Kaserne and Bern-Bollwerk, respectively.
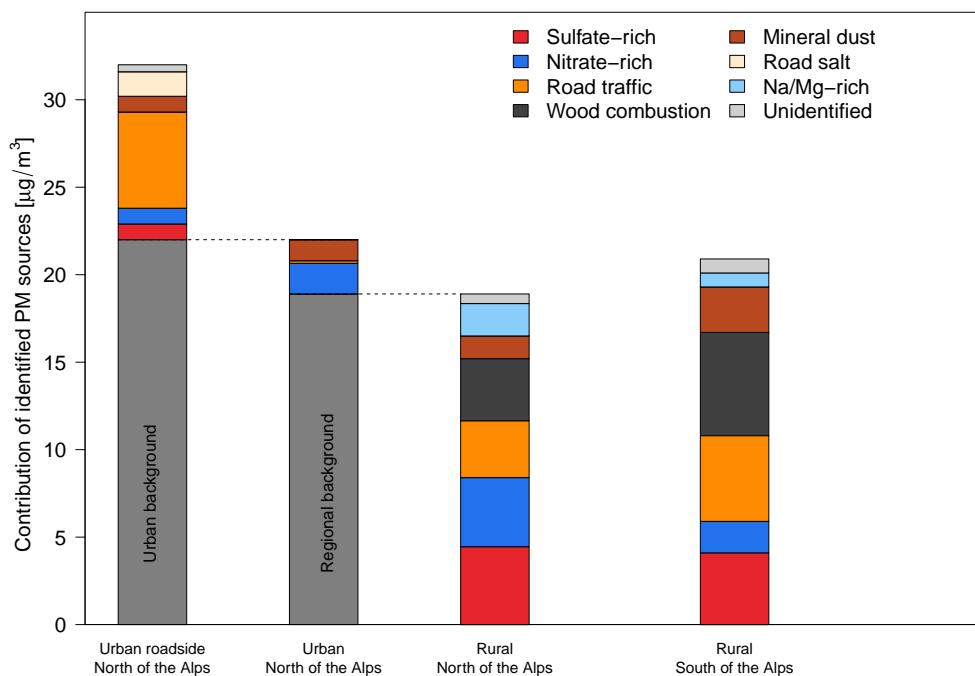
Figure A.23 – Summary of PM_{10} source apportionment for the 2008–2009 measurement period. The estimated mean annual source contributions at Magadino-Cadenazzo are considered to be representative for rural sites south of the Alps, the regional background north of the Alps is represented as the average source contributions at the suburban site Basel-Binningen and the rural site Payerne. The source contributions to the urban and roadside increments are calculated from the PMF derived sources at Zürich-Kaserne and Bern-Bollwerk, respectively.

8.2 Tables

Table A.1 – The variables/species used in the PMF models.

Variable	Notes
Aluminium	
Ammonium	
Antimony	
Arsenic	
Barium	
Bromine	Only for 1998–1999 and 2008–2009 models
Cadmium	
Calcium	
Cerium	
Chloride	
Chromium	
Cobalt	
Copper	
Elemental carbon	
Gallium	Only for 1998–1999 and 2008–2009 models
Iron	
Lanthanum	Only for 1998–1999 and 2008–2009 models
Lead	
Magnesium	
Manganese	
Molybdenum	Only for 1998–1999 and 2008–2009 models
Neodymium	
Nickel	Only for 1998–1999 and 2008–2009 models
Nitrate	
Organic carbon	
Potassium	
Rhodium	Only for 1998–1999 and 2008–2009 models
Rubidium	
Selenium	
Sodium	
Strontium	
Sulfate	
Tin	
Titanium	
Vanadium	
Yttrium	Only for 1998–1999 and 2008–2009 models
Zinc	

Table A.2 – Mean concentrations of elements in $PM_{2.5-10}$ for the 2018–2019 measurement period. Values are in $ng\,m^{-3}$ and have been rounded to three significant figures and three decimal places. For elements that have been measured by two different methods, both mean values are listed in order to facilitate a comparison of results.

Variable	Method	Bern-Bollwerk	Zürich-Kaserne	Basel-Binningen	Magadino-Cadenazzo	Payerne
Lithium	ICP-MS	0.081	0.037	0.057	0.087	0.03
Sodium	ICP-OES	141	76.3	77.1	69	59.2
Sodium	IC	147	70.5	75.8	55.9	53.3
Magnesium	ICP-OES	51.1	32.5	28.2	40.4	26.2
Magnesium	IC	27	23.6	17.1	18.1	13.1
Aluminium	ICP-OES	132	58.7	86	112	75
Phosphorus	ICP-OES	12.8	7.14	7.89	19.1	11.7
Sulfur	ICP-OES	76.7	66.4	51.3	48.8	62.6
Potassium	ICP-OES	41.2	31.1	33.3	53.6	55.3
Potassium	IC	22.2	23.2	21.6	32.4	27.8
Calcium	ICP-OES	419	254	169	159	141
Calcium	IC	401	237	158	126	118
Scandium	ICP-MS	0.02	0.005		0.078	0.024
Titanium	ICP-MS	7.91	5.14	3.8	6.97	4.35
Vanadium	ICP-MS	0.324	0.155	0.109	0.238	0.125
Chromium	ICP-MS	2.28	0.752	0.859	1.16	
Manganese	ICP-MS	7.62	3.69	1.94	3.18	1.71
Iron	ICP-OES	852	370	170	253	110
Cobalt	ICP-MS	0.075	0.064	0.053	0.066	0.033
Copper	ICP-MS	36.3	12.8	3.62	5.57	2.92
Zinc	ICP-MS	11.7	3.68	0.547	2.02	2.81
Gallium	ICP-MS	0.025	0.022	0.02	0.048	0.016
Arsenic	ICP-MS	0.022	0.013	0.038	0.089	0.044
Selenium	ICP-MS	0.018			0.014	0.017
Rubidium	ICP-MS	0.183	0.108	0.121	0.24	0.122
Strontium	ICP-MS	1.49	0.97	0.579	0.575	0.387
Yttrium	ICP-MS	0.028		0.036		0.115
Zirconium	ICP-MS	0.651	0.574			
Niobium	ICP-MS	0.021	0.055	0.037		
Cadmium	ICP-MS		0.009		0.007	0.029
Tin	ICP-MS	4.98	1.94	0.708	0.975	0.572
Antimony	ICP-MS	3.25	0.933	0.323	0.454	0.276
Cesium	ICP-MS	0.008	0.002	0.013	0.004	0.009
Barium	ICP-MS	13.3	3.4	2.78	2.52	1.31
Lanthanum	ICP-MS	0.14	0.05	0.071	0.047	0.043
Cerium	ICP-MS	0.282	0.081	0.138	0.097	0.077
Neodymium	ICP-MS	0.08	0.041	0.057	0.021	0.03
Samarium	ICP-MS	0.016	0.005	0.018		0.008
Gadolinium	ICP-MS	0.014		0.022		0.011
Terbium	ICP-MS	0.004				0.017
Dysprosium	ICP-MS	0.014	0.001	0.01		0.011
Holmium	ICP-MS			0.013		0.033
Ytterbium	ICP-MS	0.008		0.003		0.003
Hafnium	ICP-MS	0.036	0.005			
Tungsten	ICP-MS	0.104	0.01	0.006	0.112	0.023
Thallium	ICP-MS	0.001	0.001			0.005
Lead	ICP-MS	0.982	0.455	0.583	0.442	0.373
Bismuth	ICP-MS	0.3	0.256	0.106	0.082	0.07
Chloride	IC	150	25.2	34.3	25.3	15.6
Ammonium	IC				0.767	85.2
Nitrate	IC	92.3	239	364	292	492
Sulfate	IC	110	146	80.6	99.6	145

113

Table A.3 – Mean concentrations and contributions of PM_{10} PMF identified sources for five PM monitoring sites in Switzerland for three measurement periods between 1998 and 2019. All values have been rounded to one decimal place. Note that for the 2008–2009 measurement period the Saharan dust event from 15.10.2008 has not been excluded.

Period	Variable	Bern-Bollwerk $\mu g\,m^{-3}$	%	Zürich-Kaserne $\mu g\,m^{-3}$	%	Basel-Binningen $\mu g\,m^{-3}$	%	Magadino-Cad. $\mu g\,m^{-3}$	%	Payerne $\mu g\,m^{-3}$	%
1998-1999	Sulfate-rich	4.5	11.2	5.0	20.8	5.8	23.8	–	–	–	–
1998-1999	Nitrate-rich	5.1	12.8	4.2	17.3	4.2	17.2	–	–	–	–
1998-1999	Mixed anthropogenic	4.3	10.9	4.6	18.9	3.9	16.1	–	–	–	–
1998-1999	Road traffic	13.4	33.7	3.7	15.1	3.8	15.4	–	–	–	–
1998-1999	Mineral dust	5.4	13.7	4.4	18.3	3.4	14.0	–	–	–	–
1998-1999	Road salt	4.9	12.4	–	–	–	–	–	–	–	–
1998-1999	Missing	2.1	5.2	0.7	3.0	1.3	5.5	–	–	–	–
1998-1999	Sodium & magnesium-rich	–	–	1.6	6.7	2.0	8.1	–	–	–	–
2008-2009	Sulfate-rich	5.0	17.1	4.1	20.1	5.6	29.8	4.1	19.8	3.3	17.2
2008-2009	Nitrate-rich	6.6	22.5	5.7	27.5	2.2	11.7	1.8	8.5	5.7	30.0
2008-2009	Road traffic	8.9	30.3	3.4	16.6	3.2	17.0	4.9	23.6	3.3	17.2
2008-2009	Wood combustion	3.4	11.7	3.5	17.0	4.2	22.2	5.9	28.5	2.9	15.3
2008-2009	Mineral dust	3.4	11.7	2.5	12.1	1.0	5.4	2.6	12.3	1.6	8.4
2008-2009	Road salt	1.4	4.9	–	–	–	–	–	–	–	–
2008-2009	Missing	0.5	1.7	0.1	0.4	0.4	2.0	0.8	3.7	0.7	3.8
2008-2009	Sodium & magnesium-rich	–	–	1.3	6.4	2.2	11.9	0.8	3.7	1.5	8.1
2018-2019	Sulfate-rich	3.7	17.2	4.2	27.1	3.6	26.0	4.5	30.2	4.7	36.0
2018-2019	Nitrate-rich	3.2	15.1	4.0	26.0	3.1	22.0	1.9	12.6	3.1	23.6
2018-2019	Road traffic	7.3	34.1	3.4	21.7	3.9	27.9	3.1	21.0	1.1	8.1
2018-2019	Wood combustion	2.9	13.7	2.0	13.1	1.8	12.9	3.2	21.7	2.5	18.7
2018-2019	Mineral dust	3.8	17.6	1.7	11.0	1.4	10.1	1.9	13.0	1.5	11.5
2018-2019	Missing	0.5	2.2	0.2	1.1	0.1	1.1	0.2	1.4	0.3	2.1